OPTIMIZATION OF SOLAR ASSISTED OCEAN THERMAL ENERGY
CONVERSION PLANT DESIGN AND SYSTEM PERFORMANCE

NOR AMYRA HANA BINTI MOHD YUSOFF

UNIVERSITI TEKNOLOGI MALAYSIA

UNIVERSITI TEKNOLOGI MALAYSIA

DECLARATION OF THESIS / UNDERGRADUATE PROJECT PAPER AND COPYRIGHT

Author's full name : NOR AMYRA HANA BINTI MOHD YUSOFF

Date of birth : 10 SEPTEMBER 1989

Title : OPTIMIZATION OF SOLAR ASSISTED OCEAN THERMAL ENERGY CONVERSION PLANT DESIGN AND SYSTEM PERFORMANCE

Academic Session : 2016/2017 - 2

I declare that this thesis is classified as :

☐ **CONFIDENTIAL** (Contains confidential information under the Official Secret Act 1972)*

☐ **RESTRICTED** (Contains restricted information as specified by the organization where research was done)*

/ **OPEN ACCESS** I agree that my thesis to be published as online open access (full text)

I acknowledged that Universiti Teknologi Malaysia reserves the right as follows:

1. The thesis is the property of Universiti Teknologi Malaysia.
2. The Library of Universiti Teknologi Malaysia has the right to make copies for the purpose of research only.
3. The Library has the right to make copies of the thesis for academic exchange.

Certified by :

_____
SIGNATURE

890910-07-5050
(NEW IC NO. /PASSPORT NO.)

Date :

_____
SIGNATURE OF SUPERVISOR

_____
NAME OF SUPERVISOR

Date :

NOTES : * If the thesis is CONFIDENTAL or RESTRICTED, please attach with the letter from the organization with period and reasons for confidentiality or restriction.

"I hereby declare that I have read this thesis and in my
opinion this thesis is sufficient in terms of scope and quality for the
award of the degree of Master of Philosophy"

Signature   : ....
Name of Supervisor   : DR NOR'AZIZI BIN OTHMAN
Date   : ....

BAHAGIAN A – Pengesahan Kerjasama*

Adalah disahkan bahawa projek penyelidikan tesis ini telah dilaksanakan melalui kerjasama

antara _____ dengan _____

Disahkan oleh:

Tandatangan   :   ....   Tarikh :   ....

Nama   :   ....

Jawatan   :   ....
(Cop rasmi)

* Jika penyediaan tesis/projek melibatkan kerjasama.

BAHAGIAN B – Untuk Kegunaan Pejabat Sekolah Pengajian Siswazah

Tesis ini telah diperiksa dan diakui oleh:

Nama dan Alamat Pemeriksa Luar   :   _____

_____

Nama dan Alamat Pemeriksa Dalam   :   _____

_____

Nama Penyelia lain (jika ada)   :   _____

Disahkan oleh Timbalan Pendaftar di Sekolah Pengajian Siswazah:

Tandatangan :   _____   Tarikh :   _____

Nama   :   _____

OPTIMIZATION OF SOLAR ASSISTED OCEAN THERMAL ENERGY
CONVERSION PLANT DESIGN AND SYSTEM PERFORMANCE

NOR AMYRA HANA BINTI MOHD YUSOFF

A thesis submitted in fulfilment of the
requirements for the award of the degree of
Master of Philosophy

Malaysia-Japan International Institute of Technology
Universiti Teknologi Malaysia

JUNE 2017

I declare that this thesis entitled "*Optimization of Solar Assisted Ocean Thermal Energy Conversion Plant Design and System Performance*" is the result of my own research except as cited in the references. The thesis has not been accepted for any degree and is not concurrently submitted in candidature of any other degree.

Signature   :   ....

Name   :   NOR AMYRA HANA BT MOHD YUSOFF

Date   :   …………………………………………

This thesis is gratefully dedicated to my beloved husband, parents and family.

ACKNOWLEDGEMENTS

I thank Allah SWT for His blessing and mercy until I accomplished my thesis.

First of all, my gratitude sincerely goes to my beloved father and mother who always give me advices and dreams to be an excellent daughter. My second gratitude belongs to my beloved husband who has offered unwavering support and encouragement during the past years of this journey. He has cheered me on when I was discouraged and 100% confident on my ability to get this done. Thank you for your support and console.

My gratitude is dedicated to all lectures for their contributions to the direction and richness of this research. Without their thoughtful and encouragement this thesis would not have taken shape.

Last but not least, I humbly extend my gratitude to all concerned persons who co-operated with me in this regard.

ABSTRACT

Ocean Thermal Energy Conversion (OTEC) is a power generation method that utilizes the temperature difference that exists between the warm surface seawater and cold deep seawater. An OTEC plant is generally limited to operations with a temperature difference of at least 20 °C, where cold seawater needs to be withdrawn from at least 1000 m depth to maintain its performance. However, the potential of using this energy in the Malaysia-Thailand Joint Development Area (MTJDA) is low due to very shallow sea levels ranging from only 55 to 65 m. Therefore in the absence of the required depth, an alternative method using solar collectors are introduced to boost the sea surface temperature in order to maintain the required temperature difference. This research reports the results of optimization of 100 kW Solar Assisted Ocean Thermal Energy Conversion (SOTEC) cycle and its system performance. This system is composed of a turbine, condenser, evaporator, pump and flat plate solar collector. In SOTEC, the inlet temperature of existing seawater of 26.7 °C is raised to 40 °C by using a typical flat plate solar collector. Design and simulations were carried out under an annual solar radiation of 196.8 W/m^2 found in Kota Bharu, in order to estimate the potential required effective area of solar collector that can raise to the specified temperature. Simulation was conducted using the mathematical modeling and numerical study of the Organic Rankine Cycle (ORC). All the analysis was done using Visual Fortran Programming system. The results showed that the proposed SOTEC plant can potentially achieve the net power output of 92.1 kW with a net Rankine cycle efficiency of 5.4 % when a flat plate solar collector of 29155 m^2 is installed. Overall, the obtained results provided important insights from a thermodynamic perspective of combining a sustainable energy from the ocean with solar thermal energy to improve the overall system performance. Overall with the presence of solar collectors, OTEC technology is no more limited to deep oceans only but can be implemented at any ocean with specific required collector area.

ABSTRAK

Penukaran Tenaga Terma Lautan (OTEC) adalah satu kaedah penjanaan kuasa yang menggunakan perbezaan suhu yang wujud di antara permukaan air laut yang panas dan air laut dalam yang sejuk. Namun, kekurangan fasiliti OTEC adalah keperluan operasi yang memerlukan perbezaan suhu sebanyak 20 °C dan perbezaan ini hanya boleh dicapai pada kedalaman 1000 m bagi mengekalkan prestasinya. Walau bagaimanapun, potensi menggunakan tenaga boleh diperbaharui di *Malaysia-Thailand Joint Development Area* (MTJDA) adalah rendah kerana kedalaman air lautnya yang cetek iaitu di antara 55 hingga 65 m. Pada kedalaman sebegitu, penggunaan pengumpul suria dapat menaikkan suhu permukaan air dan perbezaan suhu yang dikehendaki dapat dicapai. Kajian ini melaporkan keputusan pengoptimuman 100 kW tenaga yang terhasil daripada kitaran Penukaran Tenaga Terma Lautan Solar (SOTEC). Sistem ini terdiri daripada turbin, pemeluwap, penyejat, pam dan pengumpul suria. Dalam sistem SOTEC, suhu air laut panas adalah 26.7 °C dan dapat dinaikkan ke 40 °C dari suhu asal dengan pengumpul suria. Reka bentuk dan simulasi telah dijalankan dengan menggunakan nilai sinaran suria tahunan di Kota Bharu sebanyak 196.8 W/m^2 bagi menganggar luas pengumpul suria yang boleh meningkatkan suhu tersebut. Simulasi dijalankan dengan menggunakan model matematik dan kajian berangka Rankine Kitaran Organik (ORC). Semua analisis telah dilakukan dengan sistem *Visual Fortran Programming*. Keputusan menunjukkan bahawa sistem SOTEC berpotensi mencapai kuasa output bersih 92.1 kW dengan kecekapan haba bersih sebanyak 5.4% jika luas pengumpul suria yang dipasang adalah 29155 m^2. Keputusan yang diperolehi ini dapat meningkatkan prestasi sistem dari segi perspektif termodinamik apabila menggabungkan tenaga lestari dengan tenaga haba solar. Secara keseluruhannya, dengan kehadiran pengumpul suria, teknologi OTEC tidak lagi terhad kepada lautan dalam tetapi boleh dilaksanakan di mana-mana lautan dengan luas pengumpul suria tertentu.

TABLE OF CONTENTS

LIST OF TABLES

LIST OF FIGURES

LIST OF ABBREVIATIONS

COP - Coefficient of Performance

CSIRO - Commonwealth Scientific and Industrial Reseach Organisation

FiT - Feed-in Tariff

GHG - Greenhouse Gasess

GSW - Gibbs Seawater

GWP - Global Warming Potential

HDPE - High Density Polyethylene

LTTD - Low Temperature Thermal Desalination

MTJDA - Malaysia Thailand Development Area

NELHA - Natural Energy Laboratory of Hawaii Authority

NIOT - National Institute of Ocean Technology

ODP - Ozon Depletion Potential

OTEC - Ocean Thermal Energy Conversion

RE - Renewable Energy

SEDA - Sustainable Energy Development Authority

SOTEC - Solar Ocean Thermal Energy Conversion

LIST OF SYMBOLS

Q_u -   Useful heat gain

Q_E -   Liquid-side heat flow in the evaporator

Q_C -   Liquid-side heat flow in the condenser

Q_{ewf} -   Working fluid-side heat flow in the evaporator

Q_{cwf} -   Working fluid-side heat flow in the condenser

m -   Fluid mass flow rate

c_p -   Specific heat of fluid

$c_{p,ws}$ -   Specific heat of warm seawater

$c_{p,cs}$ -   Specific heat of cold seawater

T_i -   Inlet temperature

T_o -   Outlet temperature

A_{sc} -   Flat plate solar collector area

F_R -   Collector heat removal factor

S -   Radiation flux

U_L -   Collector heat transfer coefficient

I -   Radiation intensity

η -   Efficiency of flat plate solar collector

η_T -   Turbine efficiency

η_G -   Generator efficiency

η_{th}	-	Net thermal efficiency
η_G	-	Net efficiency
m_{ws}	-	Mass warm seawater flow rate
m_{cs}	-	Mass cold seawater flow rate
m_{wf}	-	Mass working fluid flow rate
T_{wsi}	-	Warm seawater inlet temperature
T_{wso}	-	Warm seawater outlet temperature
T_{csi}	-	Cold seawater inlet temperature
T_{cso}	-	Cold seawater outlet temperature
U	-	Overall heat transfer coefficient
h	-	Enthalpy
ΔH	-	Head difference
ΔT_{lm}	-	Log mean temperature difference
L_{ws}	-	Warm seawater length pipe
L_{cs}	-	Cold seawater length pipe
L_E	-	Evaporator length plate
L_C	-	Condenser length plate
W_N	-	Net power
$W_{T\text{-}G}$	-	Turbine generator power
$W_{P,ws}$	-	Warm seawater pumping power
$W_{P,cs}$	-	Cold seawater pumping power
C	-	Coefficient factor
V	-	Velocity
D_{eq}	-	Equivalent diameter

σ - Clearance

d - Inner diameter pipe

λ - Friction loss

g - Gravitational acceleration

LIST OF APPENDICES

CHAPTER 1

INTRODUCTION

Energy use is directly linked to well-being and prosperity across the world. Meeting the growing demand for energy in a safe and environmentally responsible manner is an important challenge. A key driver of energy demand is the human desire to sustain and improve ourselves, our families and our communities. There are around seven billion people on Earth and population growth will likely lead to an increase in energy demand, which depends on the adequacy of energy resources. In addition, increasing population and economic development in many countries have serious implications for the environment, because energy generation processes (e.g., generation of electricity, heating, cooling, and shaft work for transportation and other applications) emit pollutants, many of which are harmful to ecosystems. Burning fossil fuels results in the release of large amounts of greenhouse gases, particularly carbon dioxide.

1.1   Background of the Study

Nowadays, human activity is overloading our atmosphere with carbon dioxide and other global warming emissions, which trap heat, steadily increase the planet's

temperature, and significantly create harmful impacts on our health, our environment, and climate. As such, the environmental impact of electricity generation is significant. This is due to the fact that modern society uses large amounts of electrical power. Besides that, as the waste products are dispersed directly into the air, it creates pollution and thus affects human health when breathing.

1.1.1 Electricity from Renewable Energy

The demand for electricity in Malaysia rises rapidly every year and in 2013 as shown in Figure 1.1 consumed 4511.97 kWh. By 2020, its electricity consumption is expected to increase by 30 % from its present value to 124,677 GWh. The TNB has recently announced that there is 4.5 % electricity demand growth in Peninsular Malaysia with its latest peak demand at 17,788 MW on 20th April 2016. This has reflected an improvement of 5.2 % as compared to the peak demand of 16,901 MW recorded two years ago on 11th June 2014.[1]
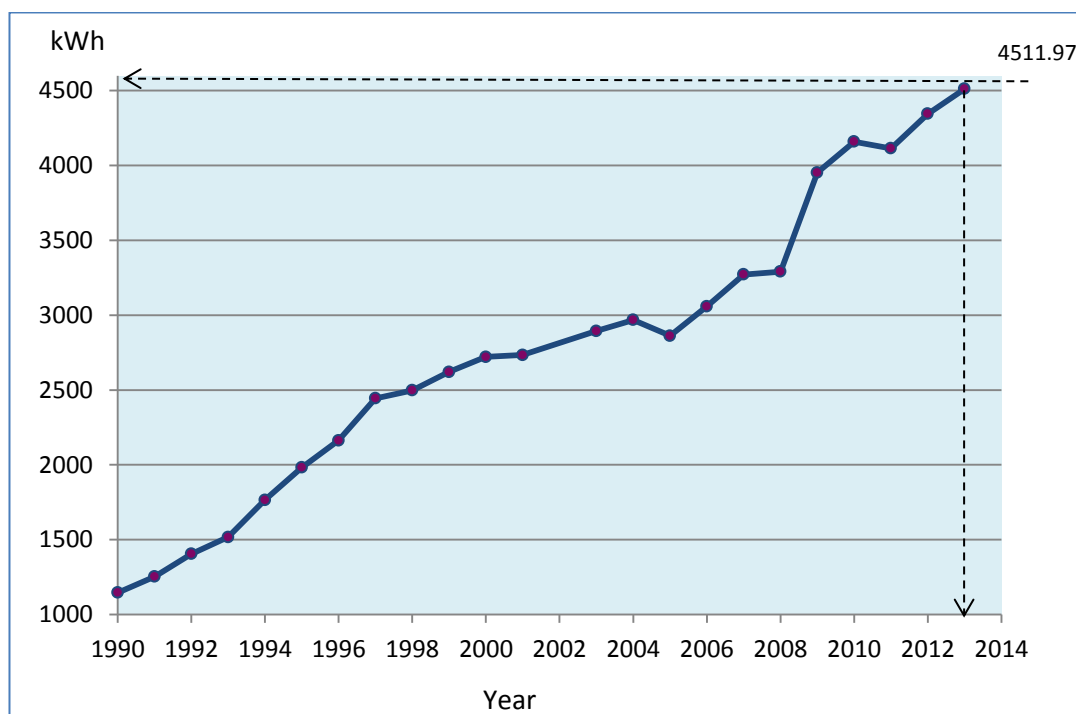
Figure 1.1   Electricity demands Per Capita in Malaysia [2]

The average electricity consumed per household in Malaysia is about 251 kWh per month, which means, one household releases 171.68 kg of carbon dioxide per month[3]. This gas effect extends from human to water resources, farm produce, forest, animals and another habitat. Besides, this negative gas, increase the greenhouse gasses (GHG) emission which cause harmful and pollution to the environment as seen in Figure 1.2. Any type of energy produced from renewable energy is called green energy because they generate less impact on the environment and is sustainable. In order to survive this situation, many companies have started inventing new technology to extract electricity from renewable energy sources like wave, wind, and solar. They are some of the examples of producing electricity without pollution. Undoubtedly, every type of electricity generation will have some impact, but some sources are much greener than others. Therefore, it is important that new technology like Ocean Thermal Energy Conversion (OTEC) be seen as the productive solution for maintaining the environmental benign and sustainability with zero CO_2 emission.
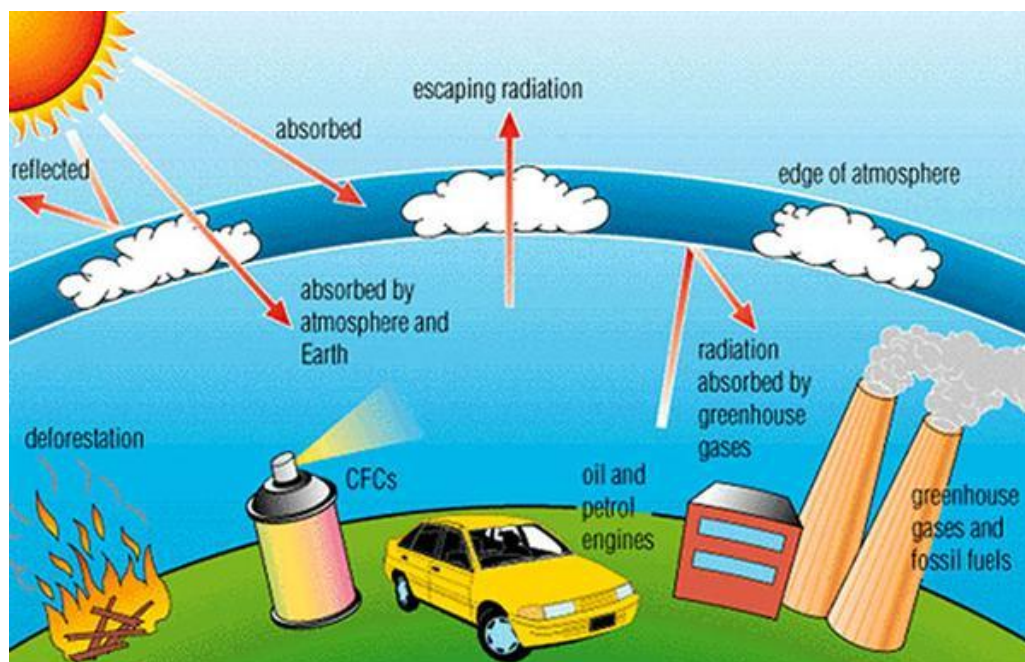
Figure 1.2   Environmental Issues-Greenhouse effect [4]

1.1.2   Ocean Thermal Energy Conversion (OTEC)

Ocean thermal energy conversion is a system of converting heat energy into electricity by using the temperature difference between hot surface water and cold deep sea water [5-7]. This concept was first proposed by D'Arsonval in 1881 and it was followed by other researchers [8]. Numerous efforts have been directed at improving the system performance of OTEC through theoretical and experimental studies conducted by researchers on the major component of OTEC system [9, 10]. A closed OTEC cycle requires a refrigerant, such as ammonia, R-134a, R-22 or R-32 as working fluid to transmit energy to warm and cold seawater in evaporator and condenser respectively. OTEC is a firm power (24/7), clean energy source, environmentally sustainable and capable of providing massive levels of energy. Several pilot studies of 10 MW OTEC plants are under development by US companies such as Lockheed Martin, Makai Ocean Engineering and Ocean Thermal Energy Corporation. Many researchers, have studied the implementation of OTEC in the tropical area [11-13] as it is located near to the equator where it's characterized by hot average temperature all year round and high monthly precipitation. In any case, even in the tropical territory, the temperature contrast between hot surface seawater and cool seawater is just 20 - 25 °C and the best thermodynamic proficiency could be accomplished just lies in the extent 3-5% requiring large seawater flow rate for power generation [14]. Nevertheless, in a typical OTEC plant, the net power efficiency is between 50 - 80 % of the system. This results in high cost of electricity generated by OTEC cycle.

Most of the earth's surface is covered by ocean where its upper layer of the ocean captures and stores the sunlight coming from the sun. The seas cover more than 70 % of Earth's surface and catch an expansive part of the sun's warmth in the upper layers, making them the world's largest solar collectors and energy storage system. The stored solar energy could provide 300 times the world's consumption of electricity. Utilizing just a small portion of this energy, can cover the global energy need. However, the research conducted by Saitoh and Yamada has proven that increasing temperature difference is the most effective solution to improve the thermal efficiency of a thermodynamic power generation cycle [15]. The idea of an

integrated ocean thermal energy cycle and solar thermal energy is to improve the cycle efficiency by widening the temperature difference. Furthermore, in order to reduce cost, some study has reported on the results of OTEC system combined with solar pond. However, solar pond requires larger capacity area and difficult to be installed offshore. This combination of OTEC and typical solar collectors best known as SOTEC system could be another possible way to improve the cycle efficiency at low-electricity cost. Reference is made to the famous literature review, in OTEC technology the minimum temperature differential is at least 20°C. This situation could be achieved by drawing cold sea water at depth of 1000m in the ocean. However with the presence of solar collector, OTEC technology is no longer limited to deep water but can also be developed in shallow sea water with reasonable solar collector area.

1.1.3 Potential OTEC in Malaysia

Up until now the global map has not yet shown that Malaysia has a potential area for generating OTEC. In the year 2008, the marine group did a study along South China sea and affirmed that Malaysia has an incredible capability for OTEC by producing power and hydrogen fuel, located in North-Borneo also known as Sabah Trough as shown in Figure 1.3. In reality, ocean thermal energy conversion is a technology that uses a concept of the temperature difference between surface water, which being heated by the sunlight and deep sea water which is much colder. The basic components of OTEC cycle are evaporator, condenser, turbine, and pump. Besides producing electricity, OTEC can also provide the possibility of other co-product like fresh water, waste cooling water for aquaculture and agriculture sector, air conditioning and hydrogen fuel.

Point	Latitude (N)	Longitude (E)
A	8° 39' 41"	115° 42' 46"
B	8° 01' 26"	116° 02' 36"
C	7° 39' 47"	115° 59' 28"
D	5° 54' 03"	114° 13' 57"
E	6° 39' 55"	113° 29' 47"
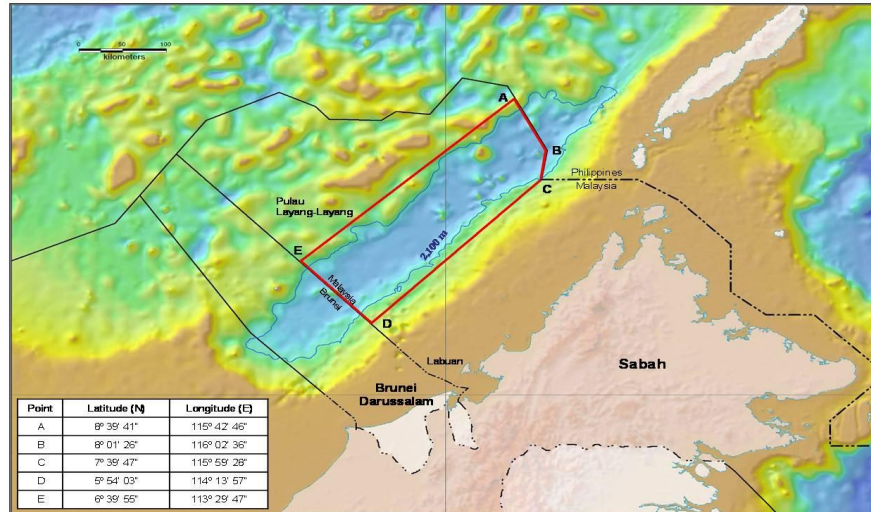
Figure 1.3   Sabah Trough [16]

The temperature at the bottom of the sea is about 4 °C located at depth of 1000 m while 28 °C at the surface of Sabah Trough as in Figure 1.4. Therefore, Malaysia has the potential to generate renewable energy due to temperature difference over 20 °C.
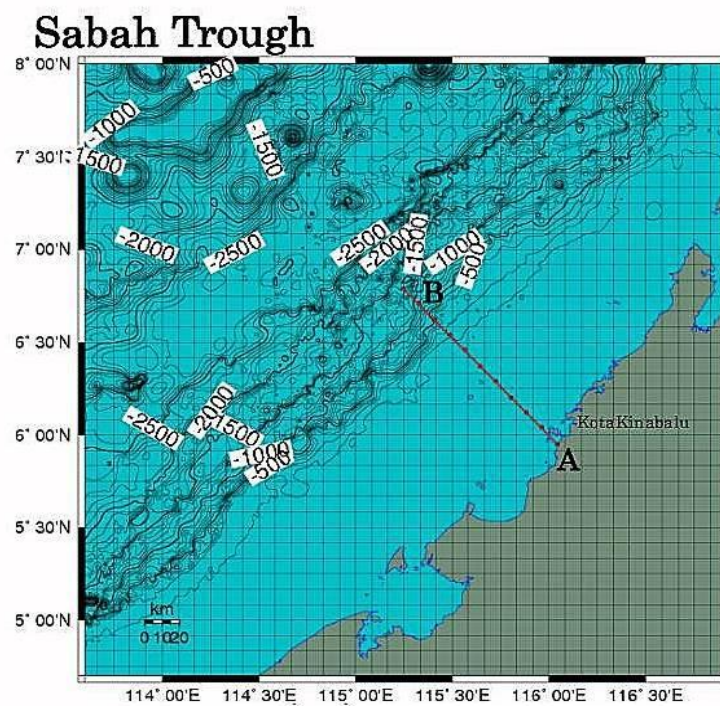
Figure 1.4   Potential OTEC in Malaysia [16]

Figure 1.5 shows the graph depicting temperature versus depth in the Sabah trough. As we know water is not perfectly transparent as nearly all of its sunlight is absorbed in the surface layer which heats up. As we realize that water is not superbly straightforward about all daylight is caught up in the surface layer which warms up. Presently, wind and waves flow the water on the surface layer conveying the warmth inside of it to some degree, and the temperature might remain entirely uniform for the initial hundred meters, yet underneath the blended layer, the temperature drops quickly from 20 °C with an extra of 1000 m to 1500 m depth. This area of rapid transition is called thermocline and below it the temperature continues to drop with depth but very gradually. Generally, thermocline varies with latitude and season but it is permanent in the tropics, variable in the temperate climates is strongest during the summer and is weak to non-existent in the polar regions where the water is cold from the surface to the bottom.
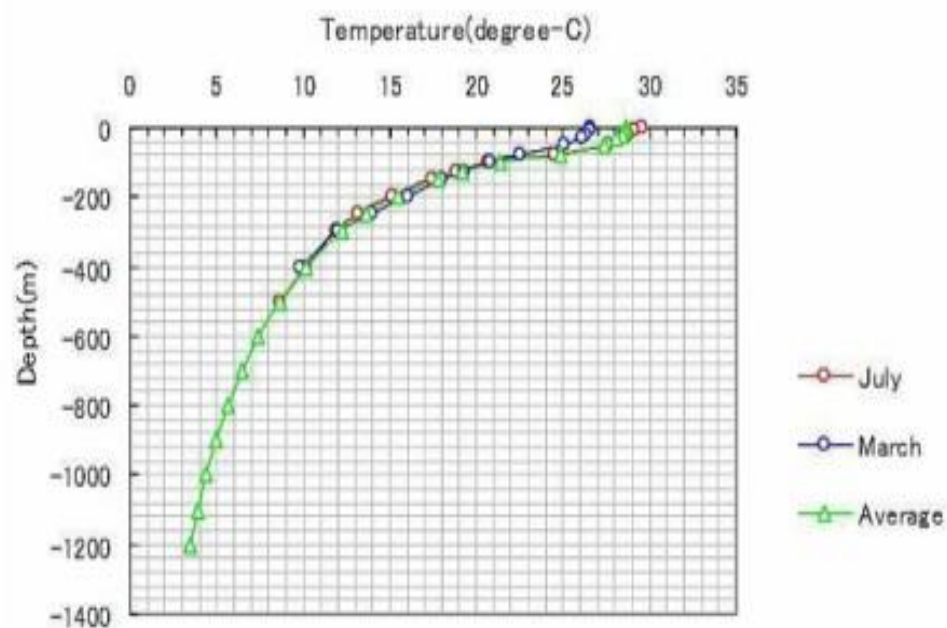
Figure 1.5   The graph temperature versus depth at Sabah Trough [17]

1.1.4   Site Potential of Solar-OTEC (SOTEC) plant

This ocean thermal energy (readily available) not only has the potential of improving energy supply and consumption system in Malaysia and Thailand as well as assisting in carbon footprints reduction. Other spinoff activities include district cooling, temperate crop farming, mineral and fresh water production, aquaculture, lithium extraction, and a host of other activities are possible with the exploration of the ocean thermal energy [18, 19]. Apart from electricity generation, there are several potentials for other co-products such as mariculture, district cooling and temperate crop farming (with chilled water), lithium extraction, etc. of technology. In general, the deep ocean temperature ranges between $1 - 7$ °C, depending on the depth. Currently, ocean thermal energy conversion technology would require a temperature difference of 20 °C and above, therefore the potential of ocean thermal energy conversion is also a function of ocean depth. Figure 1.6 shows the potential site of SOTEC, an area located in the Malaysia-Thailand Joint Authority Development Area (MTJDA), overlapping continental shelf area of 7,250 square kilometers and being claimed by both Malaysia and Thailand. This territory is located in the lower part of the Gulf of Thailand close to the South China Sea. In 1979, both nations have consented to jointly investigate and exploited non-living regular assets for the common and approach advantages of the two nations.

The objective of the Research Chess Fund is to support any research and development in the field of science and technology relating to either exploration or exploitation of petroleum or natural resources for the Joint Development Area (JDA). (Regulation 7, Part IV Malaysia-Thailand Joint Authority (Payments of Royalty and Other Proceeds from Petroleum Production to the Governments) Regulations 2004). Besides exploring and producing oil and gas, MTJDA has yet to explore other non-living resources, especially the renewable energy resources including ocean thermal energy. The UTM-OTEC team has proposed a research and development project to MTJDA where the technology of solar-assisted thermal energy generation for the current state of ocean thermal energy conversion to electricity be utilized. Besides, that various engineering tests will be conducted for any advancement in heat-exchange or working fluids by deploying nano-materials/nano-technologies and

further tests on the application of membrane technology for the production of mineral water from the 'shallow sea'. Interest by MTJDA party on the idea is encouraging, but the results of this project is still pending and under discussion between both party.
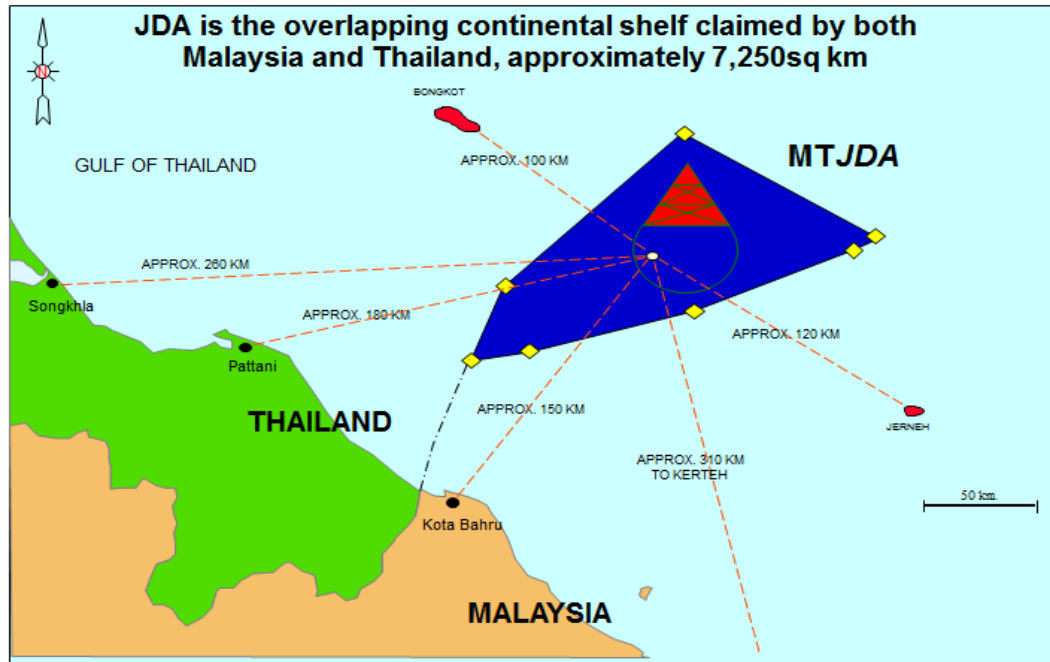
Figure 1.6   Malaysia-Thailand Joint Development Area (MTJDA) [20]

1.2   Problem Statement

The electric power industry is playing an important role in Malaysia's economic development and electricity supply has become a vital factor in sustaining the well-being of the people. The electricity generation in Malaysia is mainly from fossil fuel. However, burning of fossil fuels like coal, oil, gas or hydropower for producing electricity would create by-products such as CO_2, SO_2 and NO_2. They would then pollute when released into the environment, changing the planet's climate and harming ecosystems. Thus, it is necessary to consider the energy (non-renewable) especially in the framework of natural resources-economy-and the environmental analysis. Solar energy is a major renewable energy source with the potential to meet many of challenges facing the world. Solar is safe alternative which

can replace current fossil fuels like coal and gas for generation of electricity. Therefore, OTEC has become one of the productive solutions to maintain the environmental benign and sustainability. However, the main technical challenge in OTEC system is the presence of small temperature difference between hot surface sea water and cold deep sea water. The thermodynamic efficiency of the OTEC cycle typically lies between 3-5% with the need of huge amount of seawater flow rate [21, 22]. OTEC technology can only be operated with the minimum temperature difference of 20 °C where the cold seawater need to be withdrawn at 1000 m depth to get 4 °C as shown in Figure 1.5. In the Malaysia-Thailand Joint Development Area, the potential of using renewable energy is low, due to not only to low wind but also low wave action. Apart from that, the sea level is so shallow (55 m ~ 65 m) that no ocean thermal energy could be harnessed economically.

1.3 Objective of the Study

The objectives of the study are:

i. To develop a validated simulation model for a SOTEC system.

ii. To study the effect of operational parameters on the thermodynamic performance of SOTEC cycle.

iii. To identify the optimal design and operating parameters for 100 kW SOTEC system.

1.4 Scope of the Study

The scope of this study can be divided into several parts as listed below:

i. The propose SOTEC system is based on the mathematical and simulation study by using FORTRAN programming.

ii.   Reference power output for SOTEC cycle is 100 kW.

iii.   The designed OTEC system is considered as an illustrative base system that allows the thermodynamic analysis of its off-design operation when solar collector is integrated as an additional component.

iv.   The proposed SOTEC system will be validated by the thermodynamic performance of the same scale turbine power.

v.   The variable operational parameters are mass warm sea water flow rate, cold seawater flow rate and working fluid flow rate.

vi.   The analysis targets are based on thermodynamics and design aspects such the minimum warm seawater flow rate and optimum solar collector area to generate 100 kW turbine power.

vii.   The selection of the working fluid will be presented to optimize the system performance.

viii.   The study will be conducted based on the available solar data in Kota Bharu due to lack of accurate data at MTJDA.

1.5   Significance of the Study

Currently, with the high demand of electricity, it results in the need for sophisticated and green technology. The study of the performance of SOTEC is seen as one of the alternatives to fulfill the necessity of electricity in our daily life. Ocean thermal energy conversion cycle is the technology that makes use of the temperature difference between warm surface seawater and cold deep seawater (~1000m). Based on the previous study of OTEC cycle, the purpose of installing a solar collector is to increase the warm seawater surface temperature and create a larger temperature

differential. This results in improvement of the thermodynamic performance such as net power output and net Rankine efficiency. Although there has been numerous research conducted on the performance of SOTEC cycle, but there is still no study has been conducted at shallow sea water. At shallow seawater, OTEC technology can be implemented by installing the solar collector to boost the warm seawater temperature in order to maintain the temperature difference. This study can provide the readers as either as reference or guides in constructing SOTEC cycle at shallow seawater for offshore power supply.

CHAPTER 2

LITERATURE REVIEW

Energy plays a critical role in driving almost all practical processes and is essential to sustain life. Energy exists in several forms, e.g., light, heat, electricity. Concerns exist regarding limitations on easily accessible supplies of energy resources and the contribution of energy processes to global warming as well as various other environmental concerns as air pollution, acid precipitation, ozone depletion, forest destruction, and radioactive emissions. There are various alternative energy options to fossil fuels, including solar, geothermal, hydropower, wind and nuclear energy. The use of available natural energy resources is limited due to their reliability, quality and density.

2.1   Malaysian Energy Demand

Almost all the things that we use every day cannot either be made or used without energy. An important aspect of it is energy saving where it has been an elusive quest for many of us living in the urban developed cities. We do need energy for everything especially in our household. This is more so in this day and age that we live in, energy is the most important aspect of modern living and convening source. We use energy for everything, in our home and office basically for performing our daily tasks.

We have provided Table 2.1 on the Malaysia final energy demand by sources from the years 2010 until 2015. However, it should be noted that the current data is not available yet and as such the 2015 data presented in Table 2.1 is only based on estimated data as it was compiled before the end of 2015. For year 2010, the electricity demand was 8,993 kilo tonne of oil equivalent (ktoe) to 11,996 ktoe in 2015 with an estimated average annual growth rate of 5.9 %. The total energy demand for 2010 increased from 41,476 kilo tonne of oil equivalent (ktoe) to 53,222 ktoe in 2013 and for 2015 it is expected to increase to 57,123 ktoe. Thus, its average annual growth rate from 2011 to 2015 for all energy demand sources is expected to be 6.6 %. Final energy demand per capita increased from 1.5 toe/person in 2010 to 1.8 toe/person in 2013 and is expected to increase to 1.9 toe/person in 2015.

Table 2.1: Final Energy Demand, 2010-2015, 10th Malaysia Plan [23]

Final Energy Demand[1] by Sources, 2010-2015

Source	Kilo Tonne of Oil Equivalent[2] (ktoe)			% of Total			Average Annual Growth Rate (%)
	2010	2013	2015[e]	2010	2013	2015[e]	2011-2015[e]
Petroleum Products	24,403	29,132	32,389	58.8	54.7	56.7	5.8
Natural Gas	6,254	12,015	10,225	15.1	22.6	17.9	10.3
Electricity	8,993	10,536	11,996	21.7	19.8	21	5.9
Coal and Coke	1,826	1,539	2,513	4.4	2.9	4.4	6.6
Total	41,476	53,222	57,123	100	100	100	6.6
Final Energy Demand per capita (toe/person)	1.5	1.8	1.9				5.0

Notes: [1] Final energy demand refers to the quantity of energy delivered to final users including transformed energy
[2] One tonne oil equivalent to 7.6 barrels
[e] Estimates
Source: Energy Commission and Economic Planning Unit

Table 2.2 shows the final energy demand by sectors, for the years 2010-2015 and during the 10th Malaysian Plan. In realtion to sectors, transportation consumed 42.3 % and automatically dominated the total energy demand in year of 2013. This is due to the fact that most of the drivers preferred to drive their own vehicles instead of carpooling to protect their privacy, thus it is expected to increase the amount of energy consumption yearly. Though transportation conveys substantial socioeconomic benefits, but at the same time it does give negative impact to the environment. This is especially so in the urban areas, where transportation forms a

significant source of air pollutants, released gases such as NOx, carbon monoxide, hydrocarbon and lead. An alternative that can be used to minimize gas emission is by introducing fuel vehicles where it uses fuel cell instead of gasoline or diesel to power the motor vehicles. By using the fuel cell it can generate less CO_2 gas emission through renewable energy resources.

Table 2.2: Final Energy Demand by Sectors, 2010-2015, 10th Malaysia Plan [23]

Sector	Kilo Tonne of Oil Equivalent[2] (ktoe)			% of Total			Average Annual Growth Rate (%)
	2010	2013	2015[e]	2010	2013	2015[e]	2011-2015[e]
Transportation	16,828	22,522	23,535	40.6	42.3	41.2	6.9
Industrial	12,928	13,384	13,367	31.2	25.1	23.4	0.7
Residential and Commercial	6,951	7,378	10,339	16.8	13.9	18.1	16.4
Non-Energy	3,696	9,111	8,968	8.9	17.1	15.7	19.4
Agriculture and Forestry	1,074	827	914	2.6	1.6	1.6	-3.2
Total	41,476	53,222	57,123	100	100	100	6.6

Notes: [1] Final energy demand refers to the quantity of energy delivered to final users including transformed energy
[2] One tonne oil equivalent to 7.6 barrels
[e] Estimates
Source: Energy Commission and Economic Planning Unit

2.2 Malaysian Energy Supply

Primary energy is that energy found in natural environment such as coal, oil, natural gas and wood, nuclear fuels (uranium), the sun, the wind, tides, mountain lakes, the rivers (from which hydroelectric energy can be obtained) and the Earth heat that supplies geothermal energy. They can be used directly from the source through a transformation of primary energy; the secondary energy can be made. Electricity is a secondary resource and can be generated by a number of different primary sources. In Table 2.3, the primary energy supply in Malaysia shows its supply by sources from 2010 to 2015 and they derive from natural gas and crude oil which are expected to still remain as the main sources in 2017. This is by taking a look on the pattern. From 2010 to 2015, the total supply of energy increased from 76,809 ktoe to 95,802 ktoe. However, the total share of fossil fuels namely crude oil and natural gas as well as coal and coke declined in 2013, while the share of

hydropower had steadily increased. This change in the share of energy sources reflects the decreasing dependency on fossil fuel and can be regarded as a positive sign for renewable energy, though hydropower has steadily increased over time.

Table 2.3: Primary Energy Supply by Sources, 2010-2015 [23]

Primary Energy Supply[1] by Sources, 2010-2015

Sector	Kilo Tonne of Oil Equivalent[2] (ktoe)			% of Total			Average Annual Growth Rate (%)
	2010	2013	2015[e]	2010	2013	2015[e]	2011-2015[e]
Natural Gas	35,447	39,973	42,441	46.1	44.6	44.3	3.7
Crude Oil	25,008	31,877	29,507	32.6	35.6	30.8	3.4
Coal and Coke	14,777	15,067	20,118	19.2	16.8	21.0	6.4
Hydro	1,577	2,688	3,736	2.1	3.0	3.9	18.8
Total	76,809	89,605	95,802	100	100	100	4.5

Notes: [1] Primary energy supply refers to the supply of commercial energy that has not undergone a transformation process to produce energy
[2] One tonne oil equivalent to 7.6 barrels
[3] Natural gas excludes flared gas, re-injected gas and exports of liquefied natural gas
[e] Estimates

2.3 Malaysia Renewable Energy Supply

In 2011, the Renewable Energy Act was introduced and since 1 December 2011 the renewable energy (RE) development was enforced together with the Feed-in Tariff (FiT) mechanism. The system provides FiT approval holders, which include either individuals or companies eligible to invest in renewable energy sources such as solar power that can then be sold to the electricity grid. Sustainable Energy Development Authority (SEDA) has previously targeted 415.5 MW of RE out of total installed capacity based on approved FiT applications by 2014. However, based on figures dated 31 December 2014, only 243.4 MW was connected to the grid as shown in Figure 2.1. Through this initiative it was able to reduce GHGs emission by 432,000 $tCO_2eq.$ in 2013. There are many challenges in the RE industry, including reliability of RE plants, problems in securing adequate feedstock for long-term supply, lack of experts like RE project developers, financial personnel as well as service providers and difficulties in securing financing for RE installations. The current RE sources are mainly focused on biomass, biogas, mini hydro and solar

photovoltaic (PV) while new RE sources have not been explored extensively. In the 11th Malaysia Plan, the government has decided to enhance the utilization of RE sources by including ocean energy (OTEC). In addition, the RE capacity is expected to reach 2,080 MW by 2020, contributing to 7.8% of total installed capacity in Peninsular Malaysia and Sabah. The viability of ocean energy will be explored further in order to take advantage of Malaysia's geographical position of being surrounded by sea. In addition, the government has also encouraged the private sector to conduct training to increase the number of RE experts.

Renewable Energy Installed Capacity by Sources, 2014

Biogas 5%

Biomass 23%

Solar Photovoltaic 66%

Mini Hydro 6%
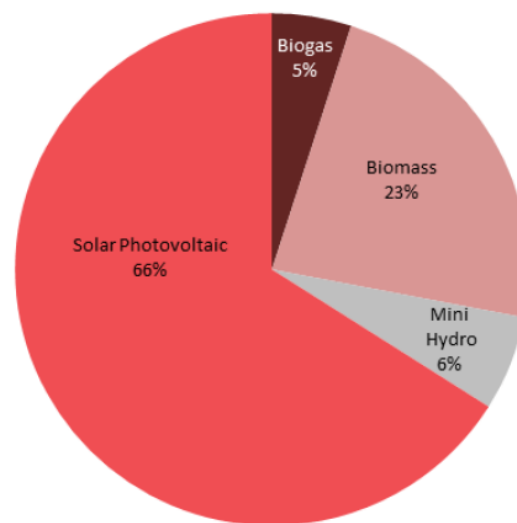
Total installed capacity in 2014: 243.4 MW

Source: Sustainable Energy Development Authority

Figure 2.1   The capacity installed from renewable energy by sources, 2014 [23]

2.4   Global Potential of Ocean Energy

For the most part, renewable energy can be characterized as the energy that originates from assets which are normally recharged, for example, sunlight, wind, rain, tides, waves, and geothermal heat. However, not all renewable energy is green and zero CO_2 emission except for power generation from ocean energy source which uses a green renewable energy method. Two sorts of energy can be delivered from

ocean energy and they are thermal energy from the sun's heat and mechanical energy from the tides and waves [24]. The source of thermal energy is fairly constant while tidal and waves are an intermittent source of energy. Though the source of mechanical energy is free but it is not available 24 hours per year like thermal energy which is OTEC. In Figure 2.2, total recoverable reserves are shown for the finite resources such as fossil fuel and nuclear resources. In considering global demographical and economical expansion trend, by year 2040 the global energy demand is estimated to increase by 30% or more, making fossil fuels duration to last a lot shorter [26]. The spheres in the middle represent the annual potential of renewable energy sources. As we can see from the figure, the total energy of wind, OTEC, biomass, hydro, geothermal, waves, currents, salinity gradient and tidal energy is only covered a small amount of the solar energy potential for a year. Despite that, due to unlimited availability of the ocean's thermal resource, OTEC is capable of generating electricity day and night throughout the year, providing a reliable source of electricity. This provides a great advantage over intermittent renewable technologies such as solar and wind.
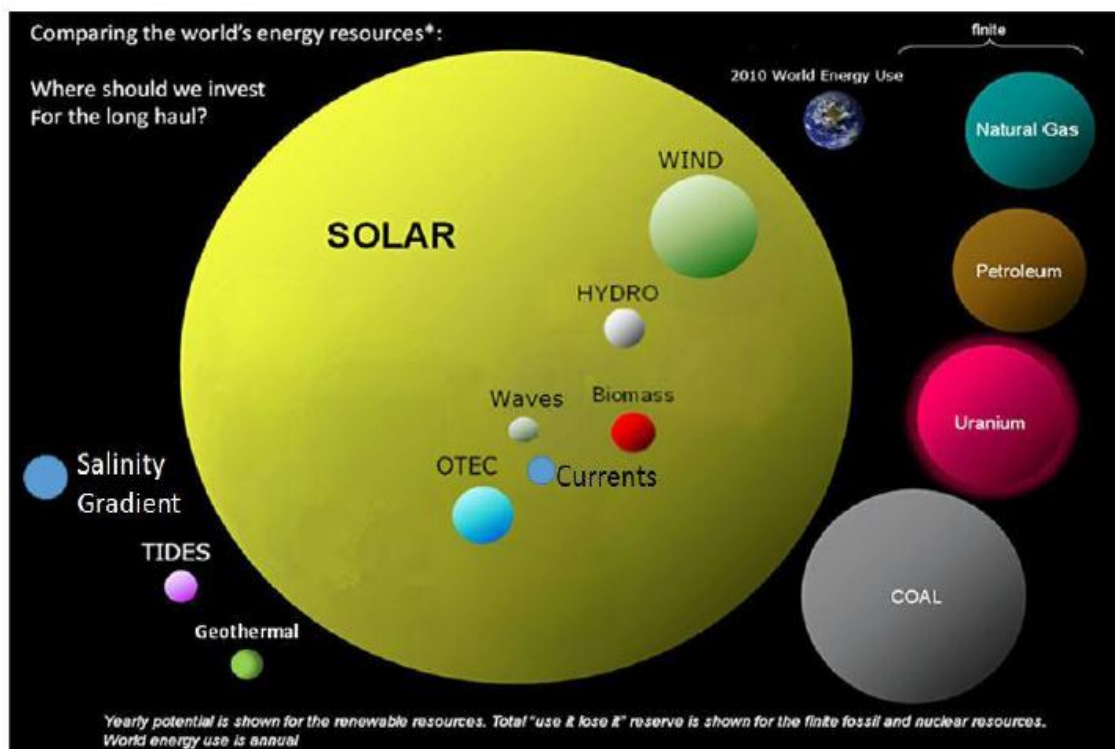
Figure 2.2 Global Sources of Energy, Renewable and Non-renewable, in perspective [25]

2.5 Ocean Thermal Energy

Ocean Thermal Energy Conversion (OTEC) is a process that can produce electricity by using the temperature difference between deep cold ocean water and warm tropical surface waters deeper layers beneath to drive the turbine. Therefore, we do not need to create a difference in temperature by burning fuel because a temperature gradient exists in the oceans naturally. An OTEC plant pumps large quantities of deep cold seawater and surface seawater to run a power cycle and produce electricity. It is firm power (24/7), a clean energy source, environmentally sustainable and capable of providing massive levels of energy. Unlike other mechanical energy (wind; tidal energy) OTEC is a stable energy supply, due to all day availability of heat which is stored on the surface of the ocean. OTEC has been viewed as an attractive technology due to its vast potential and benefits. In 1881, OTEC was introduced by D'Arsonval, other experts proclaimed that the idea would never become a reality because of the plant size and economics of developing an off-shore facility that could afford and efficiently generate significant power. But the tide is finally turning as the high cost of fossil fuels, the push toward renewable energy and advances in ocean technology are bringing OTEC's boundless power potential closer to reality than ever before. Recently, higher electricity costs, increased concerns for global warming, and a political commitment to energy security have made initial OTEC commercialization economically attractive in tropical island communities where a high percentage of electricity production is needed. Table 2.4 shows the largest operating tidal energy; Sihwa Tidal Plant and operating the Jiang Xia Power Plant. Unfortunately, due to unstable power supply the actual electricity generation was able to produce less than half of the installed capacity of the turbine power.

Table 2.4: Tidal Energy Power Plant [27, 28]

Name of Power Plant	Sihwa Power Plant	Jiangxia Power Plant
Installed capacity	254 MW	3.2 MW
Annual power	552.7 GWh	6.5 GWh
Actual Power	63.09 MW	0.7 MW

Table 2.5 (a) shows the first successful at-sea closed-cycle OTEC operation on board the Mini-OTEC, in Keahole Point, Hawaii and has been in operation for three months since it started operation in 1979. Due to various processes that must be performed on the ship in order to produce energy and transfer it, the net power output was around 15 kW. It was built at the Natural Energy Laboratory of Hawaii Authority (NELHA) mainly to demonstrate the concept. Table 2.5 (b) is the demonstration of an OTEC plant located in Kumijema Island, Okinawa, Japan. This facility operates daily except for public holiday. This plant has started its operation since April 2013 and the research is being conducted by Saga University, Japan. Table 2.5 (c) shows a 105-kilowatt project that cost about $5 million to construct which is the world's largest plant to date utilizing the evolving renewable source. It was funded by the U.S. Navy's Office of Naval Research, Hawaii Natural Energy Institute and Makai. Table 2.5 (d) shows the 100,000 litres per day (Low-temperature thermal desalination) LTTD plant which successfully conducted by National Institute of Ocean Technology, Chennai, India (NIOT). It has carried out extensive laboratory studies and set up the first land-based demonstrative plant at Kavaratti in Lakshadweep with a capacity of 100,000 litres per day. A long high density polyethylene (HDPE) pipe was deployed in a special configuration successfully. The plant has been running continuously since 2005 fulfilling the needs of the 10,000 strong local communities. Currently, 200 kW power OTEC

project is being set up by NIOT to power a desalination plant. It is still in design phase and expected to be commissioned early 2019[29].

Table 2.5: OTEC Energy Power Plant

(a) 15 kW closed cycle Mini-OTEC plant, Hawaii [30]	
(b) OTEC plant, Okinawa Japan [22]	
(c) 105 kW OTEC Energy Power Plant, Hawaii [31]	
(d) 100,000 litre per day LTTD plant at Kavaratti, Lakshadweep Islands [32]	

2.6   Principle of OTEC Cycle

The working principle of OTEC power plant is actually very simple. It is when warm water on the surface of the ocean is collected and pumped by warm seawater pump. Then, the water is pumped through the boiler/evaporator and the water vapor is used to heat ammonia, the working fluid. The ammonia vapors then extend through a turbine combined with a generator to produce power. To ensure the ammonia vapor return back to a liquid state, cold water from the deep ocean water is pumped into the condenser to cool the working liquid. The fluid is pumped back into the evaporator. The net power of the system is counted by the turbine power minus the specific energy consumption from all pumps. There are three types of OTEC design namely closed cycle, open cycle and hybrid cycle.

2.6.1   Closed-cycle OTEC

Closed Cycle OTEC D'Arsonval's original concept employed a pure working fluid that would evaporate at the temperature of warm sea water [10]. The vapor would subsequently expand and do work before being condensed by the cold sea water. This series of steps would be repeated continuously with the same working fluid, whose flow path and thermodynamic process representation constituted closed loops hence, the name 'closed cycle'. In closed-cycle OTEC, ammonia is filled inside the closed loop of the pipeline and is chosen because of its low boiling point (-33°C or 28 F) and has higher efficiency due to high sensible heat. The specific process adopted for closed cycle OTEC is the Rankine, or vapor power, cycle. Figure 2.3 shows a simplified schematic diagram of a closed cycle OTEC system. The principal components are the evaporator, condenser,turbine and pump. There are additional devices not included such as separators to remove residual liquid downstream of the evaporator and subsystems to hold and supply working fluid lost through leaks or contamination. In this system, heat transfer from warm surface sea water occurs in the evaporator, producing a saturated vapor from the working fluid. Electricity is generated when this gas expands to lower pressure through the turbine. Latent heat is transferred from the vapor to the cold sea water in the condenser and the resulting liquid is pressurized with a pump to repeat the cycle.
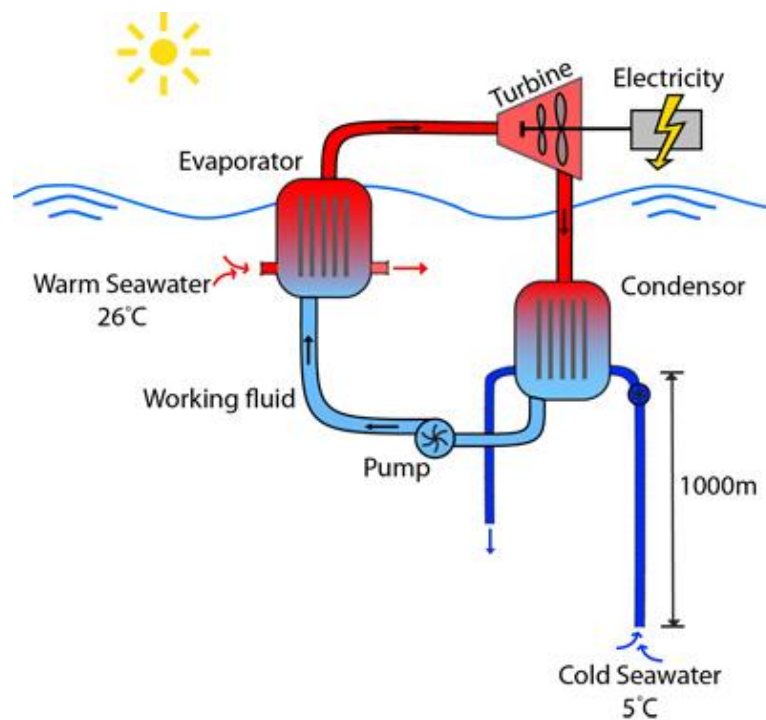
Figure 2.3   Schematic diagram of closed-cycle OTEC [33]

2.6.2 Open Cycle OTEC

The working principle of open cycle OTEC is very similar to that of closed cycle. Its only difference is that an open cycle does not use intermediate fluid or working fluid. Figure 2.4 shows the schematic diagram of open cycle OTEC system whereby the seawater itself is used to provide the thermodynamic fluid. Warm seawater is expanded rapidly into low-pressure vapor in a partially evacuated chamber where some of it 'flashes' to steam. This steam is then used to drive a steam turbine. The vapor produced by flashing warm seawater is at a relatively low pressure so it requires a very large turbine to operate effectively. Then, the expanding steam drives a low-pressure turbine attached to an electrical generator. The steam, which has left its salt behind in the low-pressure container, is almost pure fresh water. From the exhaust of the turbine, the vapor is condensed back into a liquid by exposure to cold temperatures from deep-ocean water.
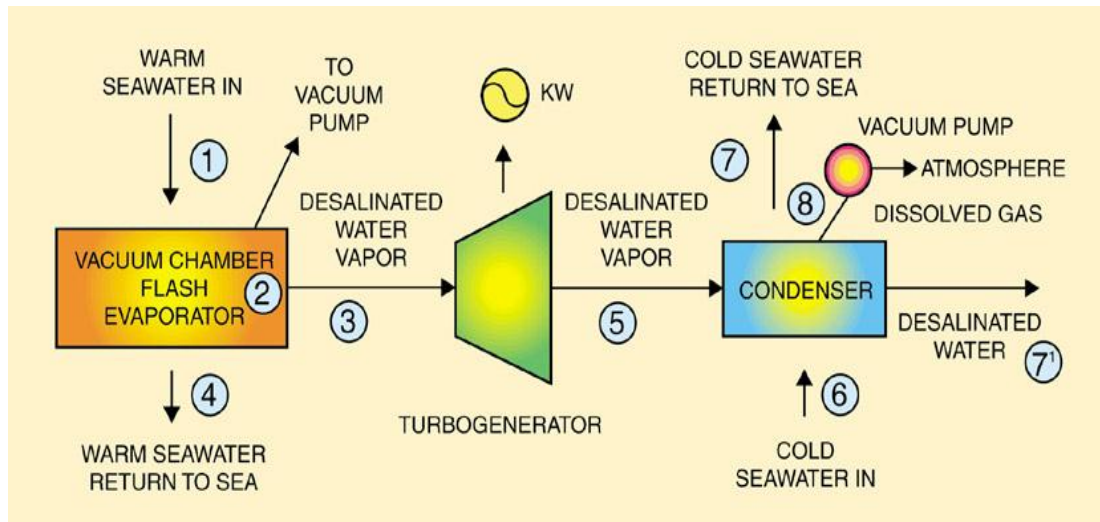
Figure 2.4   Schematic diagram of open-cycle OTEC [34]

2.6.3   Hybrid Cycle OTEC

In a hybrid system it combines the features of both the closed-cycle and open-cycle systems as shown in Figure 2.5, whereby warm seawater enters a vacuum chamber where it is flash-evaporated into steam, similar to the open-cycle evaporation process. The steam vaporizes a low-boiling-point fluid (in a closed-cycle loop) that drives a turbine to produces electricity. When the steam is condensed within the heat exchanger, the desalinated water is generated.

Figure 2.5   Schematic diagram of hybrid-cycle OTEC [35]

2.7   Solar Energy

Solar energy is an energy provided by the sun in the form of solar radiation that can be harnessed to generate electricity. Its source is free and available as long as the sun exists but with limitations in that at night time and on cloudy days where no sun is present [36]. However, during the day time, solar energy can be used again and again and might be stored in a thermal storage. Consistent and constant power supply makes solar energy useful to harness the power in remote locations [37]. Generally, it requires not much maintenance and can survive for a long time. There are no recurring costs within 10 years - 15 years [38].

2.7.1 Flat Plate Solar Collector

The normal solar collector utilized for sunlight based water warming as part of homes, structures and sun powered space warming is a flat plate collector. An average flat plate collector is a protected metal box with a glass fiber or plastic spread (called the glazing) and a dark-colored absorber plate. The absorber plate consists of an assembly of copper sheet and copper tubing. Basically, these solar collectors can heat liquid or air at temperatures less than 80°C [39]. The liquid is heated by an external source and this mechanism is called a force convection [40]. In fact, about 50% of solar heat industrial application demands for 80-160°C [41]. There are several advantages that makes flat plate solar collector was selected compared to evacuated tube collector as stated below:

i. Flat plate collector gives better performance than evacuated tube collector.

ii. For the common hot water application, flat plate collector is more efficient at delivering temperature.

iii. Flat plate collector is less expensive and gives more energy per dollar spends than evacuated tube collector.

iv. Flat plate collector usually uses thick tempered glass while evacuated use thinner glass which is easy to breaking and need to be replaced.

Great effort has been made on the development of solar energy such as an advancement of several subsystem: solar energy collectors, heat-storage containers, heat exchangers, fluid transport and distribution systems, and control systems[39]. One of the major components is a solar collector. The solar radiation from the sun strikes the surface of glazing and converting it into heat. The heat is transferred to a fluid (water in this study) flowing through the collector by force convection. The warmed liquid conveys the heat either straightforwardly to the boiling hot water or space conditioning equipment or to a capacity subsystem from which can be drawn for use around evening and on shady days. A typical configuration of flat plate solar collector is shown in Figure 2.6.
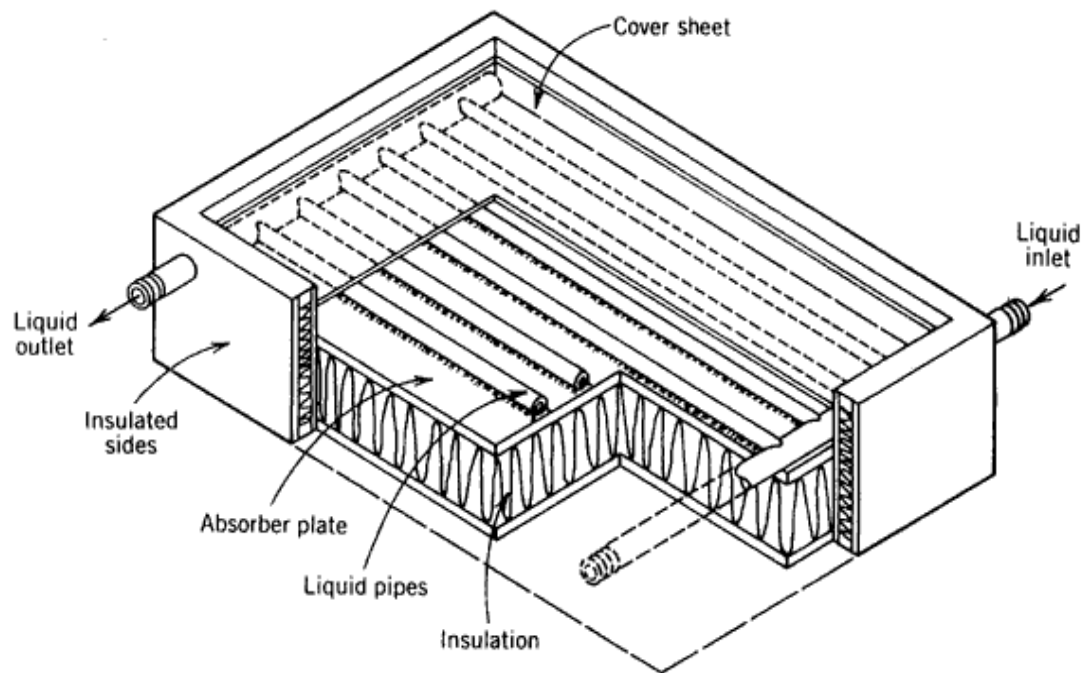
Figure 2.6   A typical liquid Flat Plate Collector [39]

2.7.2   Global Solar Radiation in Malaysia

Solar radiation is the radiation or energy that we get from the sun. It is also known as a short-wave radiation and comes in many forms, such as visible light, radio waves, heat (infrared), x-rays, and ultraviolet rays. Measurements for solar radiation are higher on clear, sunny day and usually low on cloudy days. When the sun is down, or there are heavy clouds blocking the sun, solar radiation is measured at zero. The monthly mean daily values of global solar radiation in Kuala Terengganu, Kuching, Kota Kinabalu and Kota Bharu are shown in Table 2.6.

Table 2.6: Montly mean daily values of global solar radiation for Kuala Terengganu, Kuching, Kota Kinabalu and Kota Baru [42]

Months	Global radiation (MJ/m^2/day)			
	Kuala Terengganu	Kuching	Kota Kinabalu	Kota Bharu
January	17.91	12.02	17.71	16.26
February	21.60	13.35	19.36	17.72
March	21.40	15.39	20.97	19.72
April	23.64	13.07	21.64	19.74
May	20.34	13.42	20.16	18.23
June	17.42	16.28	19.11	17.10
July	19.43	16.57	19.41	17.17
August	19.15	15.14	19.44	17.42
September	20.20	15.79	18.20	18.12
October	16.40	15.23	19.21	17.09
November	16.24	14.92	18.08	13.28
December	13.38	12.56	18.00	12.15
Annual Average	18.92	14.48	19.27	17.00

As the solar radiation data in MTJDA area is difficult to obtain, the global radiation data of Kota Bharu is selected among them since it is nearer to that potential area. Table 2.7 shows the average monthly seawater temperature in Kota Bharu.

Table 2.7: Average monthly seawater temperature in Kota Bharu [43]

Months	Temperature (°C)
January	26.7
February	27.9
March	29.8
April	29.5
May	29.9
June	29.2
July	27.9
August	29.1
September	29.1
October	29.2
November	27.1
December	27.1

2.8 Development in OTEC Technology

A lot of effort has been made in relation to ocean thermal energy conversion since it was first proposed by French physicist D'Arsonval in 1881. Due to the small temperature difference, the main technical challenge faced by OTEC is its low energy conversion efficiency which can be defined as net power divided by generated power. In a typical OTEC plant, the net power efficiency is between 50-80% of the system. Numerous extensive exploration efforts have been made to enhance the performance of the OTEC system. Subsequent to the 1980s, extensive research efforts have been made in two directions to enhance the performance of the OTEC system [44]. The first research area was aimed at increasing the efficiency of OTEC cycle by thermodynamic optimization [10, 44, 45]. Yeh et.al has theoretically investigated the dependent parameter on the net power output of OTEC to generate a maximum net power[44]. The optimization of a closed-cycle OTEC system was studied with the plate type heat exchanger using ammonia as working fluid by the Powell method [10]. However, OTEC power plants demand huge initial construction costs e.g., ~ $ 1.6B for a 100 MW OTEC power plant [28] because of the need for huge seawater mass flow rates and corresponding heat exchanger and seawater piping sizes. It would be more economically feasible if solar thermal collection is added on top of the existing power-generating and piping components to improve OTEC system.

Another research direction to be taken is towards an increase of temperature differences between the surface and deep seawater by utilizing renewable energy or waste heat sources, such as solar energy [9], geothermal energy, or waste heat of a nuclear power plant [44]. Among them, solar energy has been considered to be the most appealing renewable energy source that could be integrated with OTEC due to the ever-growing solar technology and its minimal adverse impacts to the environment. Yamada et al. [9, 44] numerically investigated the feasibility of incorporating solar energy in order to preheat the seawater in OTEC, demonstrating that the net efficiency can increase by around 2.7 times with solar preheating. In addition, recent studies have also suggested the direct use of solar energy for reheating of the working fluid to enhance the OTEC performance [9, 44, 45]. These

studies have focused on the design of solar-boosted OTEC systems, suggesting the construction of a new power plant operating at a much higher pressure ratio than the conventional OTEC system. This has been reported by Pouri et.al in the exergy and energy analysis of hydrogen production in a solar preheated OTEC cycle. Tong et.al studied the performance of CC-OTEC system with the additional solar collector at the outlet of the evaporator. They have managed to determine the most suitable working fluid and found that the appropriate net power of the cycle should be at least 50 kW [45]. This research focused on the effect of solar radiation on the exergy destruction rate and exergy efficiency [46]. Yamada et.al has carried out the simulation of 20 K and 40 K boosted temperature at the inlet of the evaporator by preheated solar to generate 100 kW of SOTEC plant and investigating the solar collector area needed at different types of solar collector[22]. Straatman and Van Sart [47] experimented using a variation of the OTEC where it is combined with an offshore solar pond which they had referred to as a hybrid system(OTEC-OSP). Aashay Tinaikar et.al [48] utilized a superheated and preheated black metallic plate of aluminium which were used to compensate the heat losses in the heat exchanger. This study also lists out the benefits and drawbacks from the proposed OTEC plant. Besides the Rankine cycle, two more types of OTEC cycles namely Uehara [49, 50] and Kalina [51, 52] cycles. Both of them are also suitable for large scale OTEC plant in the order of 4 MW or higher. These researchers has focused on the performance of solar-boosted OTEC systems, suggesting the construction of a new power plant operating at a much higher pressure ratio than the conventional OTEC system.

2.9   OTEC Plant

There are several types of the OTEC cycle namely, an open cycle, close cycle and hybrid cycle. Figure 2.7 shows the location of completed, in development, planned and proposed OTEC projects around the world. During the 70's and 80's countries like the United States, Japan, and several other countries began experimenting with OTEC systems in an effort to bring this technology into reality. It has been established that Malaysia has the capacity to generate power from OTEC

with the heat stored in the deep waters (over 700 meters in depth), covering a total area of 131,120 square kilometers, off the states of Sabah and Sarawak.
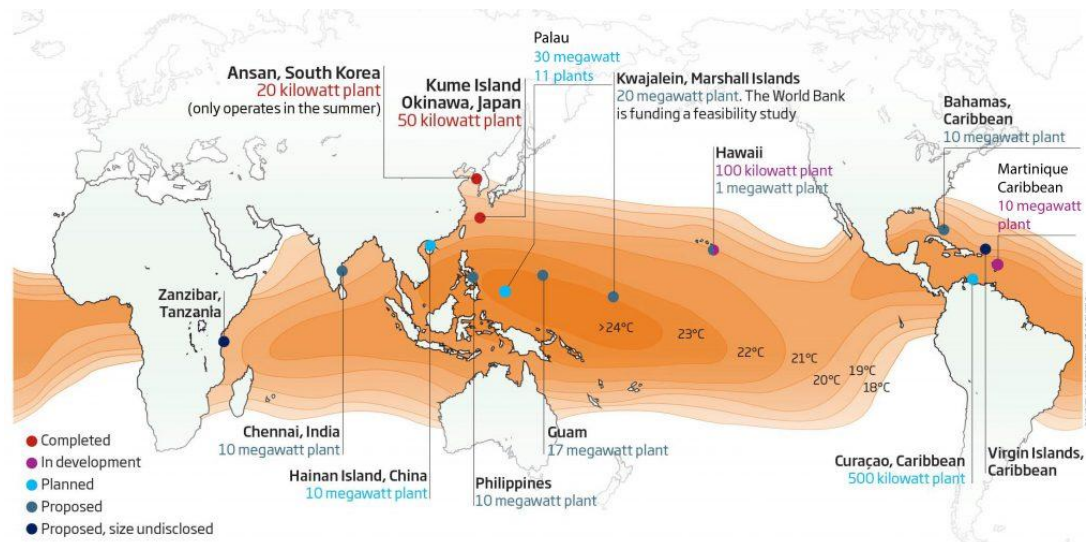
Figure 2.7   Completed, in development, planned and proposed OTEC plant around the world [35]

2.10   Conclusion

Electricity output in Malaysia is generated primarily from burning limited fossil fuel resources such as oil, coal or natural gas that have huge consequences for the environment. The government faces multi-dimensional challenges in its role to deliver reliable and affordable electricity supply to consumers as well as to support national development objectives. One of the key challenges is strong public concerns about the issues of environment due to overdependence on fossil fuels and moderate growth in renewable energy. Until 2015, Malaysia's total energy supply (95,802 ktoe) can still support the energy demands (57,123 ktoe) however, its main source of primary energy supply is still dependent on fossil fuel (natural gas and crude oil). As can be seen in Table 2.1, Malaysia's energy demand from 2010 to 2015 has increased and is expected to increase further in the future due to population

growth and sector demands (transportation, industrial, residential and commercial and etc.). It should be noted that fossil fuel is finite, by considering global demographical and economical expansion trend, thus making fossil fuels duration last a lot shorter. The decline in the total share energy supply (natural gas, crude oil, coal and coke as well) shows that renewable energy has to play a greater role in reducing the dependency of fossil fuel as primary energy supply. In the Eleventh Malaysia Plan, 2016-2020, the government continuously supports energy security and renewable energy in order to sustain the energy resources. Renewable energy has emerged as another alternative to support a continuous increase in energy demand. OTEC, a renewable energy source is seen to be the productive solution to support energy demand and maintain an environmental friendly world.

The ocean being its source is relatively abundant and is continuously being restored as long as the sun shines and natural current exist. Abundance of cold seawater flow rate is required to condense the working fluid by constructing a pipeline of approximately 1000 m in depth so as to reach 4°C. Getting water from the depths of the ocean is a difficult engineering challenge. However, at the location where the sea level is so shallow, no ocean thermal energy could be harnessed economically. In the absence of the required depth, an alternative such as a solar collector can be another opportunity to boost the sea surface temperature in order to maintain the required temperature difference for maximum efficiency of power conversion. The sun is the ultimate source of almost all kinds of energy on earth, either directly or indirectly. A typical flat plate solar collector is seen to be the most suitable selection to transform radiation from the sun into heat and transfer that heat to a fluid. Therefore, with the existence of solar collector, OTEC cycle can also be implemented in shallow sea water with an effective collector area to achieve a specific desired temperature difference without the need for constructing a long pipe.

Previous researches only focus on improving thermodynamic performance by increase the temperature difference between hot and cold seawater. Until now there still no SOTEC study has been conducted at shallow seawater where the required temperature difference 20 °C is absent. In the area where sea level is so shallow

(55~65m) such as MTJDA, ocean thermal energy could be harnessed economically with the existence of solar collector.

CHAPTER 3

METHODOLOGY

This chapter will discuss on the mechanism and theoretical approach to calculating the design point analysis for the gross power of 100 kW SOTEC system with 40°C boost inlet warm seawater temperature. In previous studies that were conducted, they were based on performance of SOTEC cycle in deep water where the cold seawater was withdrawn at 1000 m of around 4°C to boost the system performance. However, in this study, the SOTEC cycle will be designed in shallow sea water where its cold seawater will be taken from the surface of ocean. As long as the solar collector is be able to increase the warm seawater inlet temperature and create 20°C temperature difference between hot and cold seawater, the OTEC technology can be implemented in shallow water without the need for an installation of long cold pipeline. The simulation study is aimed at finding the optimization of the SOTEC cycle at shallow water and to find the design point of the cycle to achieve gross power of 100 kW. The process of determine the thermal conductance, solar collector area, size pipe diameter and type of working fluid will also be covered. The simulation model, process flow chart and system diagram will be included to boost the understanding of the system. Due to the difficulty of getting the solar radiation data at MTJDA area, the data of solar radiation will be referred to the nearby area which is at Kota Bharu (Refer Table 2.6).

3.1   Simulation Model of OTEC Cycle

Figure 3.1 shows the schematic diagram of closed Rankine cycle. Figure 3.1 (a) is the conventional OTEC system to generate electricity. In this study, Figure 3.1 (b) shows the method proposed for the installation of the solar collector at the inlet of the evaporator to preheat the warm seawater before entering the evaporator. These figures show the general arrangement of the heat exchangers, pumps, piping, turbine generator and solar collector. This system will be conducted in shallow sea water where cold seawater intake is on the surface of ocean. In Figure 3.1 (b), the warm sea water is pumped from the ocean surface and is heated by a solar collector; then the working fluid is heated and evaporated through the evaporator. A closed-cycle system is chosen to perform in SOTEC system because it is more compact than an open-cycle system and can be intended to deliver the same amount of power. Due the partial vacuum condition in open cycle it is vulnerable to the air leakages and noncondensable gasses. As consequences, some powers are required to pressurize and remove the gasses [33]. Furthermore, the specific volume of the low-pressure steam is very large compared to the pressurized working fluid used in the closed cycle system. Therefore the components must have large flow areas to ensure that steam flow does not reach a high enough velocity which could damage the turbine. Basically, a flat plate solar collector can heat liquid at temperatures less than 80°C. As previously mentioned, to generate power using existing OTEC technologies, the difference in temperature between cold and warm seawater has to be at least 20 °C. In this proposed study, we aimed to boost an additional 20°C from its minimum temperature makes the system is created to boost 40°C by solar collector. In this simulation study, an organic Rankine cycle is assumed to identify the theoretical thermal efficiency of the Rankine cycle and the numerical study will be conducted by using FORTRAN programming. Figure 3.2 shows the flow chart of the process involved in this study.

(a)

(b)
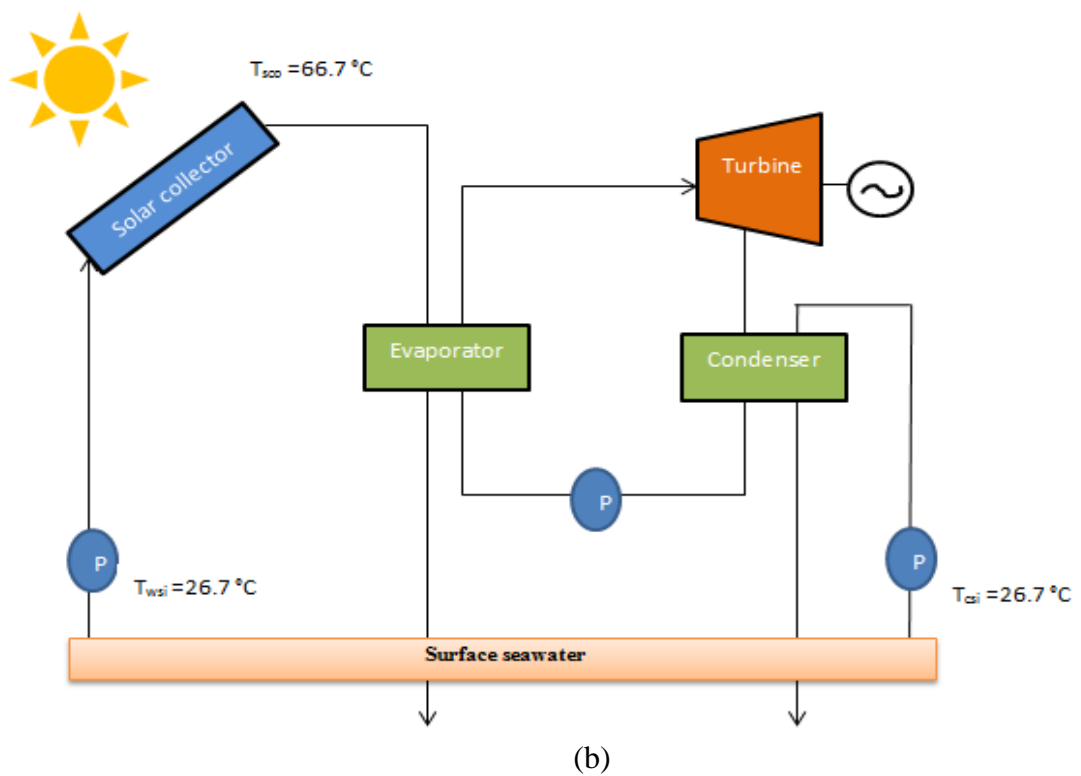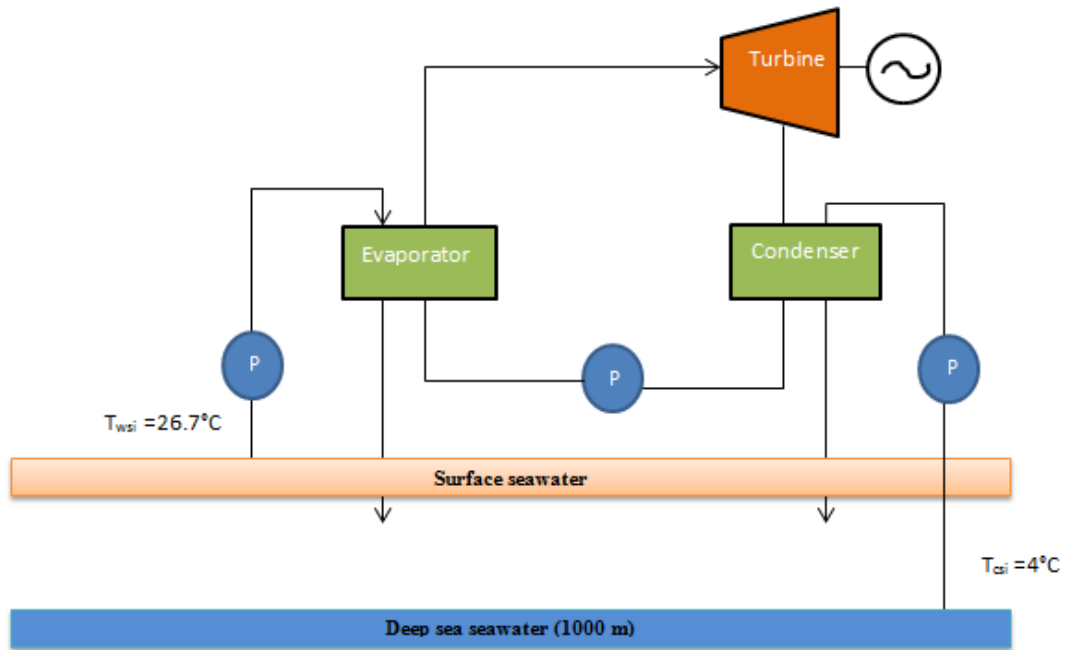
Figure 3.1   Schematic diagram of closed Rankine cycle (a) Conventional OTEC (b) Proposed SOTEC

```
                        ┌─────────────────────┐
                        │  Objective and scope │
                        │     of the study     │
                        └─────────────────────┘
                                   │
                                   ▼
┌──────────┐              ┌─────────────────┐              ┌──────────────┐
│ OTEC     │ ══════▶      │ Literature review│      ◀══════ │ Ocean energy │
│ Solar    │              └─────────────────┘              │ Previous     │
│ energy   │                       │                       │ OTEC Study   │
└──────────┘                       ▼                       └──────────────┘
                        ┌─────────────────────┐
                        │ Identify the data    │
                        │ collection and       │
                        │ methodology          │
                        └─────────────────────┘
                                   │
                                   ▼
┌────────────┐            ┌─────────────────────┐          ┌──────────────┐
│ Temperature│            │ Identify the         │          │ Flat plate   │
│ Salinity   │ ═════▶     │ operating and        │  ◀═════  │ solar        │
│ Flow rate  │            │ design parameter     │          │ collector    │
│ Pressure   │            └─────────────────────┘          └──────────────┘
└────────────┘                     │
                                   ▼
                        ┌─────────────────────┐
                        │  Developing method   │
                        └─────────────────────┘
                                   │
                                   ▼
                        (       Start        )
                                   │
                                   ▼
                        ╱────────────────────╲
                       │ Input operating and   │◀┄┄┄┄┄┄┐
               ┌──────▶│ design parameter      │       ┆
               │       │ (equation)            │       ┆
               │        ╲────────────────────╱        ┆
               │                  │                   ┆
        NO     │                  ▼                   ┆
               │          ◇ Analyse ◇                 ┆
               └──────────◇         ◇                 ┆
                           ◇       ◇                  ┆
                              │  YES                  ┆
                              ▼                       ┆
                          ╱ Output ╱┄┄┄┄┄┄┄┄┄┄┄┄┄┄┄┄┄┘
                              │
                              ▼
                         (   END   )
```

┄┄┄┄┄▶   Repeat step with various operating parameter condition

Figure 3.2   Process flow chart

3.2 Initial Condition and Assumption

Table 3.1 shows the piping condition for the system applied in the simulation study. Firstly, the warm seawater inlet will be pumped into solar collector and it is assumed to be boosted by 40°. The cold seawater inlet temperature is 26.7°C which is the lowest average seawater temperature at Kota Bharu as in Table 2.7. Overall heat transfer coefficient of the evaporator can reach 4000- 4500 W/m^2°C and 3800-4500 W/m^2°C for condenser when using ammonia as the working fluid [53]. The plate type heat exchangers is a simple and compact in size. Due to less maintenance fee and more overall heat transfer coefficient, plate heat exchanger was chosen instead of shell-tube heat exchanger [54].

Table 3.1: Piping condition for the simulation

Parameter	Value
Warm seawater pipe	
Length	50 m
Diameter	0.6 m
Cold seawater pipe	
Length (shallow sea water)	50 m
Diameter	0.6 m
Plate-type heat exchanger (as evaporator and condenser)	
Plate length	4.0 m
Clearance on seawater side	5 mm
Clearance of working fluid side	5 mm

The plant model used simplifying assumptions on heat exchanger and the constant overall heat transfer coefficient for evaporator and condenser were assumed as in Table 3.2. The components of the OTEC cycle illustrated in place in Figure 3.1 (b) are shown schematically with additional piping information in Figure 3.3 specifying the variables parameters.

Table 3.2: Input parameters to model 100kW SOTEC system

Parameter	Value
Turbine efficiency, η_T	0.85
Generator efficiency, η_G	0.96
Efficiency of all pumps, (η_{WSP}, η_{CSP}, η_{WFP})	0.85
Evaporator (plate-type heat exchanger) Overall heat transfer coefficient, U_E	4300 W/m^{2}K
Condenser (plate-type heat exchanger) Overall heat transfer coefficient, U_C	4000 W/m^{2}K
Flat plate Solar Collector Tilt angle Azimuth angle	30 ° 0 °
Sea water inlet temperature Warm sea water, T_{wsi} Cold sea water, T_{csi}	26.7 °C 26.7 °C
Ambient temperature, T_a	25 °C

3.3   Equations for Simulation

The equations for simulation follow the construction model of SOTEC plant as in Figure 3.3.

3.3.1   Organic Rankine Cycle

In the evaporator, the working fluid is evaporated to a saturated vapor by receiving heat from the warm seawater. The energy balance equation, Q_E at each side of the evaporator can be written as in Equation 3.1.

$$Q_E = m_{ws}\, c_{p,ws}\, (T_{wsi}\text{-}T_{wso}) = m_{wf}(h_1\text{-}h_4) \qquad (3.1)$$

The value of working fluid, which in general is a function of pressure and vapor quality during phase change, can be determined from PROPATH. Overall, the heat transfer coefficient and effective surface area of the evaporator correlates with the heat addition rate as shown in Equation 3.2.

$$Q_E = U_E A_E \Delta T_{lm,E} \qquad (3.2)$$

where $\Delta T_{lm,E}$ is the logarithmic mean temperature difference across the evaporator, and the effective thermal conductance $U_E A_E$ can be approximate as in Equation 3.3.

$$\frac{1}{U_E A_E} = \frac{1}{h_{wf} A_E} + \frac{1}{h_{ws} A_E} \qquad (3.3)$$

Basically the energy balance equation for the condenser is same like evaporator and written as in Equation 3.4.

$$Q_C = m_{cs} c_{p,cs}\, (T_{cso}\text{-}T_{csi}) = m_{wf}(h_2\text{-}h_3) \qquad (3.4)$$

The heat transfer area of the condenser can be defined as in Equation 3.5 below:

$$Q_C = U_C A_C \Delta T_{lm,c} \qquad (3.5)$$

The logarithmic mean temperature difference across the evaporator and condenser is correlated as in Equation 3.6 and Equation 3.7 respectively.

For condenser,

$$\Delta T_{lm,C} = \frac{T_{cso} - T_{csi}}{ln\frac{T_c - T_{csi}}{T_c - T_{cso}}}$$ (3.6)

For evaporator,

$$\Delta T_{lm,E} = \frac{T_{wsi} - T_{wso}}{ln\frac{T_{wsi} - T_E}{T_{wso} - T_E}}$$ (3.7)

3.3.2 Turbine Generator Power

The turbine generator can be calculated from the product of mass working fluid flow rate, m_{wf} and the adiabatic heat loss across the turbine. The equation is as in Equation 3.8 below:

$$W_{tur} = m_{wf}\eta_T\eta_G(h_2 - h_1)$$ (3.8)

where, η_T and η_G are the turbine isentropic efficiency and generator mechanical efficiency which assume as 0.85 and 0.96 respectively [55].

3.3.3 Warm Seawater Pumping Power

The warm seawater pumping power can be defined as in Equation 3.9.

$$W_{P,ws} = \frac{m_{ws}\Delta H_{ws}g}{\eta_{wsp}}$$ (3.9)

where ΔH_{ws} is the total head difference of the warm seawater piping, m_{ws} is mass warm seawater flow rate, g is gravitational acceleration, $9.18ms^{-2}$ and η_{wsp} is the

efficiency of the warm seawater pump. The cross sectional area of the main cold pipe can be determined as in Equation 3.10.

$$A_{ws} = \frac{\pi D_{ws}^2}{4}$$
(3.10)

where D_{ws} is the diameter pipe of cold seawater.The volumetric flow rate inside warm seawater can be calculated as in Equation 3.11.

$$Q_{ws} = \frac{m_{ws}}{\rho_{ws}}$$
(3.11)

where m_{ws} is the mass warm seawater flow rate and ρ_{ws} is density of warm seawater. Equation 3.12 shows the calculation of the flow velocity in the main warm seawater.

$$V_{ws} = \frac{m_{ws}}{A_{ws}\rho_{ws}}$$
(3.12)

The Reynold number in warm seawater diameter pipe can be calculated as in Equation 3.13 shows the equation of Reynold number.

$$Re_{ws} = \frac{\rho_{ws}V_{ws}D_{ws}}{\mu_{ws}}$$
(3.13)

where μ_{ws} is the viscosity of the warm seawater.The modified heat loss found in the warm seawater source pipe is due to friction and can be defined in Equation 3.14. The roughness for Glass-fiber reinforced pipes is assumed to be 0.003x10^{-3}m.

$$\Delta H_{ws,f} = \frac{f_{DW}V_{ws}^2(\frac{L_{ws}}{D_{ws}})}{2g\mu_{ws}}$$
(3.14)

where f_{DW} is the friction loss, L_{ws} is the warm seawater pipe length .The Reynold number in the plate heat exchanger at the evaporator calculated as in Equation 3.15.

$$Re_{ws} = \frac{\rho_{ws}V_{ws,PHE}D_{eq,ws}}{\mu_{ws}} \tag{3.15}$$

where, $V_{ws,PHE}$ is the velocity of warm seawater at the plate heat exchanger, $D_{eq,cs}$ is the equivalent diameter evaluated as in Equation 3.16.

$$D_{eq,ws} = 2\sigma \tag{3.16}$$

where σ is the clearance which assumed to be 0.005. The friction factor obtained from Taborek 1988 for 60°C chevron plate (heat exchanger design handbook) as defined in Equation 3.17.

$$f_{ws} = (4)(0.678)Re_{ws}^{-0.202} \tag{3.17}$$

Equation 3.18 shows the head loss in the plate heat exchanger at the condenser.

$$\Delta H_{cs,PHE} = \frac{f_{ws}V_{ws,PHE}^2(\frac{L_{ws}}{D_{eq,ws}})}{2g} \tag{3.18}$$

The pressure difference caused by the density difference between the warm seawater surface and cold deep seawater calculated as Equation 3.19 [56]:

$$\Delta H_{ws,d} = L_{ws} - \frac{1}{\rho_{ws}}(\frac{1}{2}(\rho_{ws} + \rho_{cs})L_{ws}) \tag{3.19}$$

ΔH_{ws} is a total head loss of warm seawater piping [46] evaluated as in Equation 3.20.

$$\Delta H_{ws} = \Delta H_{ws,f} + \Delta H_{ws,PHE} + \Delta H_{ws,d} \tag{3.20}$$

3.3.4 Cold Seawater Pumping Power

The pumping power of cold seawater can be expressed as in Equation 3.21.

$$W_{P,cs} = \frac{m_{cs} \Delta H_{cs} g}{\eta_{csp}} \tag{3.21}$$

The cross sectional area of the main cold pipe can be determine as in Equation 3.22.

$$A_{cs} = \frac{\pi D_{cs}^2}{4} \tag{3.22}$$

where Dcs is the diameter pipe of cold seawater. The volumetric flow rate inside cold seawater can be determined as in Equation 3.23.

$$Q_{cs} = \frac{m_{cs}}{\rho_{cs}} \tag{3.23}$$

where m_{cs} is the mass cold seawater flow rate and ρ_{cs} is density of cold seawater. The flow velocity in the main cold seawater can be identified by using Equation 3.24.

$$V_{cs} = \frac{m_{cs}}{A_{cs} \rho_{cs}} \tag{3.24}$$

Equation 3.25 shows how to identified the Reynold number in cold seawater diameter pipe.

$$Re_{cs} = \frac{\rho_{cs} V_{cs} D_{cs}}{\mu_{cs}} \tag{3.25}$$

where μ_{cs} is the viscosity of the cold seawater and 0.03E-3 is assumed to be the pipe roughness for Glass-fiber reinforced pipes (GRP).The modified heat loss in the cold seawater source pipe can be defined as in Equation 3.26.

$$\Delta H_{cs,f} = \frac{f_{DW}V_{cs}^2(\frac{L_{cs}}{D_{cs}})}{2g\mu_{cs}}$$

(3.26)

Where f_{DW} is the friction loss, L_{cs} is the cold seawater pipe length.The Reynold number in the plate heat exchanger at the condenser calculated as in Equation 3.27.

$$Re_{cs} = \frac{\rho_{cs}V_{cs,PHE}D_{eq,cs}}{\mu_{cs}}$$

(3.27)

where,$V_{cs,PHE}$ is the velocity of cold seawater at the plate heat exchanger,$D_{eq,cs}$ is the equivalent diameter evaluated as in Equation 3.28.

$$D_{eq,cs} = 2\sigma$$

(3.28)

where σ is the clearance which assumed to be 0.005. The friction factor obtained from Taborek 1988 for 60°C chevron plate (heat exchanger design handbook) as defined in Equation 3.29.

$$f_{cs} = (4)(0.678)Re_{cs}^{-0.202}$$

(3.29)

The head loss in the plate heat exchanger at the condenser is calculated as in Equation 3.30.

$$\Delta H_{cs,PHE} = \frac{f_{cs}V_{cs,PHE}^2(\frac{L_{cs}}{D_{eq,cs}})}{2g}$$

(3.30)

The pressure difference caused by the density difference between the warm seawater surface and cold deep seawater calculated as Equation 3.31 below [56]:

$$\Delta H_{cs,d} = L_{cs} - \frac{1}{\rho_{cs}} \left(\frac{1}{2} (\rho_{ws} + \rho_{cs}) L_{cs} \right) \tag{3.31}$$

ΔH_{cs} is a total head loss of cold seawater piping [46] evaluated as in Equation 3.22.

$$\Delta H_{cs} = \Delta H_{cs,f} + \Delta H_{cs,PHE} + \Delta H_{cs,d} \tag{3.32}$$

3.3.5 Working fluid Pumping power

The pumping power of working fluid, $W_{P,wf}$ can be identified as in Equation 3.33.

$$W_{P,wf} = m_{wf} W_{tur} \eta_T \tag{3.33}$$

3.3.6 Net Power Generation

The net power output from the system is calculated based on Equation 3.34.

$$W_{net} = W_{tur} - W_{P,wf} - W_{P,ws} - W_{P,cs} \tag{3.34}$$

By considering the turbine and pump power, the net power obtained allows the calculation of the net thermal efficiency as in Equation 3.35.

$$\eta_{th} = W_{tur} / Q_E \tag{3.35}$$

Based on the definition of cycle efficiency, net cycle efficiency should be defined as in Equation 3.36.

$$\eta_{net} = \frac{W_{net}}{W_{tur}} \qquad (3.36)$$

Point number	Specification
5	Warm water entering ORC evaporator
6	Warm water exiting the ORC evaporator to the ocean
3	Saturated liquid ammonia entering ORC pump
4	Liquid ammonia exiting ORC pump
1	Saturated vapor entering turbine
2	Saturated ammonia entering condenser
7	Cold water entering the condenser
8	Cold water outlet from condenser to the ocean
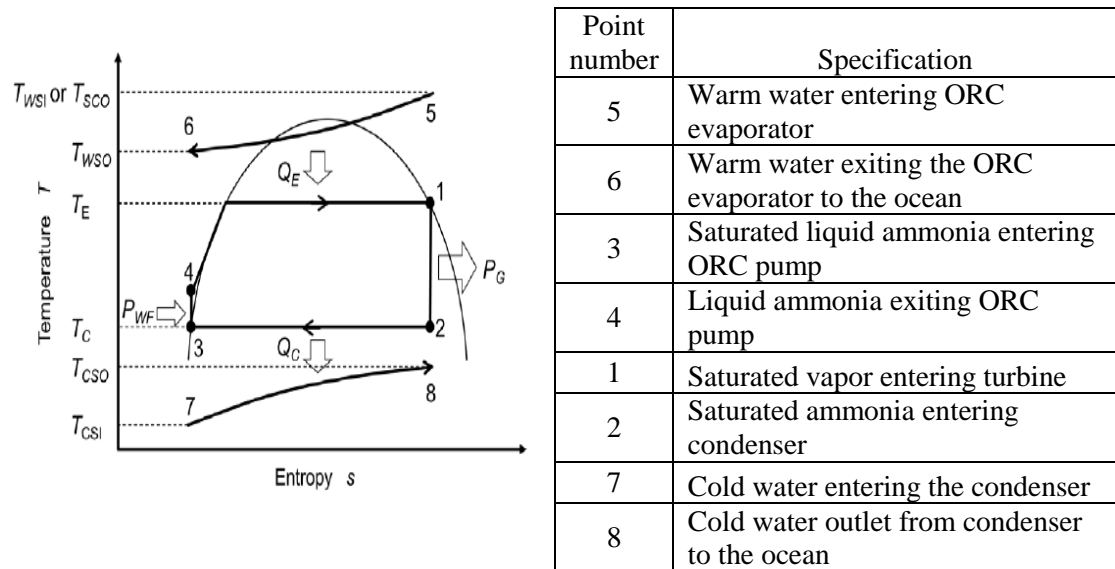
Figure 3.4   T-s diagram of the closed Rankine cycle [22]

Warm source inlet temperature, T_{wsi} and cold source inlet temperature, T_{csi} are taken at surface seawater as 26.7 ^{o}C. These values correspond, to the lowest mean average surface temperature at Kota Bharu. The design turbine power of the proposed plant, W_{tur} is 100 kW. Glass-fiber reinforced pipes of are assumed to be used for the main intake and discharge lines of both the warm and the cold seawater. Assume the warm seawater temperature at the evaporators' exit T_{wso} and calculate the liquid-side heat flow in the evaporator Q_E.

The calculation of the quantity states at each point (1-4) will be calculated by applying secant method with initial assumptions of the outlet of warm seawater and cold seawater. The evaporation and condensation temperature (T_E; T_C) can be identified by Equation 3.6 and Equation 3.7. Both values will then be used to

calculate the saturation pressure and temperature of the working fluid by using PROPATH. Besides, the enthalpy, entropy and specific volume at each point can be obtained from this program (i.e. h_{1-4}, s_{1-4} and v_{1-4}) as well. Then, evaluate the working fluid-side heat flow in the condenser, Q_{cwf} to compare with Q_c *as in Equation 3.4.* If not equal, update the cold source exit temperature assumption T_{cso} until equality is achieved. Next, the same steps will be applied in evaporator until it achieved the heat balanced between working fluid and seawater side. After specifying the flow rate of warm and cold seawater, the pumping power of cold and warm seawater, turbine power and net power generation will be determined by applying Equation 3.8 until Equation 3.34.

There are some assumptions and prediction made for this simulation study based on some criteria by acknowledging the theoretical design and real plant design. The assumptions made in the simulation are as follows [57] :

    i.   The cycle of the OTEC system based on ORC cycle.

    ii.   The main devices for the OTEC systems are steady-state and steady-flow process.

    iii.   The errors in heat transfer rate of the system calculated as 0.001.

    iv.   In ORC, the kinetic and potential energy is assumed to be neglected.

    v.   The system is assumed to have no leakage and no pressure drop.

    vi.   The saturated vapor enters the turbine at the ideal quality of the vapor.

3.3.7 Solar Energy Analysis

The equation of useful heat gained by seawater or fluid is written as shown in Equation 3.37.

$$Q_u = mc_p \, (\dot{T}_o - T_i) \tag{3.37}$$

where T_{in} and T_{out} are the inlet and outlet seawater temperature of the solar collector, m is the mass flow rate, and c_p is specific heat at constant pressure. The useful heat gain by flat plate solar collector, Q_u can be determined by using Hottle-Whillier equation as in Equation 3.38.

$$Q_u = A_p \, F_R \, [S - \dot{U}_L(T_i - T_o)] \tag{3.38}$$

where T_o is ambient temperature, F_R is heat removal factor that is defined as in Equation 3.39.

$$F_R = \frac{\dot{m} \, C_p}{U_L \, A_{sc}} [1 - e^{(-\frac{F' U_L A_{sc}}{\dot{m} C_p})}] \tag{3.39}$$

where the F' is collector efficiency factor which around 0.914 [46] and U_l overall loss coefficient[58]. Radiation flux can be calculated as in Equation 3.40.

$$S = (\alpha\tau)I \tag{3.40}$$

where $(\alpha\tau)$ is the optical efficiency and I is a molar radiation intensity. The energy efficiency of the solar flat plate collector expressed as in Equation 3.41.

$$\eta = \frac{Q_u}{IA_p} \tag{3.41}$$
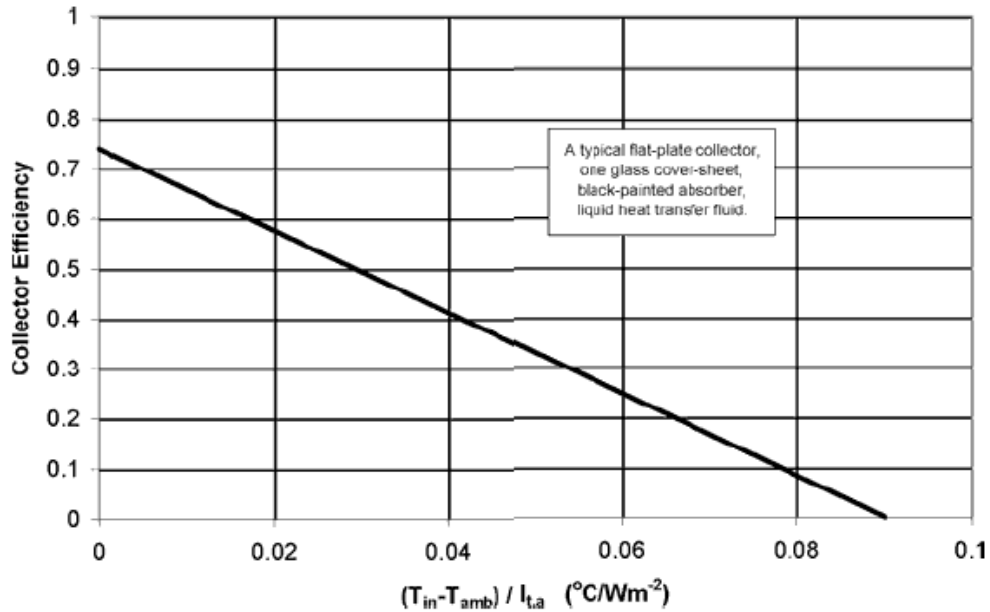
Figure 3.5 Performance of a typical flat-plate thermal collector (ambient temperature 25°C) [39]

Figure 3.5 shows the graph of collector efficiency against $(T_i\text{-}T_a)/I$ where the rate of heat loss from the solar collector is represented by the slope line $(\text{-}F_R U_L)$. The maximum collection efficiency, called as optical efficiency. This occurs when the fluid inlet temperature equals the ambient temperature $(T_i\text{=}T_a)$. For this condition $\Delta T/I$ value is zero and the intercept is $F_R (\tau \alpha)$.

    i.   The following are the assumptions applied to the present simulation of a flat-plate solar collector.

    ii.   There is no significant impact of tilt angle on the top loss coefficient of the solar collector.

    iii.   The significant impact of emissivity to the efficiency of flat plate solar collector is negligible.

3.4   Validation Process

The validation is based on the usage of software, fluid properties and comparison study of previous research that was conducted by Yamada [22].

3.4.1   Software

Visual Fortran is the programming used as it's easy to maintain and give command by user. This is one of the criteria why it was chosen rather than other programming. Due to its ability to collaborate and integrate with other software, Visual Fortran is seen as efficient, conceivable and portable. The fundamental step of the programming starts with input of parameter and followed by the process, decision and come out with the input of the program. The basic steps of the programming start by declaring the input, and then followed by the process, decision and the output of the program [59].

3.4.2   Thermodynamics Properties of the Fluids

PROPATH is a program that consist of the thermophysical properties of working fluid that is to be kept in an excel program known as E-PROPATH. The thermophysical properties of selected working fluid will be interpreted when the file is extracted into Visual Fortran program. Then the output of the system is calculated based on the input parameters.

3.4.3   Seawater

All the seawater function equation will be created as subroutine in Visual Fortran and act as call function based on specific temperature and salinity. Figure 3.6 shows the data generation of the enthalpy of seawater by GSW and CSIRO with a salinity of 35 kg/s and water by Roger and Mayhew. The result shows the enthalpy of seawater and water is different which is approximately less than 5%. This is due to

the different salinity between the two fluids. Therefore, in this study, the temperature and salinity of seawater will be calculated in order to obtain more precise result.
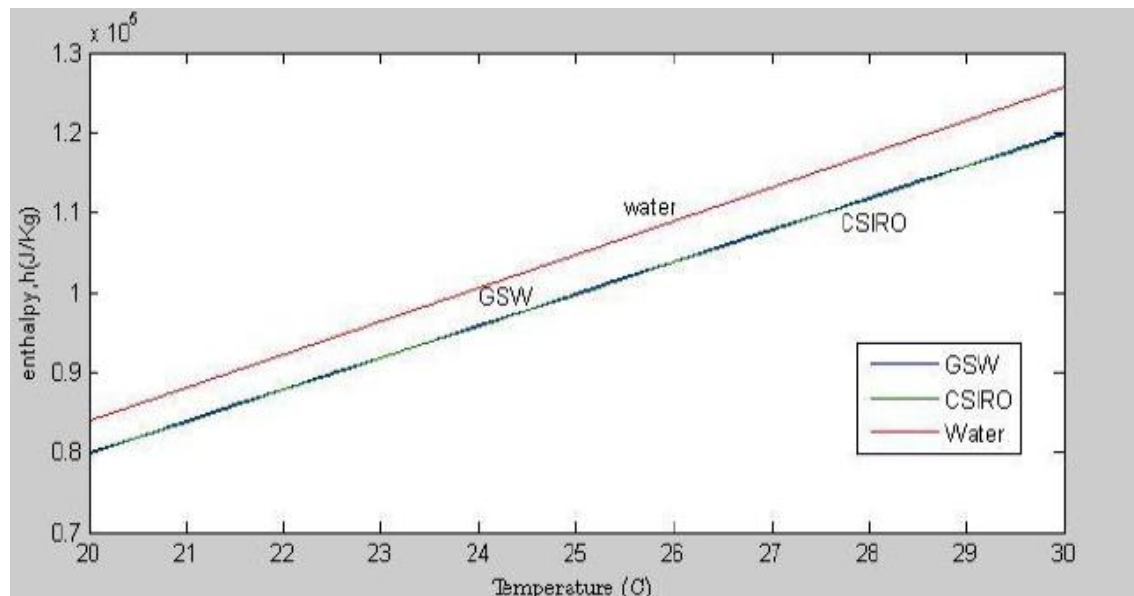
Figure 3.6 Data generation of enthalpy of seawater by GSW, CSIRO and water by Roger and Mayhew [60]

3.4.4 Program Validation

To validate the program that is going to be used in this study, the initial and piping condition is assumed to be the same as in the paper of 'Performance Simulation of Solar-boosted Ocean Thermal Energy Conversion Cycle'. The designed OTEC system is considered as an illustrative base system that allows the thermodynamic analysis of its off-design operation when solar collector is integrated as an additional component. The design-point analysis of the SOTEC system that produced turbine-generator power of 100 kW was numerically conducted using Visual Fortran. Therefore, the results obtained was compared with the results by Yamada [22]. Table 3.3 complies with the determined design parameters of the OTEC system that generates a 100 kW turbine power output. In this study, the overall results are in agreement with Yamada.et that designed the same scale OTEC system. There are noticeable that the area of evaporator and condenser is slightly difference due to different overall heat transfer coefficient by the heat exchanger which is not stated in study conducted by Yamada [22]. Table 3.4 shows the results of quantity states for 100 kW OTEC.

Table 3.3: Program Validation

Parameter	Symbol	Unit	Yamada [22] (OTEC)	This Study (OTEC)
Warm seawater				
Inlet temperature	T_{wsi}	°C	25.7	25.7
Outlet temperature	T_{wso}	°C	22.6	22.7
Cold seawater				
Inlet temperature	T_{csi}	°C	4.4	4.4
Outlet temperature	T_{cso}	°C	7.4	7.3
Solar Collector				
Inlet temperature	T_{csi}	°C	-	-
Outlet temperature	T_{cso}	°C	-	-
Flow rate				
Warm seawater	m_{ws}	kg/s	260.0	260
Cold seawater	m_{cs}	kg/s	260.0	260
Working fluid	m_{wf}	kg/s	2.6	2.52
Work Pump				
Warm seawater	W_{Pws}	kW	7.1	7.29
Cold seawater	W_{Pcs}	kW	18.6	18.62
Working fluid	W_{Pwf}	kW	1.8	1.2
Effeciency				
Rankine cycle	η_R	-	3.2	3.2
Net Rankine cycle	η_{net}	-	2.3	2.33
Evaporator				
Overall heat transfer	U_E	kW/m^2°C	-	4.3
Surface area	A_E	m^2	514	339.7
Condenser				
Overall heat transfer	U_c	kW/m^2°C	-	4.0
Surface area	A_c	m^2	478	435

Condensation temperature	T_C	°C	8.4	8.4
Evaporation temperature	T_E	°C	21.7	21.7
Net power	W_{net}	kW	72.5	72.9

Table 3.4 : Quantity state at each point (1-4) for 100 kW OTEC designed system. The positions of each point are shown as in Figure 3.3.

Point	P (kPa)	T (°C)	h (kJ/kg)	s (kJ/kg°C)	v (m^3/kg)
1	902.48	21.7	518.4	10.05	0.1420
2	580.13	8.4	463.23	10.05	0.2096
3	580.13	8.4	-723.62	5.84	0.0016
4	902.48	8.5	-723.11	5.84	0.0016

3.5   Develop a Simulation Model for 100 kW SOTEC

The development and configuration of a 100 kW SOTEC are referred in Figure 3.3. Simulation was conducted using the mathematical modeling and numerical study of the Organic Rankine Cycle (ORC). All the analysis was done using Visual Fortran Programming system.

3.5.1   Working Fluid Selection

The plant model and optimization tool will be used for working fluid selection by comparing the maximum values of net power output. This study will compare the selection of the best three working fluids which are ammonia, propane, R134a and R22 types. Several aspects should be considered under selection process of working fluid, such as the flowing losses, stability and safety. Taking into account these factors, we propose the following principle for the system as follows:

i.   Considering the environmental protection problem who's Ozon Depletion Potential (ODP) is demanded. It should have low Global Warming Potential (GWP) value.

ii.   Considering from the equipment design, we demand the low evaporation temperature/pressure to reduce the intensity requirement of turbine, evaporator and venting pipe.

iii.   Considering the low boiling points so that only a small flow rate is required to vaporize when it comes into contact with seawater in the evaporator. This is because of the fact that if the mass flow rate increases, the pumping power of the working fluid increases as in Equation 3.33.

iv.   Considering a good heat transfer properties, non-toxicity, non-flammability, high efficiency, availability and low cost.

v.   Considering the working fluid that has high mass heat of vaporization at the inlets of the evaporator and condenser.

3.5.2   Optimal Warm Seawater Flow Rate

From validation data obtained, the existence of solar collector proves that it is able to improve not only the net efficiency but also the net power output. The result has given an idea to develop a simulation model for 100 kW SOTEC in shallow water where the cold seawater will be pumped from the surface of seawater.

Meaning that, with reasonable solar collector area, the OTEC technology can also be implemented at the shallow water with minimum temperature difference of 20°C without depending on temperature gradient in seawater. Therefore, the cold seawater pipe length can be shortened to meet the sea surface level. The design point analysis of the SOTEC system producing a turbine generator power of 100 kW with 40°C additional temperature was numerically conducted using FORTRAN program. The value of useful heat gained by seawater, Q_u can be calculated by using the mass warm seawater flow rate obtained from Rankine cycle. Basically the efficiency curve of solar collector will be provided by manufacturer as shown in the Figure 3.3. The collector efficiency is depends on the inlet temperature of solar collector and solar radiation power. Once all the values are obtained, the solar collector area can be identified by applying Equation 3.40 and is based on the annual solar radiation in Kota Bharu as in Table 3.2.

3.5.3   Optimal Pipe Diameter and Thermal Conductance Selection

The selection of pipe diameter is one of the most important parameter in determining the friction loss in warm and cold seawater pumping power. In this study, the fluid flow is assumed to be at steady state flow. The mass flow rate will be the constant parameter in identifying the suitable pipe diameter. The velocity inside the pipe is related with the cross sectional area. As mentioned in Equation 3.12 and 3.24, the cross sectional area is inversely proportional to the velocity inside the pipe. For example if the pipe diameter increases, the velocity of the fluid will be slower and friction loss is reduced due to less friction that occurs in the pipe diameter. The head loss due to friction will contribute to the total head loss in both piping systems and would affect the calculation of pumping power of Equation 3.34. As such, the selection of the pipe diameter is derived from the lowest reading of the total pumping power and highest value of net power output.

Heat transfer rate of seawater and working fluid directly linked to thermal conductance in the evaporator condenser. It can be determined by fixing the value in Table 3.1 and Table 3.2. In order to generate 100 kW of turbine power, the flow rate of warm seawater, cold seawater and working fluid will be variable. The turbine

power is expected to increase with increasing thermal conductance of the evaporator and the condenser as shown in Equation 3.2 and Equation 3.5. The optimal value will be selected once the net power output is constant despite the increasing value of thermal conductance.

CHAPTER 4

RESULT AND DISCUSSION

As explained in Chapter 3, 100 kW SOTEC model has been developed with increment of 40°C of inlet warm seawater temperature. It should be noted that in the conventional OTEC system, the most stringent design condition is the mass flow rate of deep seawater, as a tremendous cost is required to construct a pipeline reaching ~1000 m depth in ocean. However, in this study, the construction of the pipeline is only on the surface of sea water due to shallow sea level at MTJDA. In this study, the most concern is design of the mass flow rate of warm seawater in solar collector, as the area is needed to increase the temperature by 40°C. Thus, the present study has identified a design point as the operation condition requiring the minimum mass flow rate of warm seawater to generate 100 kW SOTEC. Therefore, this chapter will cover the results and discussions obtained from simulation study by Fortran Programming.

4.1   Simulation results

As OTEC relies on temperature differences, it works best in the tropics, where the temperature difference is larger. As long as there is a temperature difference between hot surface and cold surface of around 20˚C, an OTEC can produce significant amounts of electricity. However, with the presence of solar collector, OTEC technology not only can be implemented in deep water but also on shallow sea water. Table 4.1 shows the simulation results of 100 kW SOTEC boosted

40˚C of inlet temperature based on the piping condition and input parameters as in Table 3.1 and 3.2. This condition indirectly create the temperature difference between warm and cold seawater ($\Delta T = T_{sco}\text{-}T_{csi}$) also equal to 40˚C where the inlet temperature of cold seawater is 26.7°C taken from the surface of ocean. The result shows that the warm seawater, cold seawater and working fluid flow rate required to increase 40˚C temperature are 23.3 kg/s, 400kg/s and 1.6 kg/s respectively. The value of warm seawater is the minimum value that is required to increase 40˚C of the temperature at the outlet of solar collector. The minimum value of mass warm seawater can minimize the solar collector area, where the relationship can be proved by Equation 3.36 until Equation 3.40. The cold seawater pumping power is highest among other pumping power due to the immense cold seawater flow rate to be pumped to achieve heat balance, therefore the net power of the system is equal to 92.15kW. The solar collector area required to boost 40˚C of SOTEC cycle is 29155 m^2 based on the annual solar radiation found in Kota Bharu (i.e 17 MJ/m^2/day equivalents to 196.8 W/m^2). The parameters that affect the solar collector area are solar radiation, I, useful heat gained by seawater, Q_u and collector efficiency, $\eta_{sc.}$ Since the temperature and solar radiation fluctuate, in order to maintain the performance, thermal storage is assumed to be installed to balance the energy demand during daytime and nighttime.

Table 4.1: Simulation results of 100 kW SOTEC boosted 40˚C (T_{sco}-T_{wsi}) at shallow seawater based on annual solar radiation

Parameters	Symbol	Unit	Value
Warm sea water			
Inlet temperature	T_{wsi}	°C	26.7
Outlet temperature	T_{wso}	°C	47.8
Cold sea water			
Inlet temperature	T_{csi}	°C	26.7
Outlet temperature	T_{cso}	°C	27.7
Solar collector			
Inlet temperature	T_{sci}	°C	26.7
Outlet temperature	T_{sco}	°C	66.7

Evaporation temperature	T_E	°C	47.7
Condensation temperature	T_C	°C	28.1
Net power	W_N	kW	92.1
Pumping power for : Warm sea water	W_{Pws}	kW	0.54
Cold sea water	W_{Pcs}	kW	5.39
Working fluid	W_{Pwf}	kW	1.96
Flow rate : Warm sea water	m_{ws}	kg/s	23.3
Cold sea water	m_{cs}	kg/s	400
Working fluid	m_{wf}	kg/s	1.6
Efficiency Rankine cycle	η_R	%	5.40
Net Rankine cycle	n_{net}	%	4.98
Heat transfer area : Evaporator	A_e	m^2	162.8
Condenser	A_c	m^2	575
Required solar collector	A_{sc}	m^2	29155
Annual solar radiation	I	W/ m^2	196.8

4.2 Working fluid selection

Table 4.2 shows the performance of several working fluids in SOTEC system to produce 100 kW. The parameters such as T_{sco}, T_{csi}, m_{ws} and m_{cs} are assumed to be constant so that the performance of every working fluid can clearly see. Based on this working fluid, ammonia gives a higher net power output because it is better in efficiency and has higher sensible heat. So, with only a small amount of ammonia, it

has the potential to get more net power output with less power of working fluid pump. Ammonia is produced from nitrogen cycle usually in ongoing industrial processes like chemical and agricultural industries. It has a better coefficient of performance (COP) where it uses less energy due to high sensible heat. Besides, ammonia has a zero reading of ozone depletion potential (ODP) and global warming potential (GWP), it does not give a negative impact to the environment. As results, ammonia is selected as the working fluid, which has satisfying quality according to parameters and nearly satisfies all the three principals as mentioned earlier.

Table 4.2: Comparison of SOTEC cycle with different working fluids

Parameters	Symbol /Unit	Working Fluid			
		Ammonia	Propane	R22	R134a
Mass flow rate					
Warm seawater	m_{ws} (kg/s)	23.3	23.3	23.3	24.1
Cold seawater	m_{cs} (kg/s)	400.0	400.0	400.0	400.0
Working fluid	m_{wf} (kg/s)	1.6	5.2	9.5	9.6
Temperature					
Solar collector outlet	T_{sco} (°C)	66.7	66.7	66.7	66.7
Warm seawater outlet	T_{wso} (°C)	47.8	48.1	49.1	49.3
Cold seawater outlet	T_{cso} (°C)	27.7	27.7	27.7	27.7
Cold seawater inlet	T_{csi} (°C)	26.7	26.7	26.7	26.7
Evaporation	T_E (°C)	47.7	48.0	49.0	49.2
Condensation	T_C (°C)	28.1	28.2	28.0	28.1
Turbine power	W_{tur} (kW)	100.0	100.0	100.0	100.0
Pumping power					
Working fluid	W_{Pwf} (kW)	1.96	5.93	5.57	4.07
Cold seawater	W_{Pcs} (kW)	5.39	5.39	5.39	5.39
Warm seawater	W_{Pws} (kW)	0.54	0.54	0.54	0.56
Net power	W_{net} (kW)	92.1	88.1	88.5	90.0

4.3   Optimization of warm seawater and cold seawater pipe diameter

Diameter pipe of cold seawater, D_{cs} and warm seawater, D_{ws} is one of the important parameters that control the performance of SOTEC cycle. As seen in Figure 4.1, the net power output tends to increase in logarithmic-like relationship with increasing diameter pipe of cold and warm seawater. This indicates the enhancement of pipe diameter by means does not reflect definitely on net power of the system. In both graphs provided, it show that the cold seawater and warm seawater pumping power are decreasing until 5.39 kW and 0.54 kW respectively with further increase of pipe diameter. By increasing the pipe diameter, it will cause the flow velocity of the seawater in the pipe to decrease which affects the head loss of seawater pipe of warm and cold source seawater pipe. At a certain point, if we further increase the pipe diameter the net output power remain the same. The pipe diameter is dependent on seawater flow rate intake of the system. However, if we use too small pipe diameter for that amount of flow rate, it definitely will have an effect on the power generation. As for the 100 kW SOTEC plant, at the warm seawater flow rate 23.3 kg/s, only 0.11 m of pipe diameter is needed while 0.6 m of pipe diameters required to pump 400 kg/s of cold seawater flow rate to produce 92.1 kW. Optimization is very important so as to find the optimal pipe diameter for the specific condition of the SOTEC plant in order that we do not have to spend more to get the highest net power.
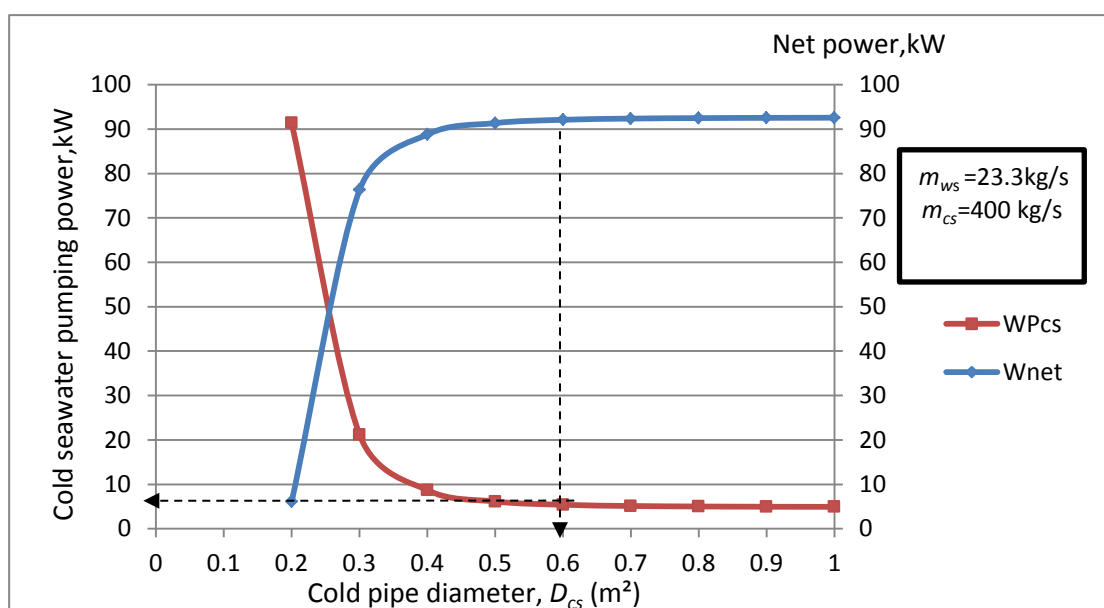
(a)
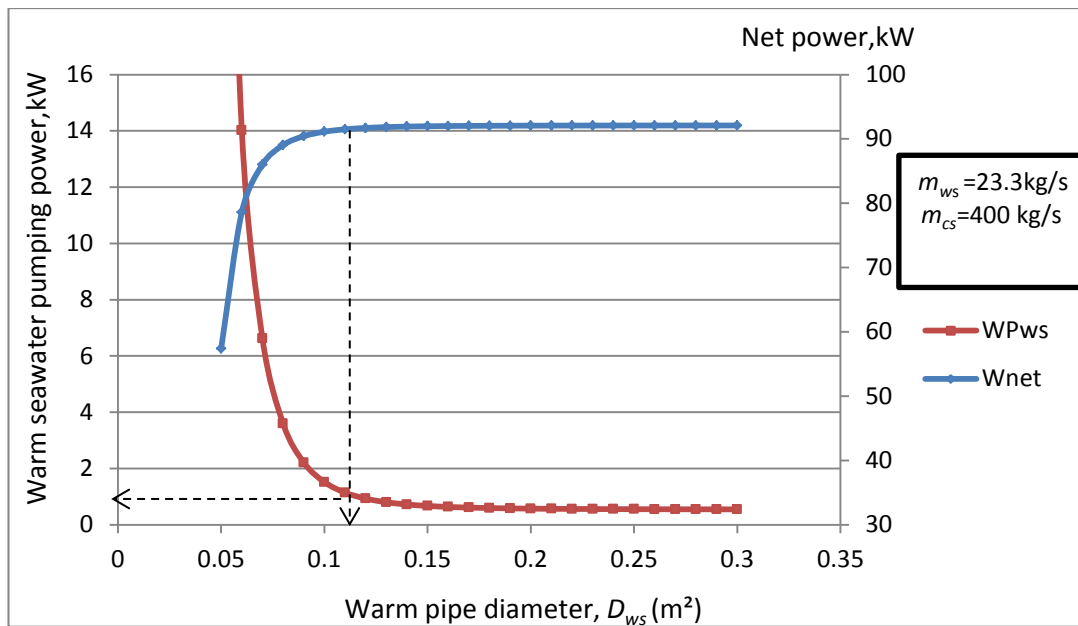
(b)

Figure 4.1 The relationship between diameter pipe and seawater pumping power on the net power output (a) Cold seawater (b) Warm seawater.

4.4 Optimization of thermal conductance at condenser and evaporator

As shown in Figure 4.2 (a), the net power output increased up to 92.1 kW when overall heat transfer area of condenser increases to 2.3 MW/°C. However, the pattern of the graph changes and after that point it remains constant. This shows that, if the overall heat transfer area keeps increasing, the net power output increases until a certain point and remain unchanged for the next reading. Referring to the graph, for a larger value of overall heat transfer area needed a lower intake of cold seawater flow rate is required in order to get a maximum net power generation. Similarly, in Figure 4.8 (b), the graph of the net power output shows an increase with increases of thermal conductance in evaporator until 92.1 kW but remain constant after $UA_E = 0.7$ MW/°C. In order to get the maximum net power output, it is just enough to have $UA_C = 2.5$ MW/K and $UA_E = 0.7$ MW/°C with seawater flow rate of cold seawater and warm seawater equal to 400 kg/s and 23.3 kg/s respectively.
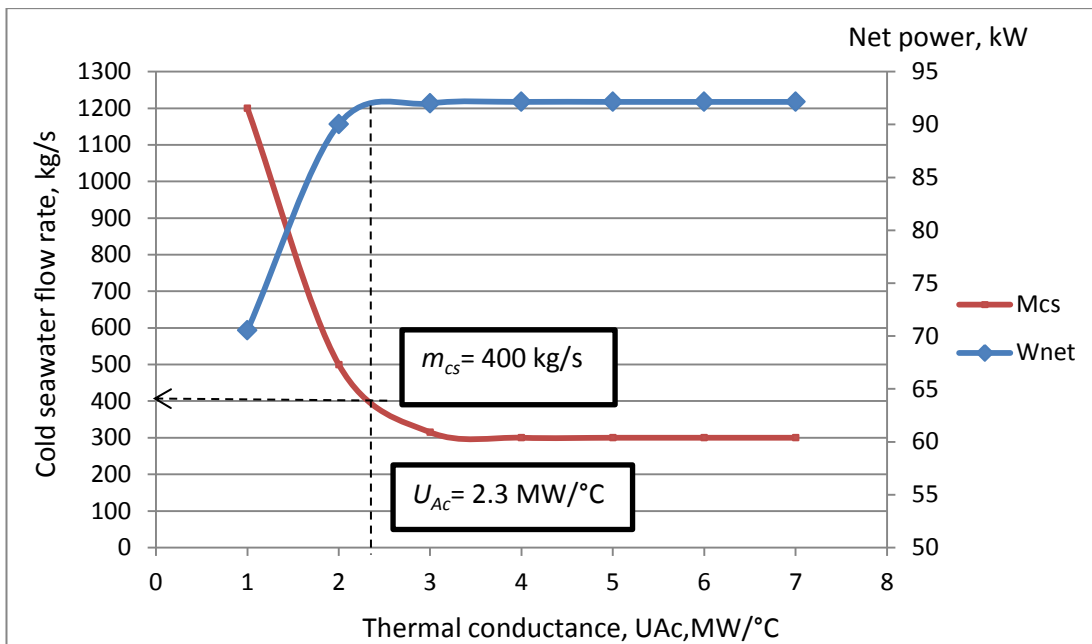
(a)
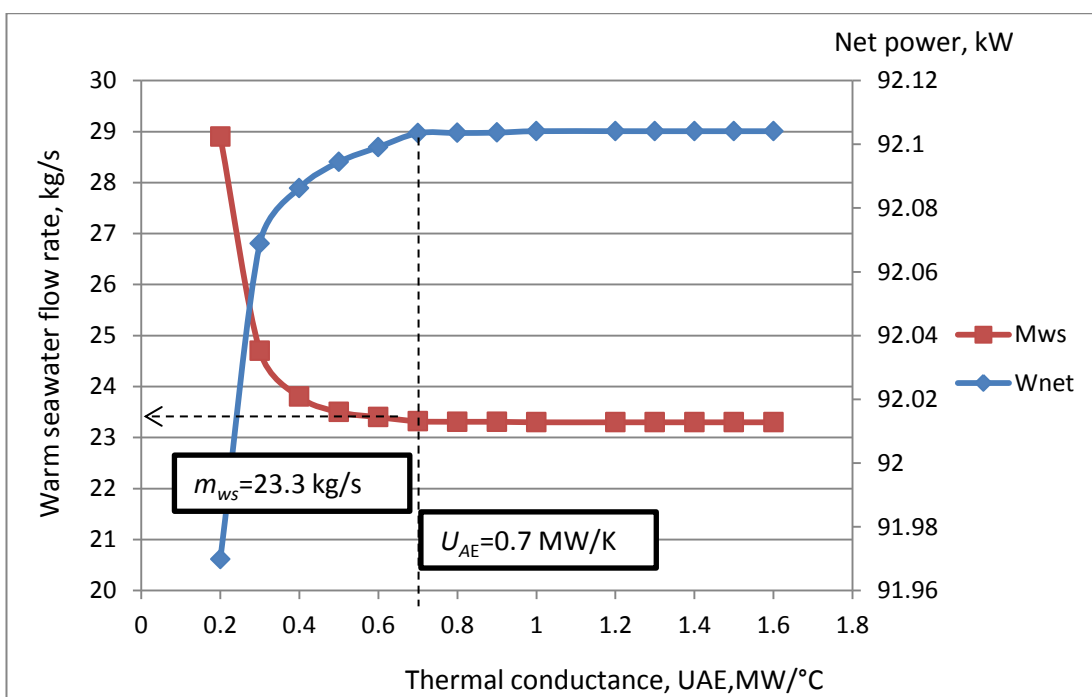
(b)

Figure 4.2 The relationship of thermal conductance to the net power output
(a) Condenser (b) Evaporator

4.5   T-S diagram

Figure 4.3 shows the T-s diagram of SOTEC cycle based on Organic Rankine cycle. Ammonia is selected as a working fluid due to its low boiling point and better performance as explained in Table 4.2. In order to achieve 100 kW turbine gross power, in the simulation study 23.3 kg/s of mass warm seawater flow rate and 400 kg/s of cold seawater flow rate with thermal conductance 0.7 MW/°C and 2.3 MW/°C were used for evaporator and condenser respectively. By applying the Equations 3.5 and 3.6 the results obtained for the evaporation temperature is 47.7°C and condensation temperature is 28.14°C. Point 1 is at inlet of turbine where the working fluid is completely in saturated vapor. Point 2 is the mixture state at the outlet of the turbine and the inlet of the condenser which the turbine is assumed to be isentropically ($s_1=s_2$). Saturated liquid state is at the outlet of condenser which is at point 3. Point 4 is at compressed liquid state, where working fluid enters the pump as saturated liquid and is compressed isentropically to the operating pressure of the evaporator.
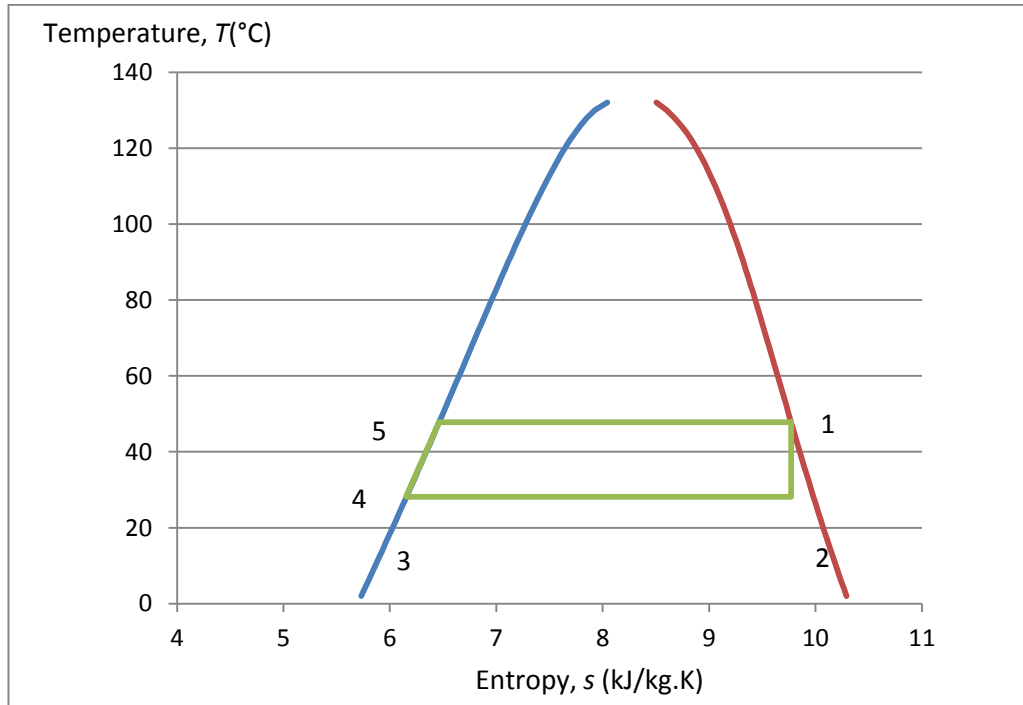
Figure 4.3   T-S diagram of 100 kW SOTEC system

4.6 The effect of temperature difference in evaporator to the net Rankine cycle and heat in evaporator, Q_E

As shown in Figure 4.4, the turbine power continues to increase with an increase of ΔT_{wsi} and attains a peak value before it starts to decline upon further increase of ΔT_{wsi}. Values of ΔT_{wsi} is around 20 °C that correspond to maximum turbine power when sea water flow rate of warm and cold seawater are set to 23.3 kg/s and 400 kg/s respectively. Equation 3.35 is able to define that turbine power does not always increases with the increases of evaporator heat input but it has its optimum value where the turbine power reached it maximum reading.
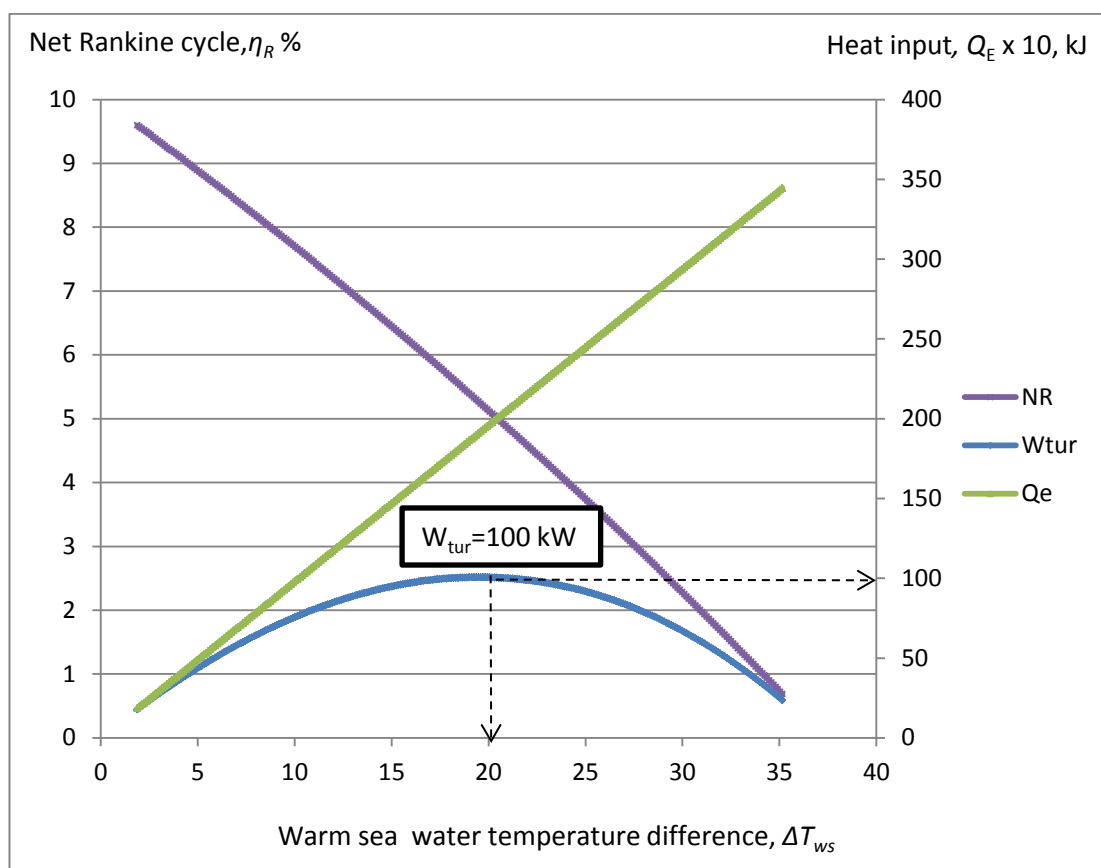
Figure 4.4 The relationship of net Rankine cycle and heat at evaporator, Q_E to the warm seawater temperature difference

4.7 The relationship of working fluid flow rate to the turbine power

As shown in Figure 4.5, the net power is about 92% of the total turbine power at the current input conditions. The main parameter that affects the net power ratio (the ratio of the net usable power to the total turbine power) is the cold and warm water pipe diameter which upon its increase, the flow velocity of the cold water in the main intake pipe decreases and so does the frictional head loss in the cold seawater pipe which is directly proportional to the square of flow velocity.
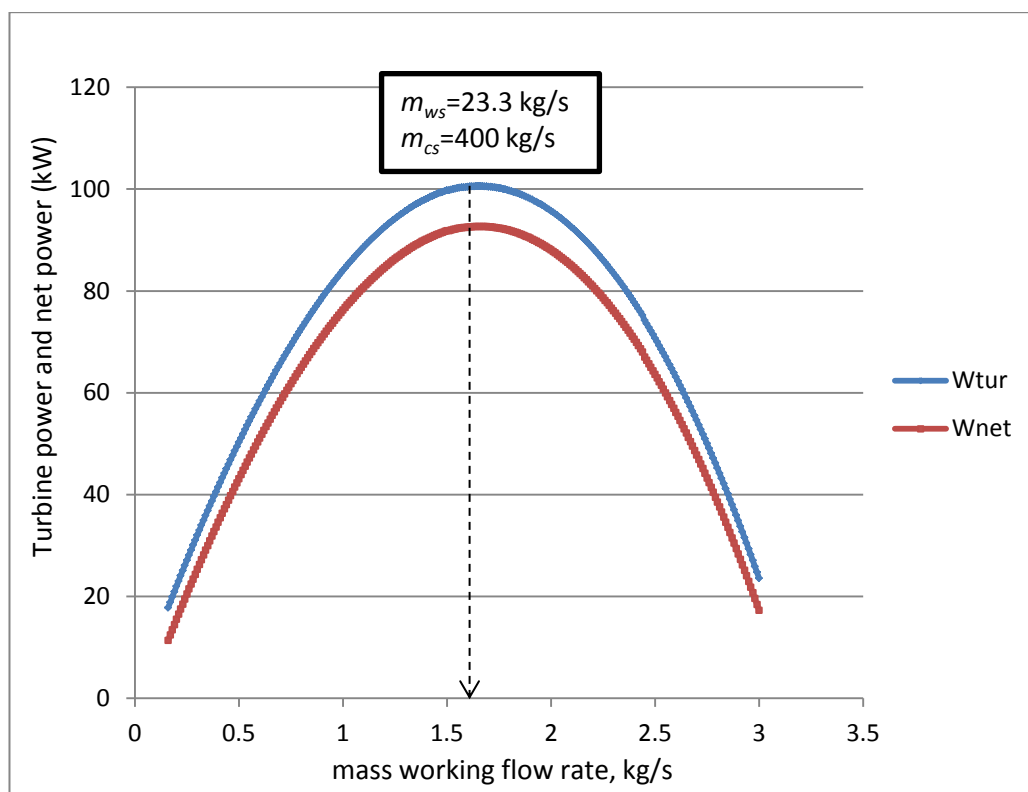
Figure 4.5 Effect of working fluid flow rate on turbine power and net power (D_{ws}=0.11m ; D_{cs}=0.6 m)

4.8 Monthly variation of net power and pumping power

Figure 4.6 shows the monthly variation of net power W_{net} and pumping powers that is required in SOTEC cycle and these figures show the design of turbine-generator with 100kW of gross power. In SOTEC cycle, the performance is based on 29155 m^2 of solar collector area and 196.8 W/m^2 the annual solar radiation in Kota Bharu. This significant result obtained by taking the mass warm seawater flow rate is equal to 23.3 kg/s. From the graph, we can see that the net power output of the system is distributed from 90 kW to 92 kW throughout the year. However, the significant result of cold seawater pumping power is slightly different for each month because of the condition where inlet temperature is higher; the intake of cold seawater flow rate need to be reduced to achieve the heat balance. This makes the cold seawater pumping power to be reduced and contribute more net power. Figure 4.6 also shows the monthly variation of the net Rankine cycle efficiency, η_{net} of SOTEC operation which lies around 5%. However, it should be noted here that the performance of SOTEC during night time is expected to be the same as the daytime due to the installation of thermal energy storage to balancing the energy between day time and night time.
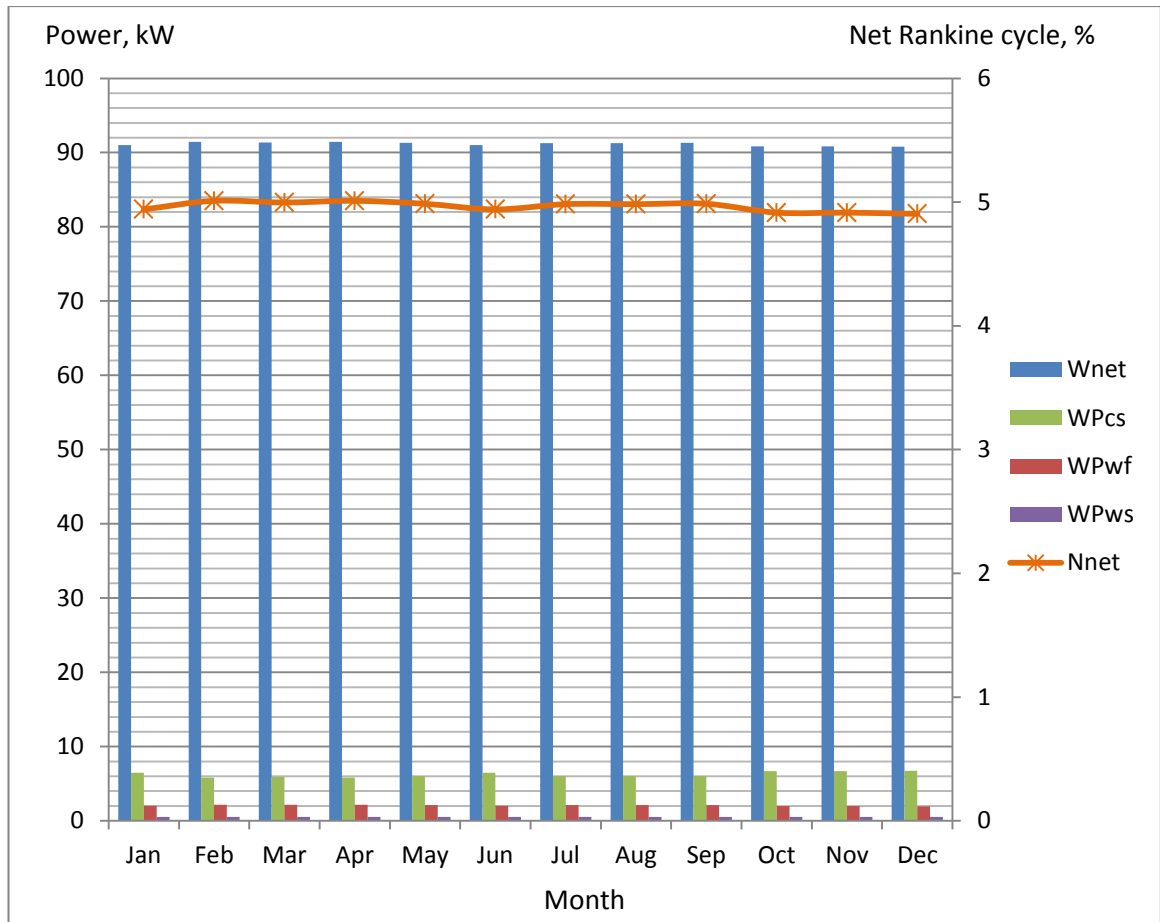
Figure 4.6   Monthly variation of net power of SOTEC plant in case of temperature increase of 40°C by flat-plate solar collector with effective area 29155 m^2

4.9   Result comparison

Until now, there still no SOTEC study has been conducted at shallow seawater where the required temperature difference is absent. Previously, Yamada [22] has studied the performance simulation of an OTEC plant that utilizes not only ocean thermal energy but also solar thermal energy as heat sources. The simulation results were presented as in Table 4.3. The cold seawater intake of the system is at 1000m depth reaching to 4.4°C. Therefore, the system was created the temperature difference about 41.3°C (T_{sco}-T_{csi}) which is higher than 40°C designed in this study. If we analyse the results of Yamada [22], the evaporation temperature, T_E is higher

than warm seawater outlet temperature, T_{wso}. This condition does not obey the *T-s* diagram of closed-Rankine cycle as shown in Figure 3.4. Even though this value can be obtained from calculation but it could not be achieved in real plant. If we look at the mass warm seawater and working fluid flow rate, both systems recorded value that is not too much different. However, the cold seawater flow rate in this system is 400kg/s which is relatively higher than 81.2 kg/s obtained by Yamada [22]. This is because the temperature of cold seawater inlet in this study is higher which is 26.7°C compared to 4.4°C. The specific heat capacity is larger at higher temperature of seawater, therefore effect on the heat at condenser. So in order to achieve the heat balanced, the mass cold seawater flow rate is larger at higher cold seawater inlet temperature. The net power output obtained is this study is 92.1 kW which is higher than 88.4 kW achieved by Yamada [22]. This is due to less total of pumping power required to pump the seawater and working fluid flow rate to operate the system. The solar collector area is inversely proportional to the solar radiation intensity. In this study, the required area to boost 40°C is larger than the study conducted by Yamada [22]. This is because, the annual solar radiation taken by Yamada [22] is the average daytime solar radiation and the system was designed to operate during daytime only, while in this study, the solar radiation is based on average daily values energy input for the whole year (24hrs). The performance of SOTEC system during night time is expected to be the same as in daytime. This due to assumption that the excess thermal energy stored in thermal storage could provide the same amount of energy for the night performance.

Table 4.3: Comparison study

Parameters	Symbol	Unit	SOTEC 20°C [22] *(Tsco-Twsi)*	This study SOTEC 40°C *(Tsco-Twsi)*
Warm sea water				
Inlet temperature	T_{wsi}	°C	25.7	26.7
Outlet temperature	T_{wso}	°C	22.8	47.81
Cold sea water				
Inlet temperature	T_{csi}	°C	4.4	26.7
Outlet temperature	T_{cso}	°C	8.5	27.7
Solar collector				
Inlet temperature	T_{sci}	°C	25.7	26.7
Outlet temperature	T_{sco}	°C	45.7	66.7
Temperature				
Evaporation	T_E	°C	41.7	47.7
Condensation	T_C	°C	8.4	28.1
Net power	W_{net}	kW	88.4	92.1
Pumping power for :				
Warm sea water	W_{Pws}	kW	3.4	0.54
Cold sea water	W_{Pcs}	kW	5.7	5.39
Working fluid	W_{Pwf}	kW	2.5	1.96
Flow rate :				
Warm sea water	m_{ws}	kg/s	16.0	23.3
Cold sea water	m_{cs}	kg/s	81.2	400
Working fluid	m_{wf}	kg/s	1.1	1.6
Heat transfer area :				
Evaporator	A_e	m^2	237	162.8
Condenser	A_c	m^2	299	575
Required solar collector	A_{sc}	m^2	5333	29155
Annual solar radiation	I	W/ m^2	457	196.8

CHAPTER 5

CONCLUSION

As a conclusion, in order to support the increase in energy demand and to reduce the dependency of fossil fuel as primary energy supply, renewable energy source like OTEC is seen to be one of the solution. However, the small temperature difference limits OTEC's performance and focus should be on the deep sea water only with minimum temperature difference of 20 °C. Immense of cold seawater flow rate withdrawn from 1000 m depth can cause it to construct a long pipeline to supply the plant. The potential of using renewable energy in the Malaysia-Thailand Joint Development Area is low, due to not only to low wind but also low wave action. Apart from that, the sea level is so shallow (55 m ~ 65 m) that no ocean thermal energy could be harnessed economically. In the absence of the required depth, an alternative such as a solar collector was introduced to boost the sea surface temperature in order to maintain the required temperature difference. The present study reports the optimization of 100 kW solar assisted OTEC for achieving inlet temperature increase of 40 °C. A simulation study approach is proposed based on mathematically based problems design to compute the optimal results. To achieve gross power 100 kW SOTEC at shallow sea water, the warm and cold seawater flow rate needed is 23.3 kg/s and 400 kg/s respectively. The optimum pipe diameter for warm seawater and cold seawater is 0.11 m and 0.6 m respectively. The overall heat transfer area for evaporator and condenser to support 100 kW SOTEC plant is 162.8 m^2 and 575 m^2. By considering the annual solar radiation value (196.8 W/m^2), the solar collector area needed to boost 40 °C temperature is 29155 m^2. The distribution of monthly net power by applying this optimal design, shows a good result of around 90 - 92 kW throughout the year. With a long-term upward trend in the prices and depletion of fossil fuels, the development of an advanced SOTEC

system will become increasingly important and promising. For future studies, the author is determined to accomplish more precise simulation study with larger scale power and to include the SOTEC plant estimation cost. These results will provide insights on thermodynamic perspective when combining sustainable energy with solar thermal energy to improve the system performance.

REFERENCES

1.   (TNB), T.N.B., *TNB,Recors improved Electricity Demand Growth.* 2016.

2.   DataBank, W.D.I.W., *Data Report.* 2017.

3.   Noordin, A.I.M., *Malaysian National News Agency. BERNAMA.* 2012.

4.   Nuketech, *Environmental Issues - Greenhouse Effect*, in *Nuketech*2012.

5.   Avery, W.H., D. Richards, and G.L. Dugger, *Hydrogen generation by OTEC electrolysis, and economical energy transfer to world markets via ammonia and methanol.* International Journal of Hydrogen Energy, 1985. 10(11): p. 727-736.

6.   Tanner, D., *Ocean thermal energy conversion: current overview and future outlook.* Renewable energy, 1995. 6(3): p. 367-373.

7.   Cavrot, D., *Economics of ocean thermal energy conversion (OTEC).* Renewable energy, 1993. 3(8): p. 891-896.

8.   Stevens, H., L. Genens, and C. Panchal, *Conceptual design of a 10 MW shore-based OTEC plant*, 1984, Argonne National Lab., IL (USA).

9.   Penny, T., et al., *Open-cycle ocean thermal energy conversion (OTEC) research: progress summary and a design study*, 1984, Solar Energy Research Inst., Golden, CO (USA).

10.   Uehara, H. and Y. Ikegami, *Optimization of a closed-cycle OTEC system.* Journal of solar energy engineering, 1990. 112(4): p. 247-256.

11.   Thorhaug, A. and J. Marcus, *The effects of temperature and light on attached forms of tropical and semi-tropical macroalgae potentially associated with OTEC (Ocean Thermal Energy Conversion) machine operation.* Botanica Marina, 1981. 24(7): p. 393-398.

12.   Larsen-Basse, J., *Performance of OTEC heat exchanger materials in tropical seawaters.* JOM, 1985. 37(3): p. 24-27.

13. Rey, M. and F. Lauro, *Ocean thermal energy and desalination.* Desalination, 1981. 39: p. 159-168.

14. Nihous, G.C., *Mapping available Ocean Thermal Energy Conversion resources around the main Hawaiian Islands with state-of-the-art tools.* Journal of Renewable and Sustainable Energy, 2010. 2(4): p. 043104.

15. Saitoh, T. and N. Yamada. *Advanced multiple Rankine cycle system including Uehara cycle for solar and ocean energy utilization.* in *Proceedings of forum on desalination using renewable energy.* 2003.

16. OTEC, U., *UTM Ocean Thermal Energy Centre.* 3rd January 2013.

17. Husain, D.M.K.A., *UTM-OTEC Research: Ocean Thermal Energy Conversion Potential in Malaysia.* drmohdkhairiabuhusain.

18. Vega, L.A., *Economics of Ocean Thermal Energy Conversion*, in *Ocean Energy Recovery: The State of the Art*1992, The American Society of Civil Engineers (ASCE). p. 1-39.

19. Ikegami, Y., *Japan Activity and Strategy of OTEC.* September 2015.

20. Ong, D.M., *The 1979 and 1990 Malaysia-Thailand Joint Development Agreements: A Model for International I Legal I Co-operation in Common Offshore Petroleum Deposit.* The International Journal of Marine and Coastal Law, 1999. 14(2): p. 207-246.

21. Aydin, H., et al., *Off-design performance analysis of a closed-cycle ocean thermal energy conversion system with solar thermal preheating and superheating.* Renewable Energy, 2014. 72: p. 154-163.

22. Yamada, N., A. Hoshi, and Y. Ikegami, *Performance simulation of solar-boosted ocean thermal energy conversion plant.* Renewable Energy, 2009. 34(7): p. 1752-1758.

23. Unit, E.P., *Sustainable Usage of Energy to Support Growth.* 2015.

24. Renewableenergyworld.com. *Renewable Energy World* 2015.; Available from: http://www.renewableenergyworld.com/index.html.

25. Abu Bakar Jaafa and Akhbariah Mohd Mahdzir, *Proceedings: 2nd National Workshop on Ocean Energy 2016.* Ocean Energy, 2016(ISBN 978-983-44732-7-3).

26. Quadrelli, E.A., *25 years of energy and green chemistry: saving, storing, distributing and using energy responsibly.* Green Chemistry, 2016. 18(2): p. 328-330.

27.   Hammons, T.J., *Tidal power.* Proceedings of the IEEE, 1993. 81(3): p. 419-433.

28.   Bae, Y.H., K.O. Kim, and B.H. Choi, *Lake Sihwa tidal power plant project.* Ocean Engineering, 2010. 37(5): p. 454-463.

29.   Ani. *India's first ocean power generation project coming up in Kavaratti, Lakshadweep.* Business Standard News September 22, 2016.

30.   Owens, W. and L. Trimble, *Mini-OTEC operational results.* Journal of Solar Energy Engineering, 1981. 103(3): p. 233-240.

31.   Ji, P., X.X. Zhou, and S. Wu. *Review on sustainable development of island microgrid.* in *Advanced Power System Automation and Protection (APAP), 2011 International Conference on.* 2011. IEEE.

32.   Raju, V. and M. Ravindran, *Ocean energy in the Indian context.* Mahasagar, 1985. 18(2): p. 211-217.

33.   Masutani, S.M. and P.K. Takahashi, *Ocean thermal energy conversion(OTEC).* Wiley Encyclopedia of Electrical and Electronics Engineering, 1999.

34.   Carlson, O., et al., *Harnessing energy flows: technologies for renewable power production.* 2014.

35.   Mutair, S. and Y. Ikegami, *Experimental study on flash evaporation from superheated water jets: Influencing factors and formulation of correlation.* International Journal of Heat and Mass Transfer, 2009. 52(23): p. 5643-5651.

36.   Anderson, D.E., *Solar energy conversion system*, 1975, Google Patents.

37.   Conserve-Energy-Future, *Advantages Of Solar Energy- Conserve Energy Future*, 2013.

38.   Markham, D., and Derek Markham. CleanTechnica. N.p., 2015. Web, *How Long Will Solar Panels Last.* 2015.

39.   Struckmann, F., *Analysis of a Flat-plate Solar Collector.* Project Report, 2008.

40.   Mathiaragan2, H.V.a.D.P., *Experimental Study on a Flat Plate Solar Collector.* International Journal of Mechanical Engineering and Research. Volume 3,(Number 6): p. 641-646.

41.   Kessentini, H., et al., *Numerical and experimental study of a flat plate solar collector with transparent insulation and overheating protection system.* 2011.

42. Muzathik, A.M., *Potential of global solar radiation in Terengganu, Malaysia.* International Journal of Energy Engineering, 2013. 3(4): p. 130.

43. *Kota Bharu Sea Temperature January Average, Malaysia, Sea Temperatures.* 2016.

44. Yeh, R.-H., T.-Z. Su, and M.-S. Yang, *Maximum output of an OTEC power plant.* Ocean Engineering, 2005. 32(5-6): p. 685-700.

45. Wang, T., et al., *Performance analysis and improvement for CC-OTEC system.* Journal of Mechanical Science and Technology, 2010. 22(10): p. 1977-1983.

46. Ahmadi, P., I. Dincer, and M.A. Rosen, *Energy and exergy analyses of hydrogen production via solar-boosted ocean thermal energy conversion and PEM electrolysis.* International Journal of Hydrogen Energy, 2013. 38(4): p. 1795-1805.

47. Straatman, P.J. and W.G. van Sark, *A new hybrid ocean thermal energy conversion–Offshore solar pond (OTEC–OSP) design: A cost optimization approach.* Solar Energy, 2008. 82(6): p. 520-527.

48. Tinaikar, A., *Ocean Thermal Energy Conversion.* International Journal of Energy and Power Engineering, 2013. 2(4): p. 143.

49. Uehara, H., et al. *The experimental research on ocean thermal energy conversion using the Uehara cycle.* in *Procedings of International OTEC/DOWA Conference, Imari, Japan.* 1999.

50. Goto, S., et al., *Construction of simulation model for OTEC plant using Uehara cycle.* Electrical Engineering in Japan, 2011. 176(2): p. 1-13.

51. Kalina, A.I., *Generation of energy by means of a working fluid, and regeneration of a working fluid*, 1982, Google Patents.

52. Zhang, X., M. He, and Y. Zhang, *A review of research on the Kalina cycle.* Renewable and Sustainable Energy Reviews, 2012. 16(7): p. 5309-5318.

53. Mochida, Y., et al., *Performance of the Heat Exchangers of a 100-kW (Gross) OTEC Plant.* Journal of Solar Energy Engineering, 1984. 106(2): p. 187-192.

54. Kakac, S., H. Liu, and A. Pramuanjaroenkij, *Heat exchangers: selection, rating, and thermal design*2012: CRC press.

55.   Hettiarachchi, H.M., et al., *Optimum design criteria for an organic Rankine cycle using low-temperature geothermal heat sources.* Energy, 2007. 32(9): p. 1698-1706.

56.   Nihous, G. and L. Vega, *Design of a 100 MW OTEC-hydrogen plantship.* Marine structures, 1993. 6(2): p. 207-221.

57.   Nakamura, S., et al. *Simulation model of integrated OTEC and desalination plant and its application.* in *ICCAS-SICE, 2009.* 2009. IEEE.

58.   Farahat, S., F. Sarhaddi, and H. Ajam, *Exergetic optimization of flat plate solar collectors.* Renewable Energy, 2009. 34(4): p. 1169-1174.

59.   Bryden, I., T. Grinsted, and G. Melville, *Assessing the potential of a simple tidal channel to deliver useful energy.* Applied Ocean Research, 2004. 26(5): p. 198-204.

60.   Sharqawy, M.H., J.H. Lienhard, and S.M. Zubair, *Thermophysical properties of seawater: a review of existing correlations and data.* Desalination and Water Treatment, 2010. 16(1-3): p. 354-380.

APPENDIX A

Vapor Pressure and Boiling Point Elevation of Seawater

Vapor (saturation) pressure, kPa

Boiling point elevation, K

Temp, °C	Salinity, g/kg												
	0	10	20	30	40	50	60	70	80	90	100	110	120
0	0.611	0.608	0.604	0.601	0.597	0.593	0.590	0.586	0.582	0.578	0.575	0.571	0.567
10	1.228	1.221	1.214	1.207	1.199	1.192	1.185	1.177	1.170	1.162	1.154	1.147	1.139
20	2.339	2.325	2.312	2.298	2.284	2.270	2.256	2.242	2.228	2.213	2.199	2.184	2.169
30	4.247	4.222	4.197	4.172	4.147	4.122	4.096	4.070	4.044	4.018	3.992	3.965	3.938
40	7.384	7.341	7.298	7.255	7.211	7.167	7.123	7.078	7.033	6.987	6.941	6.895	6.848
50	12.351	12.279	12.207	12.135	12.062	11.988	11.914	11.839	11.763	11.687	11.610	11.532	11.454
60	19.946	19.829	19.713	19.596	19.478	19.359	19.239	19.118	18.996	18.873	18.749	18.624	18.497
70	31.201	31.018	30.837	30.654	30.470	30.284	30.096	29.907	29.716	29.523	29.329	29.133	28.935
80	47.415	47.139	46.863	46.585	46.305	46.022	45.737	45.449	45.159	44.866	44.571	44.273	43.972
90	70.182	69.776	69.368	68.957	68.542	68.124	67.701	67.276	66.846	66.413	65.975	65.534	65.089
100	101.418	100.835	100.245	99.651	99.052	98.447	97.837	97.221	96.601	95.974	95.343	94.705	94.062
110	143.376	142.558	141.725	140.884	140.037	139.182	138.320	137.450	136.572	135.687	134.793	133.892	132.982
120	198.665	197.541	196.386	195.222	194.048	192.863	191.668	190.463	189.246	188.019	186.782	185.533	184.272

Temp, °C	Salinity, g/kg												
	0	10	20	30	40	50	60	70	80	90	100	110	120
0	0.000	0.067	0.138	0.213	0.291	0.373	0.458	0.547	0.640	0.736	0.836	0.939	1.046
10	0.000	0.073	0.150	0.232	0.317	0.407	0.501	0.599	0.701	0.807	0.917	1.032	1.151
20	0.000	0.079	0.163	0.251	0.344	0.442	0.545	0.652	0.764	0.880	1.002	1.128	1.258
30	0.000	0.085	0.176	0.272	0.373	0.479	0.590	0.707	0.829	0.956	1.088	1.225	1.368
40	0.000	0.092	0.190	0.293	0.402	0.517	0.637	0.764	0.895	1.033	1.176	1.325	1.480
50	0.000	0.099	0.204	0.315	0.433	0.556	0.686	0.822	0.964	1.112	1.267	1.428	1.595
60	0.000	0.106	0.219	0.338	0.464	0.597	0.736	0.882	1.035	1.194	1.360	1.532	1.711
70	0.000	0.114	0.234	0.362	0.497	0.639	0.788	0.944	1.107	1.277	1.455	1.639	1.831
80	0.000	0.121	0.250	0.387	0.530	0.682	0.841	1.007	1.181	1.363	1.552	1.748	1.952
90	0.000	0.129	0.267	0.412	0.565	0.726	0.895	1.072	1.257	1.450	1.651	1.860	2.076
100	0.000	0.138	0.284	0.438	0.601	0.772	0.952	1.139	1.335	1.540	1.752	1.973	2.203
110	0.000	0.146	0.302	0.465	0.638	0.819	1.009	1.208	1.415	1.631	1.856	2.089	2.331
120	0.000	0.155	0.320	0.493	0.676	0.868	1.068	1.278	1.497	1.725	1.962	2.207	2.462

APPENDIX B

Density and Specific Volume of Seawater

Density, kg/m

Temp, °C	Salinity, g/kg												
	0	**10**	**20**	**30**	**40**	**50**	**60**	**70**	**80**	**90**	**100**	**110**	**120**
0	999.8	1007.9	1016.0	1024.0	1032.0	1040.0	1048.0	1056.1	1064.1	1072.1	1080.1	1088.1	1096.2
10	999.7	1007.4	1015.2	1023.0	1030.9	1038.7	1046.6	1054.4	1062.2	1070.1	1077.9	1085.7	1093.6
20	998.2	1005.7	1013.4	1021.1	1028.8	1036.5	1044.1	1051.8	1059.5	1067.2	1074.9	1082.6	1090.3
30	995.7	1003.1	1010.7	1018.2	1025.8	1033.4	1040.9	1048.5	1056.1	1063.6	1071.2	1078.7	1086.3
40	992.2	999.7	1007.1	1014.6	1022.1	1029.5	1037.0	1044.5	1052.0	1059.4	1066.9	1074.4	1081.8
50	988.0	995.5	1002.9	1010.3	1017.7	1025.1	1032.5	1039.9	1047.3	1054.7	1062.1	1069.5	1076.9
60	983.2	990.6	998.0	1005.3	1012.7	1020.0	1027.4	1034.7	1042.1	1049.5	1056.8	1064.2	1071.5
70	977.8	985.1	992.5	999.8	1007.1	1014.5	1021.8	1029.1	1036.5	1043.8	1051.2	1058.5	1065.8
80	971.8	979.1	986.5	993.8	1001.1	1008.5	1015.8	1023.1	1030.5	1037.8	1045.1	1052.5	1059.8
90	965.3	972.6	980.0	987.3	994.7	1002.0	1009.4	1016.8	1024.1	1031.5	1038.8	1046.2	1053.5
100	958.4	965.7	973.1	980.5	987.9	995.2	1002.6	1010.0	1017.4	1024.8	1032.2	1039.6	1047.0
110	950.9	958.3	965.8	973.2	980.6	988.1	995.5	1003.0	1010.4	1017.8	1025.3	1032.7	1040.2
120	943.1	950.6	958.1	965.6	973.1	980.6	988.1	995.6	1003.1	1010.6	1018.1	1025.6	1033.1

Specific volume, m³/kg

Temp, °C	Salinity, g/kg												
	0	**10**	**20**	**30**	**40**	**50**	**60**	**70**	**80**	**90**	**100**	**110**	**120**
0	0.00100	0.00099	0.00098	0.00098	0.00097	0.00096	0.00095	0.00095	0.00094	0.00093	0.00093	0.00092	0.00091
10	0.00100	0.00099	0.00099	0.00098	0.00097	0.00096	0.00096	0.00095	0.00094	0.00093	0.00093	0.00092	0.00091
20	0.00100	0.00099	0.00099	0.00098	0.00097	0.00096	0.00096	0.00095	0.00094	0.00094	0.00093	0.00092	0.00092
30	0.00100	0.00100	0.00099	0.00098	0.00097	0.00097	0.00096	0.00095	0.00095	0.00094	0.00093	0.00093	0.00092
40	0.00101	0.00100	0.00099	0.00099	0.00098	0.00097	0.00096	0.00096	0.00095	0.00094	0.00094	0.00093	0.00092
50	0.00101	0.00100	0.00100	0.00099	0.00098	0.00098	0.00097	0.00096	0.00095	0.00095	0.00094	0.00094	0.00093
60	0.00102	0.00101	0.00100	0.00099	0.00099	0.00098	0.00097	0.00097	0.00096	0.00095	0.00095	0.00094	0.00093
70	0.00102	0.00102	0.00101	0.00100	0.00099	0.00099	0.00098	0.00097	0.00096	0.00096	0.00095	0.00094	0.00094
80	0.00103	0.00102	0.00101	0.00101	0.00100	0.00099	0.00098	0.00098	0.00097	0.00096	0.00096	0.00095	0.00094
90	0.00104	0.00103	0.00102	0.00101	0.00101	0.00100	0.00099	0.00098	0.00098	0.00097	0.00096	0.00096	0.00095
100	0.00104	0.00104	0.00103	0.00102	0.00101	0.00100	0.00100	0.00099	0.00098	0.00098	0.00097	0.00096	0.00096
110	0.00105	0.00104	0.00104	0.00103	0.00102	0.00101	0.00100	0.00100	0.00099	0.00098	0.00098	0.00097	0.00096
120	0.00106	0.00105	0.00104	0.00104	0.00103	0.00102	0.00101	0.00100	0.00100	0.00099	0.00098	0.00098	0.00097

APPENDIX C

Specific Internal Energy and Enthalpy of Seawater

Specific internal energy, kJ/kg

Temp, °C	Salinity, g/kg												
	0	**10**	**20**	**30**	**40**	**50**	**60**	**70**	**80**	**90**	**100**	**110**	**120**
10	42.0	41.2	40.5	39.7	39.0	38.2	37.5	36.7	36.0	35.2	34.5	33.7	33.0
20	83.9	82.7	81.4	80.2	78.9	77.7	76.5	75.2	74.0	72.8	71.5	70.3	69.1
30	125.7	124.0	122.3	120.6	118.8	117.1	115.4	113.7	112.0	110.2	108.5	106.8	105.1
40	167.5	165.3	163.1	160.9	158.7	156.5	154.3	152.1	149.9	147.7	145.5	143.3	141.1
50	209.3	206.6	203.9	201.3	198.6	195.9	193.2	190.5	187.8	185.1	182.4	179.8	177.1
60	251.1	248.0	244.8	241.6	238.4	235.3	232.1	228.9	225.8	222.6	219.4	216.2	213.1
70	293.0	289.3	285.7	282.0	278.4	274.7	271.0	267.4	263.7	260.1	256.4	252.8	249.1
80	334.9	330.7	326.6	322.5	318.3	314.2	310.0	305.9	301.8	297.6	293.5	289.4	285.2
90	376.9	372.3	367.6	363.0	358.4	353.8	349.1	344.5	339.9	335.3	330.7	326.0	321.4
100	419.0	413.9	408.8	403.7	398.6	393.5	388.4	383.3	378.2	373.0	367.9	362.8	357.7
110	461.2	455.6	450.0	444.4	438.9	433.3	427.7	422.1	416.5	410.9	405.3	399.7	394.2
120	503.6	497.5	491.4	485.4	479.3	473.2	467.2	461.1	455.0	448.9	442.9	436.8	430.7

Specific enthalpy, kJ/kg

Temp, °C	Salinity, g/kg												
	0	**10**	**20**	**30**	**40**	**50**	**60**	**70**	**80**	**90**	**100**	**110**	**120**
10	42.1	41.4	40.6	39.8	39.1	38.3	37.6	36.8	36.1	35.3	34.6	33.8	33.1
20	84.0	82.8	81.5	80.3	79.0	77.8	76.6	75.3	74.1	72.9	71.6	70.4	69.1
30	125.8	124.1	122.4	120.7	118.9	117.2	115.5	113.8	112.1	110.3	108.6	106.9	105.2
40	167.6	165.4	163.2	161.0	158.8	156.6	154.4	152.2	150.0	147.8	145.6	143.4	141.2
50	209.4	206.7	204.0	201.4	198.7	196.0	193.3	190.6	187.9	185.2	182.5	179.8	177.2
60	251.2	248.1	244.9	241.7	238.5	235.4	232.2	229.0	225.9	222.7	219.5	216.3	213.2
70	293.1	289.4	285.8	282.1	278.5	274.8	271.1	267.5	263.8	260.2	256.5	252.9	249.2
80	335.0	330.8	326.7	322.6	318.4	314.3	310.1	306.0	301.9	297.7	293.6	289.5	285.3
90	377.0	372.4	367.7	363.1	358.5	353.9	349.2	344.6	340.0	335.4	330.8	326.1	321.5
100	419.1	414.0	408.9	403.8	398.7	393.6	388.5	383.4	378.3	373.1	368.0	362.9	357.8
110	461.4	455.8	450.2	444.6	439.0	433.4	427.8	422.2	416.6	411.1	405.5	399.9	394.3
120	503.8	497.7	491.6	485.6	479.5	473.4	467.3	461.3	455.2	449.1	443.1	437.0	430.9

APPENDIX D

Latent Heat of Vaporization and Specific Entropy of Seawater

Latent heat of vaporization, kJ/kg

Temp, ºC	Salinity, g/kg												
	0	10	20	30	40	50	60	70	80	90	100	110	120
0	2500.9	2475.9	2450.9	2425.9	2400.9	2375.9	2350.8	2325.8	2300.8	2275.8	2250.8	2225.8	2200.8
10	2477.2	2452.5	2427.7	2402.9	2378.1	2353.4	2328.6	2303.8	2279.0	2254.3	2229.5	2204.7	2180.0
20	2453.6	2429.0	2404.5	2379.9	2355.4	2330.9	2306.3	2281.8	2257.3	2232.7	2208.2	2183.7	2159.1
30	2429.8	2405.5	2381.2	2356.9	2332.6	2308.3	2284.0	2259.7	2235.4	2211.1	2186.8	2162.5	2138.2
40	2406.0	2381.9	2357.9	2333.8	2309.7	2285.7	2261.6	2237.6	2213.5	2189.4	2165.4	2141.3	2117.3
50	2382.0	2358.1	2334.3	2310.5	2286.7	2262.9	2239.0	2215.2	2191.4	2167.6	2143.8	2120.0	2096.1
60	2357.7	2334.1	2310.5	2287.0	2263.4	2239.8	2216.2	2192.7	2169.1	2145.5	2121.9	2098.3	2074.8
70	2333.1	2309.8	2286.4	2263.1	2239.8	2216.4	2193.1	2169.8	2146.4	2123.1	2099.8	2076.5	2053.1
80	2308.1	2285.0	2261.9	2238.8	2215.8	2192.7	2169.6	2146.5	2123.4	2100.4	2077.3	2054.2	2031.1
90	2282.6	2259.7	2236.9	2214.1	2191.3	2168.4	2145.6	2122.8	2100.0	2077.1	2054.3	2031.5	2008.7
100	2256.5	2233.9	2211.3	2188.8	2166.2	2143.7	2121.1	2098.5	2076.0	2053.4	2030.8	2008.3	1985.7
110	2229.7	2207.4	2185.1	2162.8	2140.5	2118.2	2095.9	2073.6	2051.3	2029.0	2006.7	1984.4	1962.1
120	2202.1	2180.1	2158.1	2136.1	2114.1	2092.0	2070.0	2048.0	2026.0	2003.9	1981.9	1959.9	1937.9

Specific entropy, kJ/kg K

Temp, ºC	Salinity, g/kg												
	0	10	20	30	40	50	60	70	80	90	100	110	120
10	0.151	0.152	0.150	0.146	0.141	0.135	0.128	0.121	0.113	0.105	0.096	0.086	0.076
20	0.296	0.295	0.291	0.286	0.279	0.271	0.263	0.254	0.244	0.234	0.224	0.213	0.201
30	0.437	0.433	0.428	0.420	0.412	0.403	0.393	0.382	0.371	0.360	0.348	0.336	0.323
40	0.572	0.567	0.560	0.551	0.541	0.530	0.519	0.507	0.495	0.482	0.469	0.456	0.442
50	0.704	0.697	0.688	0.678	0.666	0.654	0.642	0.628	0.615	0.601	0.587	0.573	0.557
60	0.831	0.823	0.813	0.801	0.788	0.775	0.761	0.746	0.732	0.717	0.701	0.686	0.669
70	0.955	0.945	0.934	0.921	0.907	0.892	0.877	0.861	0.845	0.829	0.812	0.795	0.777
80	1.075	1.064	1.051	1.037	1.022	1.006	0.989	0.972	0.955	0.937	0.919	0.901	0.882
90	1.193	1.180	1.166	1.150	1.133	1.116	1.098	1.080	1.061	1.042	1.023	1.003	0.983
100	1.307	1.293	1.277	1.260	1.242	1.223	1.204	1.184	1.164	1.144	1.123	1.101	1.079
110	1.419	1.403	1.386	1.367	1.348	1.327	1.307	1.285	1.263	1.241	1.219	1.195	1.171
120	1.528	1.511	1.492	1.472	1.450	1.428	1.406	1.382	1.359	1.335	1.310	1.285	1.259

APPENDIX E

Specific Heat and Thermal Conductivity of Seawater

Specific heat at constant pressure, J/kg K

Temp, °C	Salinity, g/kg												
	0	10	20	30	40	50	60	70	80	90	100	110	120
0	4206.8	4142.1	4079.9	4020.1	3962.7	3907.8	3855.3	3805.2	3757.6	3712.4	3669.7	3629.3	3591.5
10	4196.7	4136.7	4078.8	4022.8	3968.9	3916.9	3867.1	3819.2	3773.3	3729.5	3687.7	3647.9	3610.1
20	4189.1	4132.8	4078.2	4025.3	3974.1	3924.5	3876.6	3830.4	3785.9	3743.0	3701.8	3662.3	3624.5
30	4183.9	4130.5	4078.5	4027.8	3978.6	3930.8	3884.4	3839.4	3795.8	3753.6	3712.7	3673.3	3635.3
40	4181.0	4129.7	4079.6	4030.7	3982.9	3936.4	3891.0	3846.7	3803.7	3761.8	3721.1	3681.6	3643.2
50	4180.6	4130.8	4081.9	4034.1	3987.3	3941.5	3896.6	3852.9	3810.1	3768.3	3727.5	3687.8	3649.0
60	4182.7	4133.7	4085.5	4038.3	3992.0	3946.5	3902.0	3858.3	3815.5	3773.7	3732.7	3692.6	3653.4
70	4187.1	4138.5	4090.6	4043.6	3997.3	3951.9	3907.4	3863.6	3820.6	3778.5	3737.2	3696.7	3657.0
80	4194.0	4145.3	4097.3	4050.1	4003.7	3958.1	3913.3	3869.2	3825.9	3783.5	3741.7	3700.8	3660.7
90	4203.4	4154.2	4105.9	4058.3	4011.5	3965.4	3920.2	3875.7	3832.0	3789.1	3746.9	3705.6	3665.0
100	4215.2	4165.4	4116.4	4068.2	4020.9	3974.3	3928.5	3883.6	3839.4	3796.0	3753.5	3711.7	3670.8
110	4229.4	4178.8	4129.1	4080.2	4032.2	3985.1	3938.7	3893.3	3848.6	3804.9	3761.9	3719.9	3678.6
120	4246.1	4194.7	4144.2	4094.6	4045.9	3998.2	3951.3	3905.4	3860.3	3816.2	3773.0	3730.7	3689.4

Thermal conductivity, W/m K

Temp, °C	Salinity, g/kg												
	0	10	20	30	40	50	60	70	80	90	100	110	120
0	0.572	0.571	0.570	0.570	0.569	0.569	0.568	0.568	0.567	0.566	0.566	0.565	0.565
10	0.588	0.588	0.587	0.587	0.586	0.585	0.585	0.584	0.584	0.583	0.583	0.582	0.582
20	0.604	0.603	0.602	0.602	0.601	0.601	0.600	0.600	0.599	0.599	0.598	0.598	0.597
30	0.617	0.617	0.616	0.616	0.615	0.615	0.614	0.614	0.613	0.613	0.612	0.612	0.611
40	0.630	0.629	0.629	0.628	0.628	0.627	0.627	0.626	0.626	0.625	0.625	0.624	0.624
50	0.641	0.640	0.640	0.639	0.639	0.638	0.638	0.637	0.637	0.636	0.636	0.635	0.635
60	0.650	0.650	0.649	0.649	0.648	0.648	0.647	0.647	0.647	0.646	0.646	0.645	0.645
70	0.658	0.658	0.658	0.657	0.657	0.656	0.656	0.655	0.655	0.655	0.654	0.654	0.653
80	0.665	0.665	0.665	0.664	0.664	0.663	0.663	0.663	0.662	0.662	0.661	0.661	0.661
90	0.671	0.671	0.670	0.670	0.670	0.669	0.669	0.669	0.668	0.668	0.667	0.667	0.667
100	0.676	0.675	0.675	0.675	0.674	0.674	0.674	0.673	0.673	0.673	0.672	0.672	0.672
110	0.679	0.679	0.679	0.678	0.678	0.678	0.677	0.677	0.677	0.676	0.676	0.676	0.675
120	0.682	0.681	0.681	0.681	0.680	0.680	0.680	0.679	0.679	0.679	0.679	0.678	0.678

APPENDIX F

Dynamic Viscosity and Kinematic Viscosity of Seawater

Dynamic viscosity x 10^3, kg/m s

Temp, ºC	Salinity, g/kg												
	0	**10**	**20**	**30**	**40**	**50**	**60**	**70**	**80**	**90**	**100**	**110**	**120**
0	1.791	1.820	1.852	1.887	1.925	1.965	2.008	2.055	2.104	2.156	2.210	2.268	2.328
10	1.306	1.330	1.355	1.382	1.412	1.443	1.476	1.511	1.548	1.586	1.627	1.669	1.714
20	1.002	1.021	1.043	1.065	1.089	1.114	1.140	1.168	1.197	1.227	1.259	1.292	1.326
30	0.797	0.814	0.832	0.851	0.871	0.891	0.913	0.936	0.960	0.984	1.010	1.037	1.064
40	0.653	0.667	0.683	0.699	0.716	0.734	0.752	0.771	0.791	0.812	0.833	0.855	0.878
50	0.547	0.560	0.573	0.587	0.602	0.617	0.633	0.649	0.666	0.684	0.702	0.721	0.740
60	0.466	0.478	0.490	0.502	0.515	0.528	0.542	0.556	0.571	0.586	0.602	0.618	0.635
70	0.404	0.414	0.425	0.436	0.447	0.459	0.471	0.484	0.497	0.510	0.524	0.538	0.553
80	0.354	0.364	0.373	0.383	0.393	0.404	0.415	0.426	0.437	0.449	0.462	0.474	0.487
90	0.315	0.323	0.331	0.340	0.349	0.359	0.369	0.379	0.389	0.400	0.411	0.422	0.434
100	0.282	0.289	0.297	0.305	0.313	0.322	0.331	0.340	0.350	0.359	0.369	0.380	0.390
110	0.255	0.262	0.269	0.276	0.283	0.291	0.299	0.308	0.316	0.325	0.334	0.344	0.354
120	0.232	0.238	0.245	0.251	0.258	0.265	0.273	0.280	0.288	0.297	0.305	0.314	0.323

Kinematic viscosity x 10^7, m^2/s

Temp, ºC	Salinity, g/kg												
	0	**10**	**20**	**30**	**40**	**50**	**60**	**70**	**80**	**90**	**100**	**110**	**120**
0	17.92	18.06	18.23	18.43	18.65	18.90	19.16	19.46	19.77	20.11	20.46	20.84	21.24
10	13.07	13.20	13.35	13.51	13.69	13.89	14.10	14.33	14.57	14.82	15.09	15.38	15.67
20	10.04	10.16	10.29	10.43	10.58	10.75	10.92	11.10	11.30	11.50	11.71	11.93	12.17
30	8.01	8.12	8.23	8.36	8.49	8.63	8.77	8.93	9.09	9.26	9.43	9.61	9.80
40	6.58	6.68	6.78	6.89	7.00	7.13	7.25	7.38	7.52	7.66	7.81	7.96	8.11
50	5.53	5.62	5.71	5.81	5.91	6.02	6.13	6.24	6.36	6.48	6.61	6.74	6.87
60	4.74	4.82	4.91	4.99	5.08	5.18	5.28	5.38	5.48	5.59	5.70	5.81	5.93
70	4.13	4.20	4.28	4.36	4.44	4.52	4.61	4.70	4.79	4.89	4.98	5.08	5.19
80	3.65	3.71	3.78	3.85	3.93	4.00	4.08	4.16	4.25	4.33	4.42	4.51	4.60
90	3.26	3.32	3.38	3.45	3.51	3.58	3.65	3.73	3.80	3.88	3.96	4.04	4.12
100	2.94	3.00	3.05	3.11	3.17	3.24	3.30	3.37	3.44	3.51	3.58	3.65	3.73
110	2.68	2.73	2.78	2.84	2.89	2.95	3.01	3.07	3.13	3.20	3.26	3.33	3.40
120	2.46	2.51	2.55	2.60	2.65	2.71	2.76	2.82	2.88	2.93	3.00	3.06	3.12

APPENDIX G

Surface Tension and Prandtl Number of Seawater

Surface tension x 10³, N/m

Temp, °C	Salinity, g/kg												
	0	**10**	**20**	**30**	**40**	**50**	**60**	**70**	**80**	**90**	**100**	**110**	**120**
0	75.65	75.85	76.01	76.14	76.25	76.35	76.43	76.51	76.57	76.64	76.69	76.75	76.80
10	74.22	74.47	74.66	74.82	74.96	75.07	75.17	75.26	75.35	75.42	75.49	75.56	75.62
20	72.74	73.03	73.25	73.44	73.59	73.73	73.85	73.96	74.05	74.14	74.22	74.30	74.37
30	71.19	71.53	71.78	71.99	72.17	72.32	72.46	72.58	72.69	72.79	72.88	72.97	73.05
40	69.60	69.97	70.25	70.49	70.68	70.86	71.01	71.14	71.26	71.38	71.48	71.57	71.66
50	67.94	68.35	68.66	68.92	69.13	69.32	69.49	69.64	69.77	69.89	70.01	70.11	70.21
60	66.24	66.68	67.01	67.29	67.53	67.73	67.91	68.07	68.21	68.35	68.47	68.58	68.69
70	64.48	64.95	65.31	65.61	65.86	66.07	66.27	66.44	66.59	66.73	66.87	66.99	67.10
80	62.67	63.17	63.55	63.87	64.13	64.36	64.56	64.75	64.91	65.06	65.20	65.33	65.44
90	60.82	61.34	61.74	62.07	62.35	62.59	62.80	62.99	63.16	63.32	63.47	63.60	63.73
100	58.91	59.45	59.87	60.22	60.51	60.76	60.98	61.18	61.36	61.52	61.67	61.81	61.95
110	56.96	57.52	57.96	58.31	58.61	58.87	59.10	59.31	59.50	59.67	59.82	59.97	60.10
120	54.97	55.54	55.99	56.36	56.67	56.93	57.17	57.38	57.57	57.75	57.91	58.06	58.20

Extrapolated data

Prandtl number

Temp, °C	Salinity, g/kg												
	0	**10**	**20**	**30**	**40**	**50**	**60**	**70**	**80**	**90**	**100**	**110**	**120**
0	13.18	13.21	13.25	13.31	13.40	13.50	13.63	13.78	13.94	14.13	14.34	14.56	14.81
10	9.32	9.36	9.41	9.48	9.56	9.65	9.76	9.87	10.00	10.14	10.30	10.46	10.64
20	6.95	7.00	7.06	7.12	7.19	7.27	7.36	7.46	7.56	7.67	7.79	7.92	8.05
30	5.40	5.45	5.51	5.57	5.63	5.70	5.78	5.86	5.94	6.03	6.13	6.23	6.33
40	4.34	4.38	4.43	4.49	4.54	4.60	4.67	4.74	4.81	4.88	4.96	5.04	5.13
50	3.57	3.61	3.66	3.71	3.76	3.81	3.87	3.93	3.99	4.05	4.12	4.18	4.25
60	3.00	3.04	3.08	3.12	3.17	3.22	3.27	3.32	3.37	3.42	3.48	3.54	3.60
70	2.57	2.60	2.64	2.68	2.72	2.76	2.81	2.85	2.90	2.94	2.99	3.04	3.09
80	2.23	2.27	2.30	2.33	2.37	2.41	2.45	2.49	2.53	2.57	2.61	2.66	2.70
90	1.97	2.00	2.03	2.06	2.09	2.13	2.16	2.20	2.23	2.27	2.31	2.35	2.39
100	1.76	1.78	1.81	1.84	1.87	1.90	1.93	1.96	1.99	2.03	2.06	2.10	2.13
110	1.59	1.61	1.63	1.66	1.69	1.71	1.74	1.77	1.80	1.83	1.86	1.89	1.93
120	1.45	1.47	1.49	1.51	1.54	1.56	1.59	1.61	1.64	1.67	1.70	1.73	1.76

.

APPENDIX H

OTEC Simulation Process Flow Chart

```
                    ┌──────────────────┐
                    (      Start        )
                    └──────────────────┘
                             │
                             ▼
                    ╱───────────────────╲
                   ╱    Input data        ╲
                   ╲  T_wsi, T_csi, m_ws, m_cs ╱
                    ╲───────────────────╱
                             │
                             ▼
                    ┌──────────────────┐
           ┌───────►│ Guess T_wso,T_cso │
           │        └──────────────────┘
           │                 │
           │                 ▼
           │        ┌──────────────────┐
           │        │ Calculate water  │
           │        │   properties     │
           │        └──────────────────┘
           │                 │     E<0.0001 Secant method
           │                 ▼
           │        ┌──────────────────┐
           │        │ Calculate Q_E,T_E │◄──────┐
           │        └──────────────────┘        │
           │                 │                   │
           │                 ▼                   │
           │        ┌──────────────────┐        │
           │        │ Calculate Q_C,T_C │        │
           │        └──────────────────┘        │
           │                 │                   │
           │                 ▼                   │
           │        ┌──────────────────────┐    │
           │        │ Compute h1,h2,h3,h4,Qcwf │  │
           │        └──────────────────────┘    │
           │                 │                   │
   Update  │   NO            ▼                   │
 T_wso,T_cso│        ╱───────────────╲           │
           └───────◄  lQc-Qcwfl<E     ╲          │
                    ╲───────────────╱           │
                             │ YES               │
                             ▼    T_cso           │
                    ┌──────────────────┐         │
                    │  Compute Q_ewf    │         │
                    └──────────────────┘         │
                             │                    │
                             ▼          NO        │
                    ╱───────────────╲             │
                    ╲ I Q_E-Q_ewfl<E ╱───────────┘
                    ╲───────────────╱
                 T_wso    │ YES
                          ▼
                 ┌──────────────────────┐
                 │ End of OTEC Calculation│
                 └──────────────────────┘
```
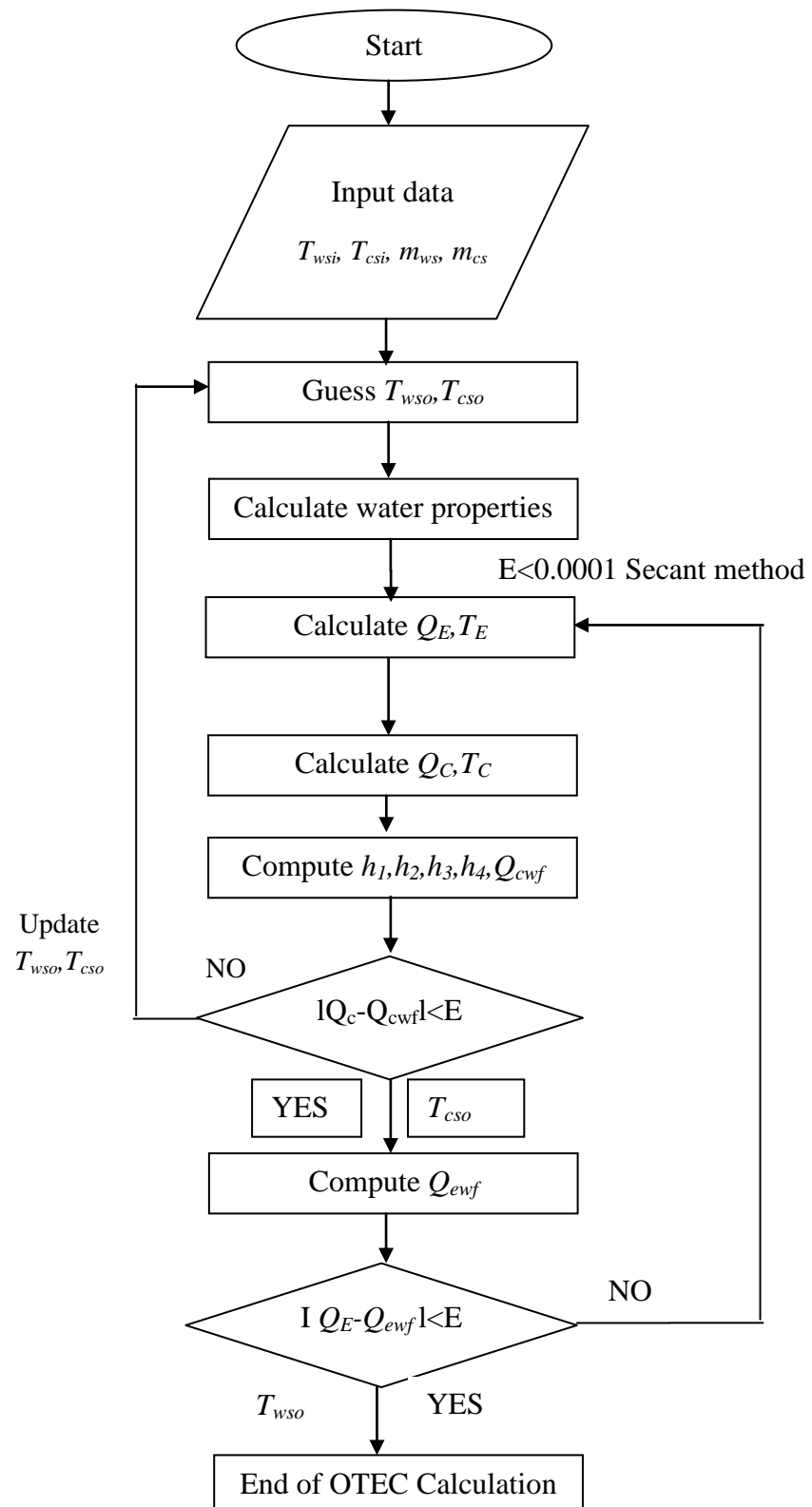
APPENDIX I

Process Flow Diagram for Closed Cycle SOTEC

APPENDIX J

Formulae and FORTRAN Subroutine

```
implicit real(a-z) !varibale declaration
call kpames(3,1)    !Temperature(c) Pressure(Pa) mass(kg)
call KPAMES(3,1)


This is calculation for preheated OTEC,BOOST 20K at theinlet of
turbine

mcs=400          !mass cold seawater flow rate,kg/s
mws=23.3         !mass warm seawater flow rate, kg/s
Dws =0.11        !Diameter of warm seawater pipe(m)
Dcs=0.6          !Diameter of cold seawater pipe(m)
NT=0.85          !turbine isentropic efficiency
NG=0.96          !generator mechanical efficiency
ETAp=0.85        !efficiency of all pumps
UAe=700000       !thermal conductance at evaporator, W/oC
UAc=2300000      !thermal conductance at condenser, W/oC
Ue=4300          !overall heat transfer coefficient,W/m2.oC
Uc=4000          !overall heat transfer coefficient,W/m2.oC
VwsPHE=0.475     !assumed seawater velocity at plate evaporator,m/s
VcsPHE=0.305     !assumed seawater velocity at plate condenser, m/s
Lp=4             !length of evaporator and condenser plate unit is
(m)
c=0.005          !c is clearance
Deqws=2*c
Deqcs=Deqws
CWPL=50          !cold water pipe length at MTJDA(m)
DepthCS=50       !depth of cold water intake at MTJDA(m)
WWPL=50          !warm water intake pipe length(m)
DepthWS=50       !depth of warm source intake point(m)
Nsc=0.68         !efficiency of solar collector based on collector
efficiency curve analysis flat plate
I=196.8          !solar radiation intensity,W/m2 in Malaysia,
AnnualPotential Global solar radiation in Terengganu.
Ta=25            !ambient temperature in Malaysia oC
Cpsc=4185.5      !Cp at constant pressure, kJ/kg.oC


open(30,file='Tsco.csv')

write(30,888)'mws',',',',','mcs',',',',','mwf',',',',','Tsco',',',',','Twso',',',',',

1Tcso',',',',','Tcsi',',',',','Qe',',',',','Qewf',',',',','Qc',',',',','Qcwf',',',',','Wtur

     2',',',',','WPwf',',',',','WPcs',',',',','WPws',',',',','NR',',',',','Nnet',',',',','TE

3',',',',','TC',',',',','Ae',',',',','Ac',',',',','Wnet',',',',','Qu',',',',','Dws',',',',','As

     4c'

open(20,file='mass energy balance.csv')

write(20,999)'P1',',',',','P2',',',',','P3',',',',','P4',',',',','T1',',',',','T2',',',',

1,'T3',',',',','T4',',',',','h1',',',',','h2',',',',','h3',',',',','h4',',',',','s1',',',',',

2s2',',',',','s3',',',',','s4',',',',','v1',',',',','v2',',',',','v3',',',',','v4',',',',','Wp'

     3,',',',','Wtur'
```

```fortran
Tsco=66.7
Tcsi=26.7


do 200 K=0.1,3.0,0.1
mwf=K

!!!!!!!!!!!!!!!!!!!!! CALCULATION OF QE & QC !!!!!!!!!!!!!!!!!!!!!

ATcso=26.8      !Old assumption of Tcso
AErrc=10000     !Old assumption of Errc value that corresponds to
ATcso
ATwso=66.6      !Old assumption of Twso
AErre=10000     !Old assumption of Erre value that corresponds to
ATwso


Twso=66.5       !Current assumption of Twso
Tcso=26.9       !Current assumption of Tcso




Call DensityDiff (DepthCS,HeqCS,XXX,Rhocs)
DHcsDen=HeqCS !Equavelent head difference in CWP due to density
difference

CALL PROPER (44.0,Tcsi,RAMDAL,ROLTcs,BMIULcs,BNIUL,CPLcsi,SIGMAL,
1              ROS,AMIUS,ANIUS,ALH,X10)

Acs=(Pi/4)*Dcs**2  ! cross section area of the main cold source pipe
Qcs=Mcs/Rhocs       ! Volumetric flow rate (m^3/s)
Vcs=Mcs/Acs/Rhocs  !Vcs: flow velocity in the main cold source pipe
Recs=Rhocs*Vcs*Dcs/BMIULcs
rough=0.03E-3      !Pipe roughness for Glass-fiber reinforced pipes
(GRP)
CALL DarcyWeisbach (Recs,Dcs,rough,fDW)
DHcsfric=fDW*(CWPL/Dcs)*Vcs**2/(2*g) ! DHcsfric: Modified frictional
Head loss in the cold source pipe

RecsPHE=Rhocs*VcsPHE*Deqcs/BMIULcs
fcs=4*0.678*RecsPHE**(-0.202)             ! friction factor Obtained
from Taborek 1988 for 60 degrees chevron plate (heat exchanger
design handbook)
DHcsPHE=fcs*(Lp/Deqcs)*(VcsPHE**2/(2*g))  ! DHcsPHE:Head loss at the
condenser (Seawater side)
!Deqcs: Water-side Equavelent diameter =2 times the clearance
beetween plates=2*bcs

DHcsTot=DHcsDen+DHcsFric+DHcsPHE

Call DensityDiff (DepthWS,HeqWS,Rhows,XXX)
DHwsDen=HeqWS        ! Equavelent head difference in WWP due to
density difference
```

```
CALL PROPER (44.0,Tsco,RAMDAL,ROLTws,BMIULws,BNIUL,CPLwsi,SIGMAL,
1 ROS,AMIUS,ANIUS,ALH,X10)
Aws=(Pi/4)*Dws**2  ! cross section area of the main warm source pipe
Qws=Mws/Rhows       ! Volumetric flow rate (m^3/s)
Vws=Mws/Aws/Rhows  !Vws: flow velocity in the main warm source pipe
Rews=Rhows*Vws*Dws/BMIULws
rough=0.03E-3      !Pipe roughness for Glass-fiber reinforced pipes
(GRP)
CALL DarcyWeisbach (Rews,Dws,rough,fDW)
DHwsfric=fDW*(WWPL/Dws)*Vws**2/(2*g) ! DHwsfric: Modified frictional
Head loss in the warm source pipe


RewsPHE=Rhows*VwsPHE*Deqws/BMIULws
fws=4*0.678*RewsPHE**(-0.202)                ! Obtained from Taborek
1988 for 60 degrees chevron plate (heat exchanger design handbook)
DHwsPHE=fws*(Lp/Deqws)*(VwsPHE**2/(2*g))  ! DHwsPHE:Head loss at the
evaporator (Seawater side
! Deqws: Water-side Equavelent diameter =2 times the clearance
beetween plates=2*bws
DHwsTot=DHwsDen+DHwsFric+DHwsPHE


     absErre=100
     do while (absErre>0.001)

*******Calculation of Physical properties of water*****************
     CALL PROPER (44.0,Tsco,RAMDAL,ROL,BMIUL,BNIUL,CPLwsi,SIGMAL,
    1            ROS,AMIUS,ANIUS,ALH,PS)
     Qe=mws*CPLwsi*(Tsco-Twso)
     LMTDe=Qe/(UAe)
     X=exp((Tsco-Twso)/(LMTDe))
     TE=(X*Twso-Tsco)/(X-1)


             absErrc=10
        do while (absErrc>0.01)
        CALL PROPER
(44.0,Tcsi,RAMDAL,ROL,BMIUL,BNIUL,CPLcsi,SIGMAL,
    1            ROS,AMIUS,ANIUS,ALH,PS)
        Qc=mcs*CPLcsi*(Tcso-Tcsi)
        LMTDc=Qc/(UAc)
        Y=exp((Tcso-Tcsi)/LMTDc)
        Tc=((Tcso*Y)-Tcsi)/(Y-1)



!!!!!!!!!!!Calculation quantity of state!!!!!!!!!!!!!!!!!!!!!!


     !!!!!!******Point 1 Saturated vapor********!!!!!!
```

```
      T1=TE            !Saturated vapor temperature,TE
      P1=PST(T1)       !Saturated vapor pressure,TE (Pa)
      h1=HTDD(T1)      !Specific enthalpy of saturated vapor(J/kg)
      s1=STDD(T1)      !Specific entropy of saturated vapor (J/kg.K)
      v1=VPDD(P1)      !Specific volume of saturated vapor(m^3/kg)
      rho1=1.0/v1      !Density(kg/m^3)


      !!!!!!******Point 3 Saturated liquid********!!!!!!

      T3=TC            !Saturated liquid temperature,TC
      P3=PST(T3)       !Saturated liquid pressure,TC (Pa)
      h3=HTD(T3)       !Specific enthalpy of saturated liquid(J/kg)
      s3=STD(T3)       !Specific entropy of saturated liquid (J/kg.K)
      v3=VPD(P3)       !Specific volume of saturated liquid(m^3/kg)
      rho3=1.0/v3      !Density(kg/m^3)



      !!!!!!******Point 2 Wet vapor********!!!!!!


      T2=TC
      s2=s1       !Both value are same because of isentropic
expansion
      P2=P3       !Both value are same because of constant pressure
heat    rejection
      P22=PST(T2)      !Another way to calculate pressure,P
      X2=XPS(P2,s2)    !Dryness fraction,x
      h2=HPX(P2,X2)    !Specific enthalpy of mixture
      h22=HTX(T2,X2)   !Another possible way to calculate Specific
enthalpy of mixture
      v2=VTX(T2,X2)    !Specific volume(m^3/kg)
      v22=VPX(P2,X2)   !Another way to find Specific volume(m^3/kg)
      rho2=1.0/v2      !Density kg/m^3



      !!!!!!******Point 4 Compressed liquid********!!!!!!

      s4=s3            !Isentopic compression
      P4=P1            !Constant pressure heat addition
      v4=v3            !Specific volume
      T4=TPS(P4,s4)    !Temperature
      v4=VPS(P4,s4)    !Another way to calculate specific volume
      v44=VPT(P4,T4)   !Another way to calculate specific volume
      Wp=v4*(P4-P3)
      h4=h3+Wp         !Calculation of h4
      T44=TPH(P4,h4)   !Another way to calculate T4
      rho4=1.0/v4      !Density kg/m^3




   Qcwf=mwf*(h2-h3)

          Errc=(Qc-Qcwf)/Qc
```

Mass and energy balance at condenser

```
          absErrc=abs(Errc)
      IF(Errc-AErrc.EQ.0.0000000000) then
      go to 777
      ElseIF(Errc.EQ.0.0) then
      go to 777
      else
CTcso=Tcso-(Tcso-ATcso)/(Errc-AErrc)*Errc !Updated assumption for
Tcso calculated using Secant method
end if
      ATcso=Tcso
      AErrc=Errc
      Tcso=CTcso
end do          ! cold source outlet temp. adjustment loop
      Tcso=ATcso              ! restore the last Tcso value that has
achieve heat balance
```

Mass and energy balance at evaporator

```
777   Qewf=mwf*(h1-h4)

      Erre=(Qe-Qewf)/Qe
      absErre=abs(Erre)

      CTwso=Twso-(Twso-ATwso)/(Erre-AErre)*Erre !Updated assumption
for Twso calculated using Secant method
      ATwso=Twso
      AErre=Erre
      Twso=CTwso             ! Warm source outlet temp. adjustment loop
      end do
      Twso=ATwso


      !!!!!!!Heat Transfer area of evaporator!!!!!!


      Wtur=mwf*(h1-h2)*NT*NG/1000 ! Turbine Power (kW)
      WPws=mws*9.81*DHwsTot/ETAp/1000 ! Warm source pumping power
(kW)
      WPcs=mcs*9.81*DHcsTot/ETAp/1000 ! Cold source pumping power
(kW)
      WPwf=mwf*WP*ETAwf/1000          ! Working Fluid pumping power
(kW)
      Wnet=Wtur-(WPws+WPcs+WPwf)
      Qe=Qe/1000
      Qewf=Qewf/1000
      Qc=Qc/1000
      Qcwf=Qcwf/1000
      Nnet=(Wnet/Qe)*100
      NR=(Wtur/Qe)*100
      Qu=mws*Cpsc*40
      Asc=Qu/(Nsc*I)
```

Calculation for solar energy

```
      write(*,*)'        mwf,         DelTws,         DelTcso,
      write(*,*)K,Tsco-Twso,Tcso-Tcsi,Qe,Qc
      write(*,*)
      write(*,*)'      Wtur,      Wnet,          Nth'
      write(*,*)Wtur,Wnet,Nnet
      write(*,*)'---------------------------------------------
      write(*,*)
```

```
write(30,300)mws,',',mcs,',',mwf,',',Tsco,',',Twso,',',Tcso,',',

1Tcsi,',',Qe,',',Qewf,',',Qc,',',Qcwf,',',Wtur,',',WPwf,',',WPcs

2,',',WPws,',',NR,',',Nnet,',',TE,',',TC,',',Ae,',',Ac,',',Wnet,','
    3,Qu,',',Dws,',',Asc


write(20,300)P1,',',P2,',',P3,',',P4,',',T1,',',T2,',',T3,',',T4,'

1,'h1,',',h2,',',h3,',',h4,',',s1,',',s2,',',s3,',',s4,',,',v1,','
    2,v2,',',v3,',',v4,',',Wp,',',Wtur


  300  format(25(f30.10,a1))
  888  Format (A10,25(A1,A10))
  999  Format (A10,25(A1,A10))
  200 continue
      pause
      stop
      end


******** Subroutine for the evaluation of the physical properties of
water and seawater ********

      SUBROUTINE PROPER (FLUID,TR,RAMDAL,ROL,BMIUL,BNIUL,CPLX,SIGMA,
     1ROS,AMIUS,ANIUS,ALHX,PS)
      IMPLICIT DOUBLE PRECISION (A-H,O-Z)
      REAL FLUID,TR,RAMDAL,ROL,BMIUL,BNIUL,CPL,SIGMA,
     1ROS,AMIUS,ANIUS,ALH,PS,CPLX,ALHX
      IF(FLUID.EQ. 44.0) GO TO 10 ! seawater
      IF(FLUID.EQ.  1.0) GO TO 80

   10 SALINI=35
      IF(TR.GE.90.0) TR=90.0
C     PROPERTY OF SEAWATER
      IF (SALINI.EQ.35.0) GO TO 351
      GO TO 100
C  SALINITY   5 (G/KG)
   51 ROL=0.1003980E+04+0.4696572E-01*TR-0.8620546E-02*TR**2
    1    +0.8982789E-04*TR**3-0.7479379E-06*TR**4
      BMIUL=0.180300E-02-0.717149E-04*TR+0.559582E-05*TR**2
    1      -0.641336E-06*TR**3+0.464173E-07*TR**4-0.182721E-
08*TR**5
    2      +0.362904E-10*TR**6-0.284084E-12*TR**7
      BNIUL=BMIUL/ROL
      CPL=(0.99840E+00-0.71284E-03*TR+0.42115E-04*TR**2
    1-0.17541E-05*TR**3+0.42049E-07*TR**4-0.39993E-09*TR**5)
      GO TO 100
C  SALINITY  10 (G/KG)
```

```
  101 ROL=0.1008021E+04+0.1743389E-01*TR-0.4373244E-02*TR**2
     1     -0.3387101E-03*TR**3+0.1760159E-04*TR**4-0.2695644E-
06*TR**5
      BMIUL=0.181700E-02-0.712387E-04*TR+0.548122E-05*TR**2
     1       -0.639825E-06*TR**3+0.470923E-07*TR**4-0.187341E-
08*TR**5
     2       +0.374503E-10*TR**6-0.294369E-12*TR**7
      BNIUL=BMIUL/ROL
      CPL=(0.989499E+00-0.333360E-03*TR-0.483233E-06*TR**2
     1+0.816571E-06*TR**3-0.267954E-07*TR**4+0.259222E-09*TR**5)
      SIGMA=0.75860E-01-0.14400E-03*TR+0.20571E-15*TR**2
      GO TO 100
C   SALINITY   15 (G/KG)
  151 ROL=0.1012050E+04+0.127410E-01*TR-0.8268747E-02*TR**2
     1     +0.9999561E-04*TR**3-0.9882334E-06*TR**4
      CPL=(0.981194E+00-0.222857E-03*TR+0.557143E-05*TR**2)
      GO TO 100
C   SALINITY   20 (G/KG)
  201 RAMDAL=0.48810E+00+0.15550E-02*TR-0.62500E-05*TR**2
      RAMDAL=RAMDAL*4186.8/3600.0  ! Conversion from kcal/(h.m.K) to
W/(m.K)
      ROL=0.1016070E+04-0.3560383E-02*TR-0.8102232E-02*TR**2
     1     +0.1059282E-03*TR**3-0.1149564E-05*TR**4
      BMIUL=0.184400E-02-0.208556E-03*TR+0.663437E-04*TR**2
     1       -0.106683E-04*TR**3+0.886650E-06*TR**4-0.414219E-
07*TR**5
     2       +0.110045E-08*TR**6-0.155225E-10*TR**7+0.902329E-
13*TR**8
      BNIUL=BMIUL/ROL
      CPL=(0.973300E+00-0.253481E-03*TR+0.348900E-04*TR**2
     1-0.224275E-05*TR**3+0.660551E-07*TR**4-0.688889E-09*TR**5)
      SIGMA=0.76080E-01-0.14400E-03*TR+0.20571E-15*TR**2
      GO TO 100
C   SALINITY   25 (G/KG)
  251 ROL=0.1020080E+04-0.1882752E-01*TR-0.7812505E-02*TR**2
     1     +0.9834211E-04*TR**3-0.1023533E-05*TR**4
      CPL=(0.965899E+00-0.661847E-04*TR-0.215563E-05*TR**2
     1+0.890740E-06*TR**3-0.365988E-07*TR**4+0.441238E-09*TR**5)
      GO TO 100
C   SALINITY   40 (G/KG)
  401 RAMDAL=0.48600E+00+0.15750E-02*TR-0.62500E-05*TR**2 !Unit is
(kcal/(h.m.K))
      RAMDAL=RAMDAL*4186.8/3600.0  ! Conversion from kcal/(h.m.K) to
W/(m.K)
      ROL=0.1032180E+04-0.6737594E-01*TR-0.6883186E-02*TR**2
     1     +0.8069219E-04*TR**3-0.7952872E-06*TR**4
      ROS=4.8536E-03+3.2530E-04*TR+1.1621E-05*TR**2+9.3579E-08*TR**3
     1+3.4389E-09*TR**4-1.2389E-12*TR**5
      BMIUL=0.1883000E-02-0.6538610E-04*TR+0.4118355E-05*TR**2
     1       -0.4903490E-06*TR**3+0.3778692E-07*TR**4-0.1542398E-
08*TR**5
     2       +0.3120905E-10*TR**6-0.2464408E-12*TR**7
      IF (TR.LE.40.0) GO TO 405
      BMIUL=0.1228E-02-0.1263E-04*TR
  405 BNIUL=BMIUL/ROL
      CPL=(0.945300E+00+0.110916E-03*TR+0.505155E-06*TR**2
```

```
      1+0.436303E-07*TR**3-0.444281E-09*TR**4)
      SIGMA=0.76520E-01-0.14400E-03*TR+0.20571E-15*TR**2
C     ALH OF WATER
      ALH=(5.9728E+02-5.6615E-01*TR)
      GO TO 100
   80 TR=TR
!******The approximation formula of thermal conductivity is
corrected.********
      A0=0.561891472159546
      A1=0.0021543458570851
      A2=-1.51193100021209E-05
      A3=9.96463343192303E-08
      A4=-8.0045775777346E-10
      A5=4.28768613386017E-12
      A6=-1.26948021722228E-14
      A7=1.55916951042287E-17
!
      RAMDAL=A0+A1*TR+A2*TR**2+A3*TR**3+A4*TR**4+A5*TR**5
     *       +A6*TR**6+A7*TR**7
!
      ROL=0.9999E+03+0.59855E-01*TR-0.90085E-02*TR**2+.11492E-
03*TR**3
     *-.14789E-05*TR**4+.83382E-08*TR**5
      BMIUL=.179364E-02-.658458E-04*TR+.270391E-05*TR**2-.136709E-06
     **TR**3+.510685E-08*TR**4-.108895E-09*TR**5+.117816E-11*TR**6
     *-.502007E-14*TR**7
      BNIUL=.179E-05-.61731E-07*TR+.193439E-08*TR**2-.810083E-
10*TR**3
     *+.31243E-11*TR**4-.714583E-13*TR**5+.818055E-15*TR**6-
.363095E-17
     **TR**7
      CPL=(.1008E+01-.613333E-03*TR-.200833E-04*TR**2+.331805E-
05*TR**3
     *-.145833E-06*TR**4+.313889E-08*TR**5-.333333E-10*TR**6+.138889
     *E-12*TR**7)
      SIGMA=.75707E-01-.12210E-03*TR-.60954E-05*TR**2+.31807E-
06*TR**3
     *-.64803E-08*TR**4+.44936E-10*TR**5
      ROS=4.8536E-03+3.2530E-04*TR+1.1621E-05*TR**2+9.3579E-08*TR**3
     *+3.4389E-09*TR**4-1.2389E-12*TR**5
      AMIUS=8.3821E-07+3.8214E-09*TR
      AMIUS=9.8*AMIUS
      ANIUS=1.7000E-03-1.0634E-04*TR+3.3806E-06*TR**2-6.287E-
08*TR**3
     *+6.3946E-10*TR**4-2.7232E-12*TR**5
      ALH=5.9728E+02-5.6615E-01*TR

      T=273.15+TR
      XT=647.31-(273.15+TR)
      PLOG=XT/T*(3.36311+.0466834*XT+1.23776E-04*XT**2-5.30465E-08
     **XT**3+2.50335E-10*XT**4)/(1.0+0.015527*XT+3.78297E-05*XT**2)
      PS=(225.65/10.0**PLOG)*100000.0 ! 100000 converts unit from
bar to pascal
      GO TO 100
!
  100 TR=TR
      CPLX=CPL*4186.8 !4186.8 Converts from kCal to J
      ALHX=ALH*4186.8 !4186.8 Converts from kCal to J
     !  RAMDALX=RAMDAL*4186.8/3600.0  ! Conversion from kcal/(h.m.K)
to W/(m.K)
```

```fortran
        RETURN
        END

        SUBROUTINE DensityDiff (Hr,Heq,Rhows,Rhocs)
        implicit real (a-h,k,l,m,n,o-z)
        real Rho(3000)

        A=1022.96633
        B=0.0139
        C=-1.57678E-5
        D=6.29198E-9

        g=9.81 ! Acceleration of gravity
        H=int(Hr)
        SumRho=0
        DY=1   ! Y interval length

        Do 100 Y=1,H,DY            ! this Do function is to calculate
the weight of the displaced water column (Upward force)

        Rho(y)=A+B*Y+C*Y**2+D*Y**3  ! fitting equation for density
calculation as function of depth

        SumRho=SumRho+Rho(y)
100     Continue
        Rhocs=Rho(H)
        Rhows=Rho(20)

        AvgRho=1/H*SumRho

        Fdn=1.0*g
        Qcs=1.0/Rhocs
        Fup=Qcs*g*AvgRho

        W=(Fdn-Fup)*H/1000        ! specific Pumping power kW/kg
=Force/kg times distance (note that F here is force per second)

        Heq=W*1000/g    ! Equavelent hydrostatic head of cold seawater
(m)

        Return
        end




        SUBROUTINE DarcyWeisbach (Re,d,Ks,fDW)

    !This Subroutine solves the Colebrook equation by itteration to
find the value of Darcy-Weisbach friction factor f



!The Colebrook equation is applied only for turbulent flow.
!This program uses the Secant method to determine the updated value
of the parameter f being looked for.
```

```fortran
      implicit real (a-h,k,o-z)

      dh=d

      Af=0.0000005 !Old assumption of (f) value
      AErrf=100    !Old assumption of Error value that corresponds
to f
      f=0.000001   !Current assumption of (f) value
      absErrf=10   !Current assumption of the error value


      do while (absErrf>0.0001)

      x=-2*log10(2.51/(Re*f**0.5)+(Ks/dh)/3.72)! x=1/SQRT(fDW)

      fDW=(1.0/x)**2.0

      Errf=abs(fDW-f)/f
      absErrf=abs(fDW-f)/f

      Cf=f-(f-Af)/(Errf-AErrf)*Errf !Updated assumption for (f)
calculated using Secant method

      Af=f
      AErrf=Errf
      f=Cf

      End do

      RETURN
      end
```

APPENDIX K

Mass and Energy Balance

				Mass and Heat Balance for Validated 100 kW OTEC					
				T_{wsi}=25.7°C, T_{csi}=4.4°C					
				m_{ws}=m_{cs}=260 kg/s					
m_{wf}	T_{wsi}	T_{wso}	T_{cso}	T_{csi}	Q_e	Q_{ewf}	Q_c	Q_{cwf}	W_{tur}
kg/s	°C	°C	°C	°C	kJ	kJ	kJ	kJ	kW
2.49	25.70	22.71	7.26	4.40	3086.20	3086.35	2945.75	2950.48	98.7
2.49	25.70	22.71	7.26	4.40	3087.45	3087.59	2946.92	2951.66	98.8
2.49	25.70	22.71	7.26	4.40	3088.69	3088.83	2948.09	2952.85	98.8
2.49	25.70	22.71	7.26	4.40	3089.93	3090.07	2949.26	2954.04	98.9
2.49	25.70	22.71	7.27	4.40	3091.17	3091.31	2950.44	2955.22	98.9
2.49	25.70	22.71	7.27	4.40	3092.41	3092.55	2951.61	2956.41	98.9
2.49	25.70	22.71	7.27	4.40	3093.65	3093.80	2952.78	2957.60	99.0
2.49	25.70	22.70	7.27	4.40	3094.89	3095.04	2953.95	2958.78	99.0
2.49	25.70	22.70	7.27	4.40	3096.13	3096.28	2955.12	2959.97	99.1
2.49	25.70	22.70	7.27	4.40	3097.37	3097.52	2956.30	2961.16	99.1
2.50	25.70	22.70	7.27	4.40	3098.61	3098.76	2957.47	2962.35	99.1
2.51	25.70	22.69	7.28	4.40	3111.02	3111.18	2969.19	2974.21	99.5
2.52	25.70	22.67	7.30	4.40	3125.91	3126.07	2983.24	2988.45	100.0
2.53	25.70	22.66	7.31	4.40	3135.83	3136.00	2992.61	2997.95	100.3
2.54	25.70	22.65	7.32	4.40	3148.24	3148.42	3004.31	3009.82	100.7
2.55	25.70	22.64	7.33	4.40	3160.65	3160.83	3016.01	3021.68	101.1
2.56	25.70	22.63	7.34	4.40	3173.05	3173.25	3027.72	3033.55	101.5
2.57	25.70	22.62	7.35	4.40	3185.46	3185.66	3039.41	3045.42	101.9
2.58	25.70	22.60	7.36	4.40	3197.86	3198.08	3051.10	3057.29	102.3
2.59	25.70	22.59	7.37	4.40	3210.27	3210.49	3062.79	3069.15	102.7
2.60	25.70	22.58	7.39	4.40	3222.67	3222.90	3074.47	3081.02	103.1
2.61	25.70	22.57	7.40	4.40	3235.08	3235.32	3086.15	3092.89	103.5
2.62	25.70	22.56	7.41	4.40	3247.48	3247.73	3097.83	3104.76	103.9
2.63	25.70	22.54	7.42	4.40	3259.88	3260.15	3109.50	3116.63	104.3
2.64	25.70	22.53	7.43	4.40	3272.29	3272.56	3121.17	3128.49	104.7
2.65	25.70	22.52	7.44	4.40	3284.69	3284.98	3132.83	3140.36	105.1
2.65	25.70	22.51	7.45	4.40	3295.85	3296.15	3143.32	3151.04	105.5
2.67	25.70	22.50	7.47	4.40	3309.49	3309.80	3156.15	3164.10	105.9
2.68	25.70	22.48	7.48	4.40	3321.90	3322.22	3167.80	3175.96	106.3
2.69	25.70	22.47	7.49	4.40	3334.30	3334.63	3179.44	3187.83	106.7
2.70	25.70	22.46	7.50	4.40	3347.94	3348.29	3192.25	3200.89	107.1
2.71	25.70	22.45	7.51	4.40	3360.34	3360.70	3203.89	3212.75	107.5
2.72	25.70	22.44	7.52	4.40	3372.74	3373.12	3215.52	3224.62	107.9
2.73	25.70	22.42	7.54	4.40	3386.38	3386.77	3228.31	3237.68	108.4
2.74	25.70	22.41	7.55	4.40	3398.78	3399.19	3239.93	3249.54	108.8
2.80	25.70	22.33	7.62	4.40	3481.84	3482.36	3317.69	3329.06	111.4
2.82	25.70	22.32	7.63	4.40	3495.47	3496.02	3330.44	3342.11	111.9
2.84	25.70	22.29	7.66	4.40	3520.26	3520.84	3353.59	3365.85	112.6
2.86	25.70	22.27	7.68	4.40	3545.05	3545.67	3376.73	3389.58	113.4
2.88	25.70	22.24	7.70	4.40	3569.83	3570.50	3399.85	3413.32	114.2

2.90	25.70	22.22	7.73	4.40	3595.85	3596.57	3424.10	3438.24	115.1
2.92	25.70	22.20	7.75	4.40	3620.63	3621.40	3447.17	3461.97	115.9
2.94	25.70	22.17	7.77	4.40	3644.17	3644.99	3469.07	3484.52	116.6
2.96	25.70	22.15	7.79	4.40	3668.94	3669.81	3492.10	3508.26	117.4
2.98	25.70	22.12	7.81	4.40	3693.71	3694.64	3515.11	3531.99	118.2
3.00	25.70	22.10	7.84	4.40	3718.48	3719.47	3538.09	3555.73	119.0

Mass and Heat Balance of 100 kW SOTEC system									
T_{sco}=66.7°C, T_{sci}=26.7°C									
m_{ws}=23.3 kg/s, m_{cs}=400 kg/s									
m_{wf}	T_{sco}	T_{wso}	T_{cso}	T_{csi}	Q_e	Q_{ewf}	Q_c	Q_{cwf}	W_{tur}
kg/s	°C	°C	°C	°C	kJ	kJ	kJ	kJ	kW
0.16	66.70	64.81	26.80	26.70	185.25	185.26	165.63	166.01	17.78
0.20	66.70	64.34	26.83	26.70	231.52	231.60	204.73	207.80	21.98
0.30	66.70	63.15	26.90	26.70	347.40	347.48	319.83	312.76	32.03
0.40	66.70	61.97	26.96	26.70	463.39	463.41	412.56	418.45	41.47
0.50	66.70	60.79	27.02	26.70	579.17	579.36	511.84	524.85	50.26
0.60	66.70	59.60	27.09	26.70	695.29	695.31	617.21	631.96	58.37
0.70	66.70	58.42	27.15	26.70	811.18	811.26	715.45	739.79	65.83
0.80	66.70	57.24	27.22	26.70	926.86	927.15	823.82	848.32	72.58
0.90	66.70	56.06	27.28	26.70	1042.22	1043.03	924.45	957.56	78.66
1.00	66.70	54.87	27.34	26.70	1158.83	1158.87	1023.04	1067.56	84.00
1.10	66.70	53.69	27.41	26.70	1274.49	1274.59	1133.24	1178.24	88.60
1.20	66.70	52.51	27.47	26.70	1390.02	1390.26	1234.98	1289.63	92.50
1.30	66.70	51.34	27.54	26.70	1505.33	1505.84	1335.88	1401.75	95.65
1.40	66.70	50.16	27.60	26.70	1620.36	1621.32	1435.69	1514.57	98.06
1.50	66.70	48.99	27.66	26.70	1735.00	1736.69	1534.19	1628.10	99.72
1.60	66.70	47.80	27.73	26.70	1851.80	1851.85	1647.92	1662.44	100.01
1.70	66.70	46.63	27.79	26.70	1966.82	1966.92	1750.02	1857.44	100.46
1.80	66.70	45.46	27.86	26.70	2081.67	2081.85	1851.74	1973.17	99.69
1.90	66.70	44.29	27.92	26.70	2196.31	2196.61	1952.99	2089.63	98.11
2.00	66.70	43.12	27.98	26.70	2310.71	2311.21	2053.68	2206.81	95.71
2.10	66.70	41.95	28.05	26.70	2424.84	2425.63	2153.72	2324.72	92.48
2.20	66.70	40.79	28.11	26.70	2538.68	2539.87	2253.03	2443.36	88.41
2.30	66.70	39.63	28.17	26.70	2652.19	2653.91	2351.50	2562.73	83.51
2.40	66.70	38.48	28.23	26.70	2765.33	2767.75	2449.08	2682.82	77.76
2.50	66.70	37.30	28.31	26.70	2881.05	2881.10	2572.24	2803.84	70.72

2.60	66.70	36.14	28.37	26.70	2994.36	2994.44	2674.19	2925.47	63.11
2.70	66.70	34.99	28.44	26.70	3107.42	3107.54	2775.94	3047.86	54.60
2.80	66.70	33.84	28.50	26.70	3220.22	3220.40	2877.42	3171.00	45.18
2.90	66.70	32.69	28.56	26.70	3332.76	3333.01	2978.61	3294.90	34.84
3.00	66.70	31.54	28.63	26.70	3445.00	3445.36	3079.49	3419.56	23.58

APPENDIX L

Published Paper, Conference and Symposium

1. Enhancing Hydrogen Production in an Ocean Thermal Energy (Otec) System Through The Use of A Solar. Jurnal Teknologi (Sciences & Engineering) Volume 77, No.1 ,November 2015.

2. Design Optimization of Power Generation and Desalination Application in Malaysia Utilizing Ocean Thermal Energy. Jurnal Teknologi (Sciences & Engineering) Volume 77, No.1 ,November 2015.

3. International Platform in Ocean Energy for Young Researcher 2015 (Presenter),Japan

4. 3 rd International OTEC symposium Malaysia 2015 (Presenter),Malaysia